Universidade de Aveiro Departamento de Biologia
2014

DIANA RAQUEL SANTOS RIBEIRO

THE ROLE OF UROCORTIN-2 IN PULMONARY ARTERIAL HYPERTENSION

O PAPEL DA UROCORTINA-2 NA HIPERTENSÃO ARTERIAL PULMONAR

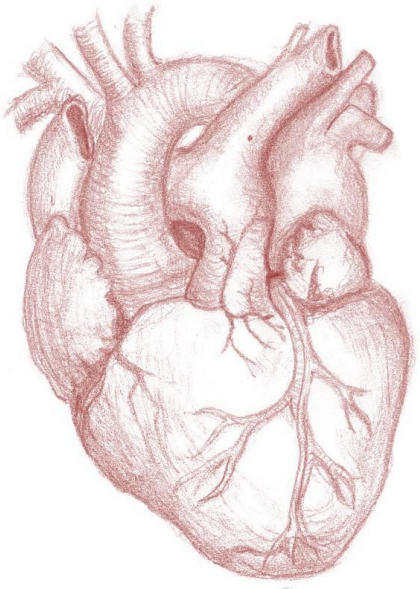

DECLARAÇÃO

Declaro que este relatório é integralmente da minha autoria, estando devidamente referenciadas as fontes e obras consultadas, bem como identificadas de modo claro as citações dessas obras. Não contém, por isso, qualquer tipo de plágio quer de textos publicados, qualquer que seja o meio dessa publicação, incluindo meios eletrónicos, quer de trabalhos académicos.

Universidade de Aveiro Departamento de Biologia
2014

DIANA RAQUEL SANTOS RIBEIRO

THE ROLE OF UROCORTIN-2 IN PULMONARY ARTERIAL HYPERTENSION

O PAPEL DA UROCORTINA-2 NA HIPERTENSÃO ARTERIAL PULMONAR

Dissertação apresentada à Universidade de Aveiro para cumprimento dos requisitos necessários à obtenção do grau de Mestre em Biologia Molecular e Celular, realizada sob a orientação científica da Professora Doutora Carmen Dulce da Silveira Brás Silva, Investigadora do Departamento de Fisiologia e Cirurgia Cardiotorácica da Faculdade de Medicina e Professora Auxiliar da Faculdade de Ciências da Nutrição e Alimentação da Universidade do Porto, e coorientação da Professora Doutora Maria Paula Polónia Gonçalves, Professora Associada ao Departamento de Biologia da Universidade de Aveiro.

Este trabalho foi desenvolvido no âmbito do projeto financiado pela Fundação para a Ciência e a Tecnologia (FCOMP-01-0124-FEDER-011051, FEDER, COMPETE, FCT PTDC/DTP-FTO/0130/2012)

À memória da minha avó Margarida da Cruz Silva

"Most people say that it is the intellect which makes a great scientist. They are wrong. It is character."

Albert Einstein

O júri

Presidente	Prof. Doutora Maria de Lourdes Gomes Pereira Professora Associada com agregação ao Departamento de Biologia da Universidade de Aveiro
Orientadora	Prof. Doutora Carmen Dulce da Silveira Brás Silva Investigadora do Departamento de Fisiologia e Cirurgia Cardiotorácica da Faculdade de Medicina e Professora Auxiliar da Faculdade de Ciências da Nutrição e Alimentação da Universidade do Porto
Arguente	Prof. Doutora Ana Patrícia Nunes Fontes de Sousa Professora Auxiliar do Instituto de Ciências Biomédicas Abel Salazar da Universidade do Porto

Agradecimentos

À minha orientadora, Professora Doutora Carmen Brás Silva, por me ter acolhido no seu grupo de trabalho e me ter dado a oportunidade de aprender e crescer, tanto como pessoa como cientista. Nunca poderei exprimir por palavras o quanto isso significa para mim e o importante que é na minha vida. Obrigado por apostar em mim e pela amizade, simpatia e compreensão que dedica a todos os que consigo trabalham. Farei das "tripas coração" para nunca a desiludir.

À Professora Doutora Paula Gonçalves por me ter apresentado esta oportunidade. Ainda, um obrigado por toda a disponibilidade e simpatia que sempre demonstrou, enquanto professora e orientadora.

Ao Professor Doutor Adelino Leite Moreira por me receber no Departamento de Fisiologia e Cirurgia Cardiotorácica da Faculdade de Medicina da Universidade do Porto.

Aos meus colegas de grupo, e hoje amigos, Mestre Pedro Ferreira, Mestre Rui Adão, Mestre Carolina Rocha e Dra. Bárbara, por todos os bons momentos passados dentro e fora do laboratório, pela entreajuda e pelos bons conselhos. Vocês são os melhores e os mais malucos que conheço. Nunca deixem morrer a criança que há em vós. Obrigado por fazerem do nosso local de trabalho um sítio espetacular.

Aos restantes membros e colegas de departamento, em especial, Glórinha, Fabi, Dudu, Dani, Mizé e Ticha por me terem acolhido no seio da vossa amizade e partilharem o vosso dia-a-dia comigo. Obrigado por fazerem deste departamento uma autêntica casa de família.

A todos os meus amigos de longa data por estarem sempre comigo, tanto nos bons como nos maus momentos. Estou certa de que só a morte nos separará. Adoro-vos, obrigado por serem quem são e por partilharem a vossa vida comigo!

À minha família e namorado, por todo o apoio e carinho incondicional que sempre me deram, por todas as oportunidades que me proporcionaram e principalmente por sempre terem acreditado em mim e nas minhas capacidades. Obrigado por me incentivarem a querer mais e melhor para o meu futuro. Vocês são tudo para mim.

Ainda, a todos que se cruzaram comigo ao longo destes anos, e que de alguma forma contribuíram para a minha formação pessoal, académica e profissional, contribuindo para a concretização desta dissertação de mestrado.

Muito Obrigado!

Palavras-chave

Hipertensão arterial pulmonar, disfunção ventricular direita, urocortina-2, recetor tipo 2 para a hormona libertadora de corticotropina.

Resumo

A hipertensão arterial pulmonar (HAP) é uma síndrome caracterizada por um aumento progressivo das resistências vasculares pulmonares e sobrecarga sobre o ventrículo direito que potencialmente levam à insuficiência cardíaca (IC) direita e consequentemente à morte. A urocortina (UCN)-2 é um péptido altamente expresso a nível cardiovascular que tem exibido efeitos terapêuticos benéficos tanto em humanos como em modelos animais de IC. Este estudo tem como principal objetivo explorar os efeitos da UCN-2 num modelo animal de IC ventricular direita (VD), secundário à HAP, e o seu impacto na função miocárdica.

Ratos *Wistar* machos receberam aleatoriamente uma injeção de monocrotalina (MCT) ou veículo. Após 14 dias, os animais foram novamente sorteados para receber tratamento com UCN-2 ou veículo. Do estudo resultaram 4 grupos experimentais: CTRL, CTRL+UCN-2, MCT e MCT+UCN-2. As avaliações ecocardiográficas, estudos hemodinâmicos e colheita de amostras para análise morfométrica, histológica e molecular foram realizados 24-25 dias após a administração de MCT.

Os animais injetados com MCT desenvolveram HAP e IC VD, demonstrado pelo comprometimento do fluxo pulmonar, dilatação VD e aumento das pressões VD, assim como um débito cardíaco diminuído. A administração de MCT também levou à hipertrofia VD. O tratamento com UCN-2 conseguiu recuperar as alterações induzidas pela HAP na função e estrutura cardíacas. Ainda, os animais MCT+UCN-2 tiveram uma maior taxa de sobrevivência quando comparados com os MCT. Os estudos moleculares revelaram uma expressão genética e uma fosforilação proteica alterada nos animais MCT, de alguns componentes do sistema UCN-2/$CRHR_2$.

Em suma, com este estudo demonstramos que o tratamento crónico com UCN-2 é capaz de restaurar as alterações induzidas pela HAP na função e estrutura cardíacas, assim como reverter as alterações na expressão de marcadores cardíacos de sobrecarga, hipertrofia, hipóxia e apoptose induzidos pela doença. Estes resultados sugerem que a via UCN-2/$CRHR_2$ tem um papel relevante na fisiopatologia da HAP e progressão para IC, representando um potencial alvo terapêutico.

Keywords

Pulmonary arterial hypertension, right ventricular dysfunction, urocortin-2, corticotropin-releasing hormone receptor 2.

Abstract

Pulmonary arterial hypertension (PAH) is a syndrome based on diverse aetiologies, characterized by a persistent increase in pulmonary vascular resistance and overload of the right ventricle (RV), leading to heart failure (HF) and death. Urocortin (UCN)-2 is a peptide highly expressed in the cardiovascular system that has shown promising therapeutic effects in several studies both in humans and animal models of HF. Thus, this study aims to explore the effects of UCN-2 treatment in an animal model of RV HF secondary to PAH and its impact on myocardial function.

Male Wistar rats (180-200g) randomly received monocrotaline (MCT, 60mg/kg) or vehicle. After 14 days, animals were randomly assigned to receive UCN-2 treatment (5μg/kg/day) or vehicle. The study resulted in 4 groups: CTRL (n=9), CTRL+UCN-2 (n=9), MCT (n=7) and MCT+UCN-2 (n=10). Echocardiographic, hemodynamic studies and sample collection were performed 24-25 days after MCT administration. Only significant results (mean±SEM, $p<0.05$) are given.

MCT animals developed PAH, demonstrated by impaired pulmonary flow, RV dilation and increased RV pressures, as well as decreased cardiac output. MCT administration also resulted in RV hypertrophy. UCN-2 treatment was able to restore PAH-induced severe abnormalities in cardiac function and structure. Moreover, Kaplan-Meier analysis showed increased survival rate for MCT+UCN-2 rats when compared with the MCT group. The molecular studies revealed an altered genetic expression of the UCN-2/$CRHR_2$ system components in the MCT animals, as shown by the increase in molecular markers of hypertrophy, overload, hypoxia and apoptosis that were reversed with UCN-2 treatment. As well as an impaired protein activation/phosphorylation seen in peptides pertaining to different signaling pathways.

In conclusion, we show that UCN-2 chronic treatment is able to restore PAH-induced severe abnormalities in cardiac function and structure, as well as to reverse the changes in the expression of markers of cardiac overload, hypertrophy, hypoxia and apoptosis induced by the disease. The beneficial effects of UCN-2 seem to be associated with the modulation of numerous signaling pathways, such as survival and proliferation. These findings suggest that the UCN-2/$CRHR_2$ pathway has a relevant role on the pathophysiology of PAH and progression to RV failure, representing a potential therapeutic target.

INDEX

INDEX OF TABLES

INDEX OF FIGURES

ABBREVIATIONS AND ACRONYMS

5-HT
5-hydroxytryptamine / Serotonin

5-HT_{1B}
Serotonin receptor type 1B

5-HTT
Serotonin transporter

6MWT
6 minute walk test

6MWD
6 minute walk distance

aa
Amino acid

AC
Adenylyl cyclase

AKAP
A-kinase anchoring protein

Akt
Protein kinase B

ALK1
Activin receptor-like kinase type 1

ANP
Atrial natriuretic peptide

APAH
Associated pulmonary arterial hypertension

AU
Arbitrary units

BMPR2
Bone morphogenetic protein receptor type 2

BNP
Brain natriuretic peptide

BW
Body weight

CaMKII
Ca^{2+}/calmodulin-dependent protein kinase II

cAMP
Cyclic adenosine monophosphate

CCB
Calcium channel blocker

cGMP
Cyclic guanosine monophosphate

CHD
Congenital heart disease

CI
Cardiac index

CO
Cardiac output

CPET
Cardiopulmonary exercise testing

CREB
cAMP response element-binding protein

CRH
Corticotropin-releasing hormone

$CRHR_1$
Corticotropin-releasing hormone receptor type 1

$CRHR_2$
Corticotropin-releasing hormone receptor type 2

CTEPH
Chronic thromboembolic pulmonary hypertension

EC
Endothelial cell

ECD
Extracellular domain

EDPVR k1
End-diastolic pressure volume relationship slope

EF
Ejection fraction

ENG
Endoglin

eNOS
Endothelial nitric oxide synthase

EPAC
Exchange protein activated by cAMP

ERA
Endothelin receptor antagonist

ERK 1/2
Extracellular signal-regulated kinases 1 and 2

ESPVR E_{es}
End-systolic pressure volume relationship slope

ET-1
Endothelin-1

ET_A
Endothelin receptor type A

ET_B
Endothelin receptor type B

GcW
Gastrocnemius weight

GPCR
G protein-coupled receptor

GSK-3β
Glycogen synthase kinase 3 beta

HE
Hematoxylin-eosin

HF
Heart failure

HR
Heart rate

HIV
Human immunodeficiency virus

HPAH
Heritable pulmonary arterial hypertension

HUVEC
Human umbilical vein endothelial cell

IL-1
Interleukin-1

IL-6
Interleukin-6

IVC
Inferior vena cava

IVS
Interventricular septum

iNOS
Inducible nitric oxide synthase

IPAH
Idiopathic pulmonary arterial hypertension

KCNK3
Potassium channel subfamily K member 3

LiW
Liver weight

LV
Left ventricle

LV+SW
Left ventricle + septum weight

LVEDP
Left ventricular end-diastolic pressure

LVEF
Left ventricular ejection fraction

LW
Lung weight

MAPK
Mitogen-activated protein kinase

MCT
Monocrotaline

mPAP
Mean pulmonary arterial pressure

NFAT
Nuclear factor of activated T cells

NF-κB
Nuclear factor kappa-light-chain-enhancer of activated B cells

NO
Nitric oxide

NOS
Nitric oxide synthase

NT-proBNP
N-terminal of the prohormone brain natriuretic peptide

p38-MAPK
p38-mitogen-activated protein kinase

PAAT
Pulmonary artery acceleration time

PAD
Pulmonary artery diameter

PAEC
Pulmonary arterial endothelial cell

PAET
Pulmonary artery ejection time

PAH
Pulmonary arterial hypertension

PAPSV
Pulmonary artery peak systolic velocity

PASMC
Pulmonary arterial smooth muscle cell

PAVTI
Pulmonary artery velocity time integral

PCWP
Pulmonary capillary wedge pressure

PDE
Phosphodiesterase

PDE-5
Phosphodiesterase type 5

PGI2
Prostacyclin or prostaglandin 12

PH
Pulmonary hypertension

PI3K
Phosphatidylinositol-3 kinase

PKA
Protein kinase A

PKB
Protein kinase B

PKC
Protein kinase C

PLB
Phospholamban

PVR
Pulmonary vascular resistance

RAA
Right atrium area

RH
Right heart

RHC
Right heart catheterization

RT-PCR
Reverse transcription polymerase chain reaction

RV
Right ventricle

RVEDD
Right ventricular end-diastolic dimension

RVEDV
Right ventricular end-diastolic volume

RVEDP
Right ventricular end-diastolic pressure

RVESP
Right ventricular end-systolic pressure

RVF
Right ventricular failure

RVH
Right ventricular hypertrophy

RVW
Right ventricle weight

SERCA
Sarco/endoplasmic reticulum Ca^{2+}-ATPase

SMAD9
Mothers against decapentaplegia homolog 9

SMC
Smooth muscle cell

SR
Sarcoplasmic reticulum

$STAT_3$
Signal transducer and activator of transcription 3

SV
Stroke volume

τ_{log}
Isovolumic relaxation constant

TAPSE
Tricuspid annular plane systolic excursion

TGF-β
Transforming growth factor-beta

TL
Tibia length

TXA_2
Thromboxane A2

UCN-1
Urocortin-1

UCN-2
Urocortin-2 or stresscopin-related peptide

UCN-3
Urocortin-3 or stresscopin

VEGF
Vascular endothelial growth factor

VEGFR-2
Vascular endothelial growth factor receptor type 2

VSMC
Vascular smooth muscle cell

WHO-FC
World Health Organization functional class

WSPH
World Symposia on pulmonary hypertension

INTRODUCTION

Overview of Pulmonary Arterial Hypertension

The term Pulmonary Hypertension (PH) encircles several disorders mainly characterized by the presence of abnormally high pulmonary vascular pressure. Pulmonary arterial hypertension (PAH), the largest group of PH, is a syndrome based on diverse aetiologies that results from restricted blood flow through the pulmonary arterial circulation resulting in increased pulmonary vascular resistance (PVR) and overload of the right ventricle (RV), leading to heart failure (HF) and death[1].

Definition

PAH is defined by a mean pulmonary artery pressure (mPAP) equal to or greater than 25mmHg at rest, and is hemodynamically characterized (Table 1) by the presence of pre-capillary PH, which implies a normal pulmonary capillary wedge pressure (PCWP) or left ventricular end-diastolic pressure (LVEDP) of 15mmHg or less with a PVR greater than 3 Wood Units (mmHg/l•min)[1, 2]. So far there is no sufficient evidence to add an exercise criterion to this definition[3].

TABLE 1. Hemodynamic definitions of Pulmonary Hypertension*

Definition	Characteristics	Clinical Group(s)
PH	mPAP ≥ 25mmHg	All
Pre-capillary PH	mPAP ≥ 25mmHg PWP ≤ 15mmHg CO normal or reduced[#]	1. PAH 3. PH due to lung diseases 4. Chronic thromboembolic PH 5. PH with unclear and/or multifactorial mechanisms
Post-capillary PH	mPAP ≥ 25mmHg PWP > 15mmHg CO normal or reduced[#]	2. PH due to left heart disease
Passive	TPG ≤ 12mmHg	
Reactive (out of proportion)	TPG > 12mmHg	

*All values measured at rest. [#]High CO can be present in cases of hyperkinetic conditions such as systemic-to-pulmonary shunts (only in the pulmonary circulation), anaemia, hyperthyroidism, etc. **Abbreviations:** CO, cardiac output; mPAP, mean pulmonary arterial pressure; PH, pulmonary hypertension; PWP, pulmonary wedge pressure; TPG, transpulmonary pressure gradient (mean PAP-mean PWP). Adapted from Galiè *et al.* (3).

Clinical Classification

Since the first World Symposia on Pulmonary Hypertension (WSPH) in 1973 held in Geneva, Switzerland, the clinical classification of PH has gone through a series of alterations. Initially, a simple classification divided only in two categories was proposed: primary and secondary PH, depending on the presence or absence of identifiable causes or risk factors[4, 5]. In the following WSPHs, new classifications have been proposed based on emerged knowledge about PH pathophysiology, clinical features and therapeutic options[5, 6].

The latest classification was established during the fifth WSPH in Nice, France, in 2013 (Table 2)[7] and individualizes five PH categories according to pathological findings, hemodynamic characteristics and similar therapy: PAH (Group 1); PH due to left heart diseases (Group 2); PH due to chronic lung disease and/or hypoxia (Group 3); chronic thromboembolic PH (CTEPH) (Group 4) and PH due to unclear multifactorial mechanisms (Group 5).

In Group 1, idiopathic PAH corresponds to sporadic disease in which there is no familial history nor identified risk factors. When PAH occurs in a familial context, it is labeled heritable PAH and emerges from germline mutations mainly in the gene coding for the bone morphogenetic protein receptor type 2 (BMPR2) (>70% cases), a member of the transforming growth factor beta (TGF-β) signaling family. Mutations like this also have been found in 11-40% of idiopathic cases with no familial record[8]. Several drugs like aminorex, fenfluramine and dexfenfluramine (appetite suppressants), and/or toxic rapeseed oil represent a clear risk factor for PAH development, therefore it represents an isolated PAH category. The last PAH group encircles several diseases closely related to PAH, such as, connective tissue diseases, human immunodeficiency virus (HIV) infection, portal hypertension, congenital heart diseases (CHD) and schistosomiasis[7, 9].

TABLE 2. Updated clinical classification of Pulmonary Hypertension (Nice, 2013)

1.	**PAH**
1.1.	Idiopathic PAH
1.2.	Heritable PAH
1.2.1.	BMPR2
1.2.2.	ALK1, ENG, SMAD9, CAV1, KCNK3
1.2.3.	Unknown
1.3.	Drugs and toxins induced
1.4.	Associated with (APAH)
1.4.1.	Connective tissue diseases
1.4.2.	HIV infection
1.4.3.	Portal hypertension
1.4.4.	Congenital heart diseases
1.4.5.	Schistosomiasis

1'.	**Pulmonary veno-occlusive disease and/or pulmonary capillary hemangiomatosis**
1''.	**Persistent PH of the newborn (PPHN)**
2.	**PH due to left heart disease** 2.1. Left ventricular systolic dysfunction 2.2. Left ventricular diastolic dysfunction 2.3. Valvular disease 2.4. Congenital/acquired left heart inflow/outflow tract obstruction and congenital cardiomyopathies
3.	**PH due to lung diseases and/or hypoxia** 3.1. Chronic obstructive pulmonary disease 3.2. Interstitial lung disease 3.3. Other pulmonary diseases with mixed restrictive and obstructive pattern 3.4. Sleep-disordered breathing 3.5. Alveolar hypoventilation disorders 3.6. Chronic exposure to high altitude 3.7. Developmental lung diseases
4.	**Chronic thromboembolic PH (CTEPH)**
5.	**PH with unclear multifactorial mechanisms** 5.1. Hematological disorders: chronic hemolytic anemia, myeloproliferative disorders, splenectomy 5.2. Systemic disorders: sarcoidosis, pulmonary histiocytosis, lymphangioleiomyomatosis, neurofibromatosis, vasculitis 5.3. Metabolic disorders: glycogen storage disease, Gaucher disease, thyroid disorders 5.4. Others: tumoral obstruction, fibrosing mediastinitis, chronic renal failure, segmental PH

Abbreviations: ALK1, activin receptor-like kinase-1 gene; BMPR2, bone morphogenetic protein receptor type II; CAV1, caveolin-1; ENG, endoglin; HIV, human immunodeficiency virus; KCNK3, potassium channel subfamily K member 3; PH, pulmonary hypertension; PAH, pulmonary arterial hypertension; SMAD9, mothers against decapentaplegic homolog 9. Adapted from Simonneau *et al.* (7).

Pathophysiology

HISTOPATHOLOGY

PAH is considered a vasculopathy, and in general, all PAH subgroups (Group 1) and other forms of PH (i.e. PH owing to lung disease and/or hypoxia) exhibit several arterial abnormalities mainly present in small pulmonary arteries and arterioles[1]. The most common pathologic features in PH are medial hypertrophy, dilation and intimal atheromas and because they are present in all forms of PH, they hold poor diagnostic value. However, PAH is characterized by **constrictive lesions**, which include medial hypertrophy, and intimal and adventitial thickening, and by **complex lesions** that includes plexiform and dilation lesions, as well as arteritis[10].

Medial hypertrophy

Is defined by an increase of the diameter of the medial layer, measured between the internal and the external elastic lamina, exceeding 10% of the arteries cross-sectional diameter. This abnormality appears in all PAH subgroups and occurs due to pulmonary arterial

smooth muscle cell (PASMC) proliferation and/or recruitment to the tunica media. This lesion is considered an early event in PAH pathogenesis but it is usually regarded as a reversible one[10].

Intimal and adventitial thickening

This occurs due to the proliferation and recruitment of fibroblasts, myofibroblasts and other connective tissue cells, and consequently by the interstitial deposition of collagen, leading to fibrosis. This thickening can be uniform (concentric) or focal (eccentric) being the former often associated with thrombotic events[11].

Plexiform lesions

This abnormality affects several vascular compartments and it's very PAH-characteristic[11]. The formation of these lesions occurs due to the local and excessive endothelial cell (EC) proliferation, which leads to the formation of capillary-like channels on a myofibroblasts, smooth muscle cells (SMC) and connective tissue-rich matrix within the arterial lumen[12]. These lesions are responsible for the expansion and partial destruction of the arterial wall, since they tend to enlarge into the perivascular connective tissue. Fibrin, thrombi and platelets are frequently encountered in these lesions[10, 13].

Dilation lesions and arteritis

The first is usually located near a plexiform lesion and is a thin-walled vein-like vessel, representing a potential cause for hemorrhages and subsequent fibrosis. In arteritis, necrotic and fibrotic tissue may accumulate in the artery wall and/or infiltration with inflammatory cells[10].

CELLULAR FACTORS

Several different cell populations are involved and contribute to these types of lesions[14]. The main mechanisms responsible for this pulmonary vascular dysfunction are the abnormal proliferation of SMC and EC, infiltration of inflammatory cells and fibrosis[15]. However, PAH cannot only be associated with cell proliferation but also with apoptotic processes, since it is supposed that an imbalance between these two events is the major responsible for the narrowing of pulmonary arteries in PAH[16].

Smooth muscle cells and fibroblasts

All forms of PAH have in common the migration and proliferation of SMC, which in general is accompanied by the migration of fibroblasts and formation of an extracellular matrix layer. This uncontrolled proliferation of SMCs ultimately leads to media hypertrophy, also contributing to the thickening of the intima and adventitia layers of the pulmonary vessels[17]. The formation of an extracellular matrix and myofibroblasts between the endothelium and internal elastic lamina is termed neointima. Another PAH characteristic feature is the increase in *vasa vasorum* neovascularization which mainly affects the adventitia, being able to expand to the media[18].

Endothelial cells

In response to shear stress, hypoxia, inflammation and/or other stimuli, ECs proliferate beyond limit and generate plexiform lesions[19]. ECs in response to these stimuli may undergo through changes in proliferative and apoptotic processes, as well as changes at the functional level. Endothelial dysfunction eventually results in a clear imbalance between the production and release of vasoconstrictors/vasodilators, activator/inhibitory growth factors, prothrombotic/antithrombotic mediators and proinflammatory/anti-inflammatory signals[20, 21].

Inflammatory cells

In certain forms of PAH (i.e. PAH associated with auto immune diseases) the inflammatory response plays an important role, since some patients improved both clinically and hemodynamically when administered immunosuppressant therapy. A fraction of patients (30-40%) have circulating auto-antibodies and elevated plasma levels of interleukin (IL)-1 and IL-6. Moreover, some inflammatory cells, such as lymphocytes and macrophages, can also be found in plexiform lesions[20].

Thrombosis and platelet dysfunction

Some PAH patients exhibit elevated plasma levels of fibrinopeptides, along with von-Willebrand factor and plasminogen activator inhibitor type 1, reflecting an abnormal coagulation process and endothelial dysfunction, respectively. Both events are very important in PAH development because they can generate or aggravate *in situ* thrombosis. Platelets also participate in vasoconstriction and vascular remodeling, since they are able to produce prothrombotic, vasoactive and mitogenic factors[22].

MOLECULAR ABNORMALITIES

The molecular abnormalities seen in PAH patients are normally associated with increased endothelin (ET)-1 levels and decreased nitric oxide (NO) and prostacyclin levels, since these factors influence vascular homeostasis, cell survival and proliferation, among other processes.

Prostanoids

Prostacyclin or prostaglandin I2 (PGI2) and thromboxane A_2 (TXA_2) belong to the prostanoids family and are produced from arachidonic acid metabolites. The former is a potent vasodilator and inhibitor of platelet activation and cellular proliferation, while TXA_2 is a vasoconstrictor and promotes these cellular mechanisms[1]. PGI2 is produced in vascular ECs and acts on vascular smooth muscle cells (VSMC) as well as circulating platelets and cells, via the cyclic adenosine monophosphate (cAMP) pathway[23]. In PAH patients, the expression of PGI2 synthase in pulmonary arteries is reduced and therefore the production of prostacyclin in ECs is evidently decreased[24].

Endothelin-1

This 21-amino acid vasoactive peptide is expressed in several mammalian tissues in different types of cells and is responsible for the regulation of vascular tone. ET-1 exerts its effects through the interaction with two types of receptors, endothelin receptor-type A (ET_A) and –type B (ET_B), which belong to the G-protein-coupled receptors (GPCRs) family and are in general highly homologous. In PASMCs, when activated, both receptors have a vasoconstrictor effect, while in pulmonary arterial endothelial cells (PAEC), ET_A is not expressed and the activation of ET_B leads to vasodilatation[25]. EC dysfunction usually leads to ET-1 overexpression, which results in vasoconstriction and reduced synthesis of NO and prostacyclin, worsening the vasoconstrictor response. The upregulation of ET-1 is also involved in inflammatory responses and increased fibrosis[15]. In PAH patients, ET-1 levels are elevated and it's clearance in the pulmonary vasculature is reduced. The plasma levels of this peptide can be correlated with the severity of PAH and its prognosis[26, 27].

Endothelial nitric oxide

NO is a 30Da lipophilic gaseous molecule that can be synthesized in mammalian tissues via activation of either one of the three NO synthase (NOS) isoforms, which have the ability to catalyze the formation of NO from L-arginine in a two-step reaction. NO is a vasodilator that modulates several physiological processes, being also capable of inhibiting leukocyte adhesion,

platelet aggregation, thrombus formation, and vascular proliferation[23]. Endothelial NOS (eNOS) can be activated either by GPCR signal transduction, which increases intracellular Ca^{2+} levels and, subsequently, levels of Ca^{2+}-calmodulin; Akt signaling; vascular endothelial growth factor (VEGF) and hormonal stimuli (e.g. estrogen and insulin)[25]. In both animal models of PH and humans with this syndrome, decreased pulmonary vascular eNOS activity is observed, along with loss of NO bioavailability, which is linked to impaired endothelium-dependent and -independent vasodilatation, increased PASMC mitogenesis and platelet aggregation[25, 28].

Phosphodiesterase inhibition

Phosphodiesterase (PDE) enzymatic activity is implicated in the endogenous degradation of cAMP[29], and currently, eleven PDE isoforms are known in mammalian tissue[30]. More specifically, in the setting of PH, PDE type-5 has gaining some interest since it was identified in elevated concentrations in PASMCs, platelets and myocytes. PDE-5 regulates cyclic guanosine monophosphate (cGMP) bioactivity via hydrolysis of cGMP to 5'-GMP and allosteric binding of cGMP to PDE-5, which induces a conformational change to the structure of the latter, that positively feeds back to promote cGMP metabolism[25]. In a setting of PAH, expression of PDE-5 is increased in both PASMCs and RV myocytes[31,32] being associated with decreased levels of NO, pulmonary vascular dysfunction and impaired RV lusitropy[33]. In PASMCs *in vitro*, PDE-5 inhibition reduces DNA synthesis/cell growth, cellular proliferation, and suppression of apoptosis[32], being also linked to decreased thrombotic burden in CTEPH, presumably by increasing bioactive cGMP levels in platelets to inhibit platelet aggregation[34].

Potassium channels

The inhibition of voltage dependant potassium channels in PASMC results in membrane depolarization and opening of voltage dependant calcium channels, which leads to an increase in $[Ca^{2+}]_i$ and cellular contraction[11]. This inhibition can result from a variety of stimuli, such hypoxia or anorexigens[35]. Some of these channels are downregulated in PAH patients[36].

Serotonin

Serotonin (5-hydroxytryptamine, 5-HT) is a vasoconstrictor agent that is also capable of promoting PASMC hypertrophy and hyperplasia[1]. While 5-HT transporter (5-HTT) facilitates the induction of proliferation since it carries 5-HT into PASMCs, the 5-HT_{1B} receptor mediates vasoconstriction, both contributing to PAH pathogenesis[37]. PAH patients usually present elevated plasmatic concentrations of 5-HT[38].

Rho proteins

Several cellular functions such as contraction, migration, proliferation and apoptosis are regulated by Rho proteins and especially Rho protein A and Rho kinases have been implicated in PAH vasoconstriction and vascular remodeling[39]. The signaling pathway involving these proteins is directly involved in 5-HTT-mediated PASMC proliferation and platelet activation during PH progression[40].

GENETIC MUTATIONS

If not associated with other clinical condition or induced by toxins, PAH can be either idiopathic or heritable. This disease segregates an autosomal dominant trait with a markedly reduced penetrance, since only 10-20% of individuals that carry the mutation will develop PAH[41]. The BMPR2 is a serine/threonine receptor kinase that belongs to the family of TGF-β. In 58-74% of PAH patients with familial history of the disease, and in 35-40% of idiopathic PAH patients, germline BMPR2 mutations can be detected[42,43]. Mutations in BMPR2 cause an aberrant signal transduction in PASMC, resulting in an imbalance between apoptosis and proliferation in favor of the latter[44]. Other two PAH predisposing genes are ALK1 that codes for Activin-Like Kinase type I receptor, present in ECs, and ENG (endoglin), and are most common in patients displaying hereditary hemorrhagic telangiectasia[45, 46]. Most recently, a few studies described mutations in more than one SMAD genes[47]. Interestingly, all genes mentioned above encode proteins involved in the TGF-β signaling pathway, which may be a trigger for pulmonary vascular remodeling since this signaling pathway controls growth, differentiation and apoptosis in different cell types[48].

The Right Ventricle

Though the development of right heart (RH) failure is secondary to pulmonary vascular remodeling in PAH, the former is the immediate cause of death in most patients. Therefore, the integrity of RV function, rather than the degree of vascular injury, is the major determinant of prognosis in PAH[49]. The abnormal changes that occur in the pulmonary arteries of PAH patients, at first leads to vessel narrowing and/or obstruction, which then results in a progressive increase in PVR and mPAP[50].

In a normal heart, the RV, which differs anatomically from the left ventricle (LV), is able to adapt and respond to an increase in load with an increase in contractility since its thin wall,

crescent shape and greater compliance give the RV the ability to adapt rapidly to changes in volume and pressure load[49].

In PAH patients, initially the RV copes with increased afterload, with an enhanced contraction and a concentric RV remodeling, while the right atrium pressure remains normal. The rise in ventricular pressures increases diastolic and systolic stretch on the RV wall, which firstly leads to an increase in muscle mass – adaptive hypertrophy – due to increased protein synthesis and cardiomyocyte size. However, if the pressure overload is maintained, the RV cannot sustain the adaptive hypertrophy and eventually dilates, without any increase in RV contractility, despite further increases in load, reaching a state called uncoupling of the RV[51].

The mechanisms involved in further adaptation of the RV and decline of its contractility are poorly understood, but it is thought to be associated with an imbalance between oxygen supply and demand[52], increased chronic sympathetic activation[53], oxidative and nitrosative stress, immune activation and cardiomyocyte apoptosis[51].

The increase in ventricular volume may also lead to tricuspid regurgitation, which results in RV volume overload and thus further RV decline. The latter is accompanied by an increase in RV contraction time and ventricular asynchrony together with a decrease in RV stroke volume (SV), leading to underfilling of the LV[54]. The impaired LV filling in concert with RV dysfunction contributes to the evident decline in cardiac output (CO) seen in severe cases of PAH, and if not interrupted, these circle of events end in RH failure and eventually death[50].

Epidemiology and Survival

PAH is a rare and seriously underdiagnosed syndrome, with an estimated prevalence of 15-50 cases per million people and an incidence of 2.4 cases per million people per year, however the prevalence in certain at-risk groups is substantially higher[55]. For instance, according to the French registry, in the associated PAH subgroup, 15.3% PAH patients had connective tissue diseases, 11.3% had congenital heart diseases, 10.4% had portal hypertension, 9.5% had anorexigen-associated PAH and 6.2% had HIV infection[43]. Idiopathic PAH is 2-4 times more common in women than in men and accounts for at least 40% of PAH cases, with associated PAH accounting for the majority of the remaining cases[55].

The published data regarding Portugal is scarce, but according to the recent Portuguese nationwide registry, in a cohort of 79 patients, 58.2% were classified as having PAH. This study showed a clear preponderance of women among PAH patients, with a female/male ratio of

1.9:1. The majority of patients were between 21 to 60 years of age. Idiopathic PAH was present in 37% of the patients, followed by connective tissue disease (26%), congenital heart disease (22%), portopulmonary hypertension (11%), familial (2%) and other etiologies (2%)[56].

In treated PAH patients, the survival rates improved to 96% after 1 year and 89% after 2 years[57]. While the untreated patients, face an estimated mean survival of 2.8 years, with 1-, 3- and 5-years survival rate of 68%, 48% and 34%, respectively[58].

Symptoms

Due to the non-specific nature of the symptoms, PAH is frequently diagnosed when patients have reached an advanced stage of disease[43]. The most common early symptoms include breathlessness, fatigue, weakness, angina, syncope and abdominal distension. Regarding physical signs, normally there is a left parasternal lift, an accentuated pulmonary component of the second heart sound, a systolic murmur of tricuspid regurgitation, a diastolic murmur of pulmonary insufficiency and a RV third sound. In a more advanced stage, patients often show a jugular vein distension, hepatomegaly, peripheral edema, ascites and cold extremities[3].

Diagnosis

The evaluation of a patient with suspected PH requires a series of tests and exams intended to confirm the diagnosis, clarify the clinical group of PH and the specific etiology within the PAH group, being also important to evaluate the functional and hemodynamic impairment present[3].

Initially, patients with suspected PAH undergo a transthoracic echocardiography, which is an ultrasound-based technique that provides several variables that can be correlated with RH hemodynamic parameters[59] and it is normally performed in cases of suspected PH, as a first approach. In order to confirm the diagnosis of PAH, a RH catheterization (RHC) is necessary and also useful to assess the severity of hemodynamic impairment and to test the vasoreactivity of the pulmonary circulation[60]. Patients with idiopathic PAH, who might benefit from long-term calcium-channel blocker (CCB) therapy are normally subjected to this acute vasodilator test, which is performed at the time of RHC through the administration of pharmacologic agents[61]. Patients with evident RH failure or hemodynamic instability are excluded from the test[3].

In patients of suspected PAH, evaluation of other potential etiologies, such as thromboembolic disease, is recommended, in order to redirect the therapy to the source of the problem[3].

Prognosis

Both clinical and hemodynamic assessments derive from patients cohort's data and therefore may not accurately reflect the prognosis of individuals with the disease. However, they yield important predictive information which may guide clinical management. Despite large inter-observer variation in the measurement, WHO functional class (WHO-FC), depicted in Table 3, remains a powerful predictor of survival.

TABLE 3. Functional classification of PH modified after the New York Heart Association functional classification according to the WHO 1998.

Class I	Patients with PH but without resulting limitation of physical activity. Ordinary physical activity does not cause undue dyspnoea or fatigue, chest pain, or near syncope.
Class II	Patients with PH resulting in slight limitation of physical activity. They are comfortable at rest. Ordinary physical activity causes undue dyspnoea or fatigue, chest pain, or near syncope.
Class II	Patients with PH resulting in marked limitation of physical activity. They are comfortable at rest. Less than ordinary activity causes undue dyspnoea or fatigue, chest pain, or near syncope.
Class IV	Patients with PH with inability to carry out any physical activity without symptoms. These patients manifest signs of RH failure. Dyspnoea and/or fatigue may even be present at rest. Discomfort is increased by any physical activity.

Abbreviations: RH, right heart; PH, pulmonary hypertension. Adapted from Galiè *et al*. (3).

Echocardiographic evaluation remains a good tool to access cardiac structure and function since it is non-invasive and generates many indices, such as pericardial effusion, right atrial area (RAA), RV and pulmonary artery dimensions[62] and RV Doppler index[63], which carry a high prognostic value. Also, tricuspid annular plane systolic excursion (TAPSE) has been reported to be of prognostic value[64]. Amongst the hemodynamic measurements, mPAP has some prognostic value, but it is less reliable as it may fall towards the end stage of the disease as the RV fails. Some studies suggest that reduced arterial O_2 saturation, low systolic blood pressure, and increased heart rate (HR) carry a worse prognosis[65].

For the assessment of exercise capacity of patients with PAH the 6-minute walk test (6MWT) and the cardiopulmonary exercise testing (CPET) are used. The former is technically

simple, inexpensive, reproducible and well standardized, and in addition to distance walked, dyspnoea on exertion (Borg scale) and finger O_2 saturation are also recorded. However, this test is not sufficiently validated in PAH subgroups and it can be influenced by body weight (BW), gender, height, age and patient motivation[66]. In CPET, gas exchange and ventilation are continuously recorded during incremental exercise. In PAH patients, O_2 uptake at the anaerobic threshold and peak exercise are reduced in relation to disease severity, as well as the peak work rate, peak heart rate, O_2 pulse and ventilatory efficiency[67].

Recently some biomarkers have emerged as an attractive non-invasive tool to monitor RV dysfunction in patients with PAH and to evaluate the prognosis severity. For instance, brain natriuretic peptide (BNP) induces vasodilatation and natriuresis as it is released from the myocardium in response to wall stress. The biologically inactive N-terminal segment (NT-proBNP), derived from the cleavage of a higher molecular weight precursor of BNP (proBNP), has an extensive half-life and is very stable even after sampling, providing a useful quantifiable marker. The baseline median value of BNP which distinguishes a good from a bad prognosis is 150pg/mL[68]. Low or decreasing BNP/NT-proBNP levels may be a useful marker of successful disease control in PAH. Increased levels of Troponin T and Troponin I in plasma represents a marker of myocardial damage and are useful prognostic indicators in acute coronary syndromes and acute pulmonary embolism. However, the monitoring value of the cardiac Troponin T levels in plasma still requires confirmation since in some patients they disappear temporarily or permanently after treatment initiation[69]. Currently there are other circulating biomarkers under investigation[70, 71], still waiting for clinical validation.

Patients who experience falling exercise capacity, syncope, hemoptysis and have signs of RV failure carry a poor prognosis. If untreated, PAH patients show a median survival of 6 months for WHO-FC IV, 2.5 years for WHO-FC III, and 6 years for WHO-FC I and II[3] (Table 4).

TABLE 4. Determinants of Pulmonary Arterial Hypertension* prognosis

Determinants of Risk	Lower Risk (Good Prognosis)	Higher Risk (Poor Prognosis)
Clinical evidence of RV failure	No	Yes
Progression of symptoms	Gradual	Rapid
WHO class‡	II, III	IV
6MW distance§	Longer (>400 m)	Shorter (<300 m)
CPET	Peak VO_2 >10.4 mL/kg/min	Peak VO_2 <10.4 mL/kg/min

Echocardiography	Minimal RV dysfunction	Pericardial effusion, significant RV enlargement/dysfunction, RA enlargement
Hemodynamics	RAP <10 mmHg, CI >2.5 L/min/m^2	RAP >20 mmHg, CI <2.0 L/min/m^2
BNP[#]	Minimally elevated	Significantly elevated

*Most data available pertains to idiopathic PAH. One should not rely on any single factor to make risk predictions. [‡]The WHO class is the functional classification for PAH and is a modification of the New York Heart Association functional class. [§]6MW distance is also influenced by age, gender, and height. [#]As there is currently limited data regarding the influence of BNP on prognosis, and many factors including renal function, weight, age and gender may influence BNP, absolute members are not given for this variable. **Abbreviations:** 6MW, 6-minute walk; BNP, brain natriuretic peptide; CI, cardiac index; CPET, cardiopulmonary exercise testing; peak VO_2, average peak oxygen uptake during exercise; RA, right atria; RAP, right atrial pressure; RV, right ventricle; WHO, World Health Organization. Adapted from Mclaughlin *et al*. (1).

Therapy

Currently the pathogenesis of PAH is poorly understood and although the existing treatments can improve clinical symptoms, they cannot cure PAH.

GENERAL MEASURES

Physical activity adapted to patient's symptoms is recommended and though there is no evidence of cardiac hemodynamic improvement, 6MWD and quality of life seem enhanced. Oxygen therapy may also be an option, especially in patients with chronic obstructive pulmonary disease while hypoxic conditions should be avoided, such as high altitude travel. Pulmonary infections should be prevented since they can deteriorate PH symptoms. Pregnancy should also be avoided since it contributes to 30-50% mortality in PAH patients[23].

In some cases, non-specific drugs such as diuretics and anticoagulants, can be administered, since they have the ability to decrease RV overload and *in situ* thrombosis, respectively, improving PAH symptoms[23].

Calcium channel blockers

Because initially vasoconstriction was assumed to be a preponderant mechanism in PAH, CCBs were introduced as part of PAH therapy and in some cases they are able to induce a beneficial vasodilator response[72,73]. This therapy is only indicated in patients that showed a positive vasodilatation reaction after inhaled NO. In the absence of acute vasoreactivity, CCB therapy must be avoided, since it can dramatically reduce CO and systemic blood pressure. Moreover, CCB is not advised in pulmonary veno-occlusive disease because of the risk of pulmonary edema[61].

SPECIFIC TREATMENT

The growing knowledge about the interplay between signaling pathways in pulmonary arterial ECs and SMCs, lung fibroblasts, and RV myocytes that occur in response to injury has led to the development of PAH-specific pharmacotherapies[23], already approved for the treatment of PAH.

Prostanoids

PGI2 or prostacyclin, is an arachidonic acid produced by ECs that induces relaxation in both systemic and pulmonary vascular smooth muscle and inhibits platelet aggregation through the increase in intracellular cAMP levels[15]. PGI2 also plays an important role in antiproliferative, antithrombotic, antimitogenic and immunomodulatory activity[23]. In fact, patients with PAH have reduced endogenous prostacyclin, which contributes to the pathogenesis of the disease[24].

Phosphodiesterase type-5 inhibitors

The vasodilator activity of NO in VSMC is achieved through the up-regulation of cGMP, whose metabolism depends on the activation of PDEs, since the latter is responsible for the hydrolytic breakdown of cGMP. Three types of PDEs enzymes can be found in pulmonary arterial contractive cells, but PDE-5 is the most expressed isoform in pulmonary circulation[23].

Endothelin receptor antagonists

ET-1 is a potent vasoconstrictor and a SMC mitogen that contributes to the development of PAH. Elevated ET-1 levels are frequently correlated with poor prognosis in PAH patients. Endothelin receptor antagonists (ERAs) act by blocking the binding of ET-1 to its receptors, inhibiting its downstream effects. So far, several types of ERAs have been identified and differ in their selectivity to ET_A and ET_B receptors[74].

In short, currently several PAH-specific drugs are available, however they are not able to cure PAH, and some of them show adverse side effects, such as teratogenic effects, hepatic function deterioration and anemia during treatment[75,76].

Animal Models of Pulmonary Hypertension

In order to better understand the pathophysiological mechanism and remodeling process behind PH, and search for novel therapeutic agents, a variety of animal models have been developed and characterized.

These experimental *in vivo* models mimic certain histological and molecular features seen in PH pathophysiology in humans. These include endothelial dysfunction, muscularization of previously non-muscular arterioles and increased medial thickness of normally muscularized arterioles, *in situ* thrombosis and plexiform lesions appearance[77]. Chemical agents[78,79], genetic techniques[80,81], environmental factors[82] and surgical procedures[83] can be used to induce PAH-associated alterations in animals (Table 5).

Currently, monocrotaline (MCT) administration and chronic exposure to hypoxia are the most widely used models of PH in translational research due to their good reproducibility and well described histopathology.

MCT is a pyrrolizidine alkaloid extracted from *Crotalaria spectabilis* seeds and when administered in rats it is metabolized by several oxidases present in the liver, producing the reactive bifunctional cross-linking compound MCT pyrrole. Because this compound has a short half-life and the pulmonary circulation represents the first major vascular bed following liver, its toxic effect concentrate on pulmonary vessels without affecting the systemic circulation[77].

After MCT injection, rats undergo a severe inflammatory reaction, followed by EC death and loss of small peripheral arteries, as well as an increase of the alveoli/arteries ratio. In the first two weeks no clinical disorder can be noticed, whereas in the following 2-4 weeks, the animal's state begins to deteriorate due to the progressive thickening of the media, muscularization of non-muscularized arteries, along with an adventitial proliferation. These abnormalities lead to a progressive increase in mPAP and PVR, ultimately leading to RV hypertrophy (RVH) and increased RV systolic pressure (from 25 to 80 mmHg). At this stage, animals show impaired breathing and cyanotic mucus membranes, acquiring also a hunched posture, being visibly sick. After 4-6 weeks of MCT-administration, animals develop severe PH with a compensatory RVH, due to the increase in PVR. Following this stage and with a progressive increase in PVR, the RV function deteriorates and eventually the animals die of RV failure. However, due to the different pharmacokinetics of MCT among different rat strains, and even between individuals, differences in time of onset and extent of toxic effects can be seen[84].

TABLE 5. Experimental animal models of Pulmonary Hypertension

	Experimental model	Animal species	Shared pathological findings in human disease
(Patho)physiological stimuli	Acute and chronic hypoxia	Bird, cow, dog, guinea pig, mouse, pig, rat, sheep	Increased muscularization of resistance vessels in chronic bronchitis, cystic fibrosis, chronic obstructive pulmonary disease, hypoventilation and chronic heart disease.
	Increased flow	Dog, pig, rat, sheep	Increased muscularization in congenital heart disease
	Vascular obstruction (air embolism, synthetic microspheres)	Dog, pig, rat, sheep	Vascular obliteration and increased muscularization in chronic pulmonary thromboembolism
Chemical and toxic stimuli	Monocrotaline (pyrrole)	Dog, rat, sheep	Increased muscularization and vascular inflammation in drug-induced PH
	α-Naphthylthiourea	Rat	Pulmonary edema and increased muscularization induced by chemotherapy
	Bleomycin	Mouse, rabbit, rat	Fibrosis and increased muscularization in interstitial lung diseases
	Group B Streptococcus	Pig, sheep	Vasoconstriction in persistent PH of the newborn
Molecular stimuli	VEGFR-2 inhibition + hypoxia	Rat	Plexiform lesions in primary PH
	Angiopoietin-I overexpression	Rat	Muscularization and vascular occlusion in primary and secondary PH
Genetic stimuli	Fawn-hooded rat	Rat	Genetic predisposition resulting in increased muscularization
	Broiler chickens	Chicken	Genetic predisposition resulting in increased muscularization
	BMPR2 knockout	Mouse	Genetic predisposition resulting in increased muscularization
	S100A4 overexpression	Mouse	Genetic predisposition resulting in plexiform lesions

Abbreviations: BMPR2, bone morphogenic protein receptor type II; PH, pulmonary hypertension; VEGFR-2, vascular endothelial growth factor receptor type II. Adapted from Marsboom *et al.* (76).

Overview of Urocortin-2/$CRHR_2$ System

Urocortins (UCNs) belong to the corticotropin-releasing hormone (CRH) family which includes CRH, fish urotensin I, frog sauvagine, UCN-1, UCN-2 (or stresscopin-related peptide) and UCN-3 (or stresscopin)[85]. The various actions of the CRH family of peptides are mediated via CRH receptors (CRHRs) that derive from two distinct genes termed $CRHR_1$ and $CRHR_2$[86].

These peptides and their receptors are ancient signaling molecules that allow organisms in development to coordinate physiological responses to a changing environment[85]. The CRH family seem to have overlapping roles in different tissues namely the immune, digestive, central nervous, reproductive and cardiovascular systems, with their relative importance in each system dependent upon their site of production, plasma distribution and specific receptor affinity[87].

UCN-2 is a peptide highly expressed within the cardiovascular system and has shown promising effects in multiple studies in both animals[88-90] and humans[91,92]. Therefore, UCN-2 expression and activity in the heart, particularly its therapeutic potential in terms of cardiac protection has gaining interest in the field of cardiovascular research.

Molecular Structure

UCN-1 is a 40 amino acid (aa) peptide related to CRH (45% sequence identity) and urotensin (63% sequence identity)[93]. The parent peptide, composed of 122 aa, has an N-terminal methionine and a consensus signal peptide sequence, whilst the carboxy terminus of the precursor contains the C-terminally amidated peptide of UCN-1. The CRH analogue peptides have a helical conformation and the C-terminal helices are amphipathic, whereas the N-terminal helices differ in their amphipathicity. The amphipathic N-terminal helices might play an important role in selectivity of the analogues to $CRHR_1$, but may not be as essential for $CRHR_2$ binding. The link between N- and C-terminal helices could also play a fundamental role in ligand-receptor interactions[94].

UCN-2, a 38 aa peptide, shows reasonable homology with rat and human CRH (34%), UCN-1 (43%) and UCN-3 (37–40%)[95]. Mouse UCN-2, but not human UCN-2, is processed at the C terminus, resulting in an amidated residue that is further cleaved to a smaller bioactive form. The prohormones of both UCN-1 and UCN-2 are heavily glycosylated and are capable of activating $CRHR_2$[96].

The $CRHR_1$ and $CRHR_2$ are membrane-bound proteins that belong to the class B1 of the family of seven transmembrane GPCRs and are encoded by two distinct genes, at least in mammals, which are expressed in numerous tissues. Both receptors, bind all members of the CRH family, albeit with different affinities[97].

Concerning receptor structure, they have an aa homology of about 70%, while exhibiting an approximately 47% divergence at the N-terminal extracellular domain (ECD), a major ligand binding site, which serves to dock peptide ligands via its C-terminal segment. This is consistent with their distinct actions and agonist selectivity, which is important for their unique physiological roles when co-expressed in the same tissue[98]. Early studies identified a number of aa within the ECD region crucial for the binding of $CRHR_1$ receptor agonists and antagonists. Both $CRHR_1$ and $CRHR_2$ ECDs contain a short consensus repeat fold, characteristic of the ECD of class B1 GPCRs and important in activating the receptor by inducing a helix formation towards the N-terminus of the ligand to generate a conformational active state[99,100].

Tissue Distribution

In the brain, UCN-1 expression is most prominent in the Edinger Westphal nucleus and lateral superior olive. UCN-1 mRNA or immunoreactivity has also been reported in other brain regions including the hypothalamus and it seems to be co-localized with dopamine. UCN-1 distribution has also been verified in peripheral tissues such as heart, adrenal gland, skeletal muscles, placenta, skin, immune system, and gastrointestinal tract[101].

UCN-2 has a similar pattern of distribution relative to UCN-1 in the mouse and rat central nervous systems. In peripheral tissues, high levels of UCN-2 have been detected in the heart, adrenal gland, placenta, stomach, skin, ovaries, gastrointestinal tract, uterine smooth muscle, skeletal muscle and peripheral blood vessels[101].

In contrast, UCN-3 exhibits a different distribution from UCN-1 and UCN-2, since it's found predominantly within the hypothalamus and amygdala. Several major UCN-3 terminal fields have been recognized, including the lateral septum and the ventromedial hypothalamus which are known to express high levels of $CRHR_2$, supporting the notion that UCN-3 is an endogenous ligand[101]. In human peripheral tissues, immunoreactive UCN-3 is expressed in the adrenals, heart and kidney (particularly the distal tubules)[102].

Regarding the receptors, $CRHR_1$ is not detected in the heart, while $CRHR_2$ is highly expressed in cardiomyocytes[86]. In the heart, $CRHR_2$ has two splice variants – $CRHR_{2\alpha}$ which is

detected in all chambers of the human heart, and $CRHR_{2\beta}$ which seems to be restricted to the left atrium[86]. This latter isoform is also found in endothelial and SMCs of the systemic vasculature[103]. This observation triggered investigation of UCN-2 as an important physiological peptide in the cardiovascular system.

The half-life of UCN-1 and -2 in humans is approximately 50[104,105] and 10 minutes[92], respectively. The exact half-life of UCN-3 in man is not yet known, but it appears to have a shorter interval of action, at least in healthy sheeps[106].

Intracellular Signaling Pathways

UCN-2 appears to exert its effects mainly through interaction with $CRHR_2$ on target cells, since it shows no appreciable binding affinity for the $CRHR_1$[107]. Upon agonist binding, CRHRs undergo a structural conformation alteration, activating the coupled heterotrimeric G protein which mediates a wide range of intracellular pathways[101].

The CRH family of peptides achieves its physiological effects mainly via activation of the adenylyl cyclase (AC)-cAMP signaling pathway[108], which initiates intracellular events resulting in post-translational modifications of target proteins by protein kinase A (PKA) and/or other kinases, and alteration of gene transcription regulation by cAMP response element-binding (CREB) proteins[109]. However, some studies[88,110] have shown that pharmacological inhibition of the cAMP/PKA pathway failed to abolish the biological effects of CRH and related agonists, suggesting that these peptides and their receptors are able to induce cellular events through alternative signaling pathways, as will be further discussed.

Several studies suggest that signaling transduction by UCN-2 and related peptides, begins by an increase in cAMP-dependent PKA activity[103, 111] and downstream PKA/A-kinase anchoring protein (AKAP) interactions[112]. UCN-2-binding to $CRHR_2$ promotes an increased activation of extracellular-signal-regulated kinase (ERK) 1/2[88, 113] and exchange proteins activated by cAMP (EPAC), which appears to play a role in cAMP-dependent ERK1/2 activation[114, 115]. The phosphatidylinositol-3 kinase (PI3K)/protein kinase B (Akt) pathway is also known to be activated by this peptide[108, 112, 116, 117], and it is particularly important in cardiac and skeletal muscle since it helps regulate phospholamban (PLB) phosphorylation, along with PKA, controlling the inhibition of sarco/endoplasmatic reticulum calcium-ATPase (SERCA)[118].

Another signaling pathway induced by $CRHR_2$ activation is Ca^{2+}/calmodulin-CaMKII, which along with PKA, is important for intracellular Ca^{2+} homeostasis given that they have the

ability to phosphorylate key Ca^{2+}-regulating proteins like the L-type Ca^{2+} channel, the ryanodine receptor and PLB[119]. The activation of these proteins leads ultimately to increased Ca^{2+} influx, sarcoplasmic reticulum (SR) Ca^{2+} content and accelerated $[Ca^{2+}]_i$ transients[119, 120]. UCN-2 also interferes with the opening of K^+ channels, leading to a hyperpolarized state, which increases the driving force for Ca^{2+} entry in the cell[121].

Regarding the NO/cGMP pathway, it seems that, in contrast to $CRHR_1$, $CRHR_2$ activation in human umbilical vein endothelial cells (HUVECs) leads to an increased expression of inducible NOS (iNOS)[122]. In pigs, UCN-2 administration induces NO release via activation of $CRHR_2$[89], leading also to increased Ca^{2+} influx since UCN-2 causes eNOS activation through $CRHR_2$-cAMP and CaMKII-dependent signaling[120].

Recently, the mechanism that leads to eNOS phosphorylation and NO release was established in isolated rabbit ventricular myocytes, where $CRHR_2$ activation through UCN-2 caused an increase in phosphorylation of Akt (Ser473 and Thr308), eNOS (Ser1177) and ERK1/2 (Thr202/Tyr204). It appears that the MEK1/2-ERK1/2 pathway is not required for stimulation of NO signaling in these cells because eNOS phosphorylation was not suppressed by inhibition of MEK1/2. The other two pathways, cAMP-PKA and PI3K-Akt, converge on eNOS phosphorylation and result in pronounced and sustained cellular NO production with subsequent stimulation of cGMP signaling since, when both of these pathways were inhibited, the UCN-2-induced increases in $[NO]_i$ were attenuated[117].

In myocytes, UCN-2 also induces the secretion of both atrial natriuretic peptide (ANP) and BNP from these cells via $CRHR_2$[123]. In SMCs, UCN-induced intracellular cAMP accumulation contributes to increased IL-6 release, and both protein kinase C (PKC) and p38 mitogen-activated protein kinase (MAPK) signaling cascades are involved downstream of this pathway[124]. Furthermore, in neonatal rat cardiomyocytes, this increase in IL-6 release was induced by $CRHR_2$, in a NF-κB-dependent manner[125], indicating that UCNs, specifically UCN-2 and UCN-3, could be important inflammation mediators.

Cells overexpressing both $CRHR_1$ and $CRHR_2$ and treated with sauvagine, a CRH-related peptide, causes PKA-mediated phosphorylation of the transcription factor CREB, which is an important intermediary step in transduction pathways arising from activation of these receptors and leading to modulation of gene transcription of target cells[108]. In addition, receptor stimulation by agonist binding increases activation of ERK1/2 independently of cAMP, revealing the possibility that PKA and MAPK may act in concert to control gene transcription in CRH-responsive cells. Sauvagine is also able to increase intracellular levels of Ca^{2+} through both

mobilization of intracellular stores and influx across the plasma membrane, which are important for muscle contraction and relaxation[108].

Markovic *et al.* showed that $CRHR_{2\beta}$ endocytosis appears to be regulated by ERK1/2 direct phosphorylation of β-$arrestin_1$ in an auto-regulatory mechanism that influences the rate and extent of β-$arrestin_1$ recruitment to the plasma membrane and interaction with $CRHR_{2\beta}$[112]. This mechanism induced AKAP250 translocation to the plasma membrane and interaction with the receptor. Furthermore, this interaction exhibits signaling selectivity since it does not appear to be important for activation of Akt, a mechanism that is mediated via $G_{i/o}$-dependent pathways involving PI3K[112].

UCN-2 differentially regulates nuclear factor of activated T-cells (NFAT) activity in cardiac myocytes from both normal and failing heart through the PI3K/Akt/eNOS/NO pathway[126] (Figure 1).

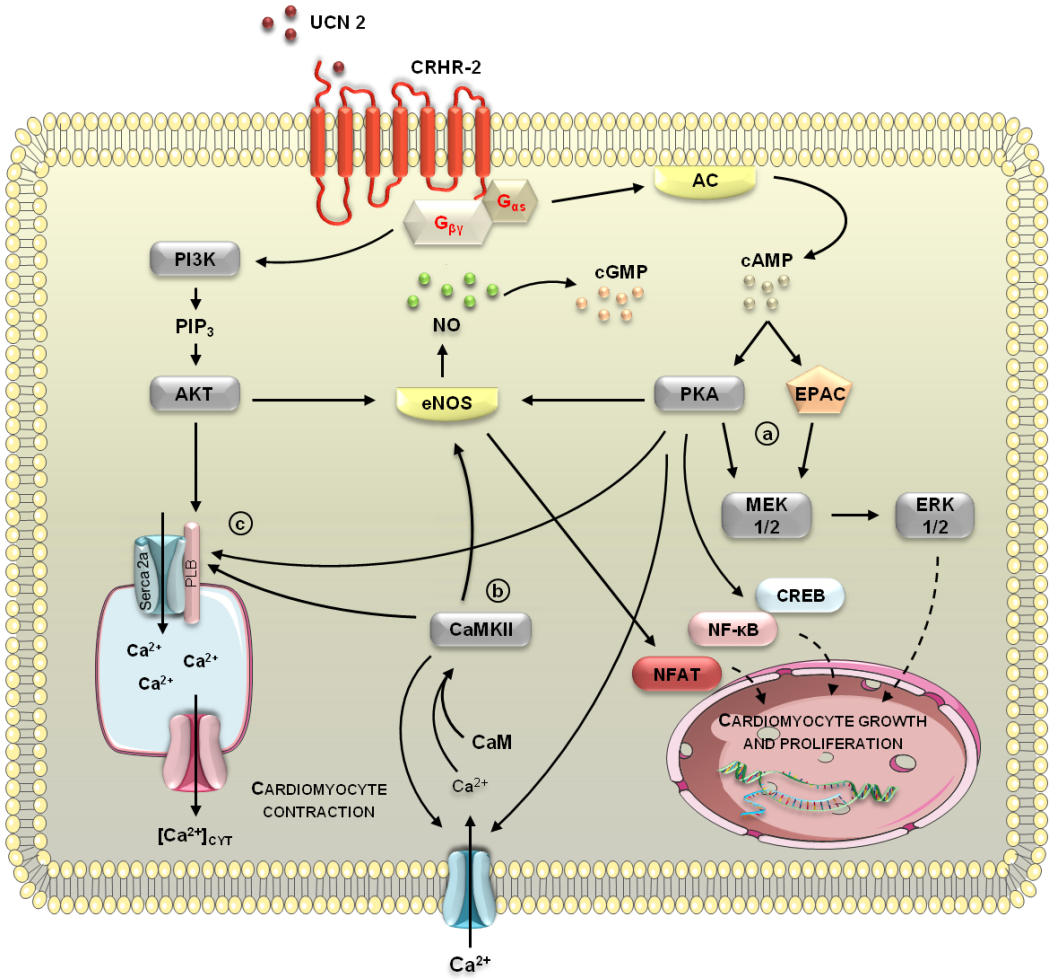

FIGURE 1. Suggested UCN-2/$CRHR_2$ signaling pathway in the cardiomyocyte. UCN-2 regulates cardiomyocyte growth and proliferation (a), homeostasis (b) and function (c). **A)** Upon UCN-2 binding to $CRHR_2$, the activation of AC, by the α-subunit of G protein, results in an increase in cAMP concentration, which promotes an increased activation of PKA and EPAC. This results in post-translational modifications of target proteins, such as ERK1/2, and alteration of gene transcription regulation by CREB and NF-κB. **B)**

The Ca^{2+}/calmodulin-CaMKII, along with PKA, is important for intracellular Ca^{2+} homeostasis, since they have the ability to phosphorylate key Ca^{2+}-regulating proteins, leading to increased Ca^{2+} influx, SR Ca^{2+} content and accelerated $[Ca^{2+}]_i$ transients. The cAMP-PKA and PI3K-Akt signaling pathways converge on eNOS phosphorylation and result in pronounced and sustained cellular NO production with subsequent stimulation of cGMP signaling. **C)** The activation of PI3K, though the βγ subunit of the G protein, leads to Akt activation which helps regulate PLB phosphorylation, along with PKA, controlling the inhibition of SERCA. NFAT regulation is mediated by PI3K/Akt/eNOS/NO signaling cascade that converges on the activation of several kinases, including GSK-3β, JNK, p38 and PKG, resulting in phosphorylation, deactivation and nuclear export of NFAT.

Abbreviations: AC, adenylate cyclase*;* cAMP*,* cyclic adenosine monophosphate; PKA, protein kinase A; EPAC, exchange proteins activated by cAMP; MEK1/2, mitogen-activated protein kinase; ERK1/2, extracellular signal-regulated kinase; CREB, cAMP response element-binding protein; NF-κB, nuclear factor kappa-light-chain-enhancer of activated B cells; eNOS, endothelial nitric oxide synthase; NO, nitric oxide; cGMP, cyclic guanosine monophosphate; CaM, calmodulin; CaMKII, Ca^{2+} /calmodulin-dependent protein kinase II; PI3K, Phosphoinositide 3-kinase; PIP3, Phosphatidylinositol (3,4,5)-trisphosphate; AKT, protein kinase B; Serca 2a, sarco/endoplasmic reticulum Ca^{2+}-ATPase; PLB, phospholamban; UCN-2, Urocortin-2; $CRHR_2$, corticotropin releasing hormone receptor type 2; NFAT, nuclear factor of activated T-cells; GSK-3β, glycogen synthase kinase 3 beta; JNK, c-Jun NH2-terminal kinase; p38, p38 mitogen-activated kinase; PKG, protein kinase G.

UCN-2/$CRHR_2$ Signaling Effects in Cardiac Function

The majority of the described actions of UCNs in the myocardium have been revealed by observations in cardiomyocytes and in animal models of heart failure. However, it is not completely clear if the protective effects of UCNs are mediated via a direct effect on cardiac myocytes or via sympathetic stimulation in reaction to decreased peripheral resistance[127].

In both rabbit[128] and mouse ventricular myocytes[119], as well as in a murine model of HF[129], UCN-2 administration enhances myocardial inotropy and lusitropy in a time- and concentration-dependent manner. These effects appear to be mediated via activation of $CRHR_2$ and subsequent stimulation of both cAMP/PKA and Ca^{2+}/calmodulin-CaMKII signaling pathways since they were abolished by antisauvagine-30, a specific $CRHR_2$ antagonist, leading to increased SR Ca^{2+} content and $[Ca^{2+}]_i$ transients, as well as an accelerated decay of the latter[119, 128]. However, in mouse cardiomyocytes, these effects were accompanied by arrhythmogenic events, triggered by spontaneous diastolic SR Ca^{2+} release[119]. On the other hand, UCN-2 is reported to increase the ventricular fibrillation threshold[130] and reduce the occurrence of arrhythmias[131] *in vivo*. Evidence of the UCNs actions to improve intracellular handling[132] and perhaps inhibit efferent cardiac sympathetic nerve activity[133], might explain the peptide's anti-arrhythmic effects in the whole animal. Other beneficial cardiac effects of UCNs include their ability to improve cardiac bioenergetics (through preservation of high-energy phosphate stores)[134].

In the pig, local intracoronary administration of UCN-2 also has the ability to increase coronary blood flow as well as myocardial function[89]. In addition, an immediate improvement of left ventricular fractional shortening and circumferential fiber shortening velocity after an

acute injection of UCN-2 has been described in rats. These positive effects were maintained even at 5 weeks after treatment[135].

Recently, Walther *et al.* demonstrated that UCN-2 differentially regulates NFAT activity in cardiac myocytes from both normal and failing hearts, having a crucial role in the regulation of gene expression in cardiac development, maintenance of an adult differentiated cardiac phenotype and remodeling processes[126].

UCN-2/CRHR$_2$ Signaling Effects in Vascular Function

UCN-2/CRHR$_2$ system effects are not limited to the heart, since in both pulmonary and systemic vasculature the activation of this receptor and the following pathway seems to exert a potent and consistent relaxation of the vessels.

In rat thoracic aorta, UCN-2 and -3 wield more potent vasodilator effects than CRH, and since this relaxation response was abolished in the presence of both AC and PKA inhibitors, this effect is likely to be mediated by signaling pathways involving these peptides[136].

Indeed, in both healthy[137] and animal models of HF[129], UCN-2 administration causes a reduction in arterial blood pressure. Furthermore, the selective CRHR$_2$ antagonist, astressin$_2$-B, abolished UCN-2-induced hypotensive activity while having no effect on basal arterial blood pressure, indicating that UCN-2 induces hypotension through peripheral CRHR$_2$[137]. Dieterle *et al.* also showed an immediate and sustained lowering of blood pressure in hypertensive rats, with no reflex rise in HR[135]. Several mechanisms have been postulated for the blood pressure-lowering effects of the UCNs, including a direct smooth muscle relaxant effect in combination with an associated reduction in plasma concentrations of vasoconstrictor hormones. Grossini *et al.* showed that UCN-2 administration in the anaesthetized pig primarily increases coronary blood flow and myocardial function through the release of NO and activation of CRHR$_2$. In this study, the blockade of NOS abolished only the coronary effects, whereas blockade of subtype 2 of the CRH receptors abolished both cardiac and coronary effects[89].

Ex vivo studies in human internal mammary artery[138] and in rat coronary artery[139] propose both endothelium-dependent and -independent mechanisms for vasorelaxation, which involves the release of NO that in turn stimulates Ca^{2+}-activated K^+ channels in vascular smooth muscle via cGMP-dependent pathways[138].

Additionally, another important role for the UCN-2/CRHR$_2$ system is its contribution to the angiogenesis process, being a critical component of the pathway necessary for tonic

inhibition of adult neo-vascularization. Bale *et al.* demonstrated that mice deficient in $CRHR_2$ become hypervascularized postnatally. On the other hand, the activation of this receptor *in vitro* results in reduced release of VEGF from SMCs, inhibition of SMC proliferation and inhibition of capillary tube formation in collagen gels[140].

Recently, Emeto *et al*. reported that in human aortic vascular SMCs, UCN-2 significantly inhibited Akt phosphorylation and proliferation in a dose-dependent manner by promoting a G_1 cell-cycle arrest, reinforcing the role of UCN-2 in the regulation of cell proliferation[141]. Moreover, endothelial UCN has potent antioxidative properties and is up-regulated by inflammatory cytokines and pitavastatin[142].

UCN-2/CRHR$_2$ Signaling Effects in Heart Failure

Given the potent vasorelaxant and inotropic effects of UCN-2, interest has grown in its role in the pathophysiology of HF and its potential therapeutic value in this disease. Several studies with UCN-2 in different animal models and in human clinical studies have demonstrated the beneficial effects of the peptide in the setting of cardiac failure.

In both adult rabbit ventricular myocytes[128] and in a murine model of HF[129], UCN-2 administration enhanced myocardial inotropy and lusitropy, increasing cell shortening and accelerating relaxation in a time- and concentration-dependent manner. These effects are induced via $CRHR_2$ receptor-mediated stimulation of PKA[128].

In contrast to limited UCN-2 bioactivity in healthy sheep, the therapeutic administration in animals with pacing-induced HF induced rapid and dose-dependent increases in CO and reductions in peripheral resistance and left atrial pressure[90]. The prolonged administration of UCN-2 in the same animal model also produced the beneficial effects seen above, except in a sustained way of action[143], supporting a role for UCN-2 in pressure/volume homeostasis in HF. Additionally, UCN-2 co-treatment with an existing proven treatment such as furosemide, a diuretic agent, resulted in enhancement of beneficial hemodynamic effects compared with either agent alone, together with augmented renal responses with less rennin activation and no exacerbation of potassium loss[144].

UCN-2/CRHR$_2$ Signaling Effects in Myocardial Ischemia

Myocardial ischemia frequently leads to cardiomyocyte apoptosis and necrosis, even with subsequent restoration of blood flow to the affected area, which has caused research to focus on trying to prevent cardiomyocyte death after an ischemic event. In this context, UCNs appear to have a cardioprotective role with increased expression and peptide release observed following ischemia stimulation[145].

On the other hand, neonatal cardiomyocytes treated with either 1-10nM of UCN-2 or -3 results in ERK1/2 phosphorylation, and the inhibition of MEK 1/2 obstructs their cardioprotective effects[88]. Brar *et al.* suggested that UCN-2 and -3 have a cardioprotective role in situations of ischemia/reperfusion injury acting via the MAPK pathway and reducing infarct size[88].

Moreover, as mentioned above, CRHR$_2$-deficient mice become hypervascularized postnatally and the activation of this receptor reduces VEGF release from SMCs, suppresses SMC proliferation and impedes capillary tube formation[140]. These studies demonstrate a critical role for CRHR$_2$ in the regulation of angiogenesis and remodeling of both juvenile and adult vasculature, suggesting this receptor may be a potential target to modulate angiogenesis in diseases such as cardiovascular ischemia.

UCN-2/CRHR$_2$ Signaling Effects in Other Cardiovascular Diseases

Dieterle *et al*. reported that chronic UCN-2 treatment was able to improve cardiac and vascular function through an immediate sustained blood pressure reduction without affecting the HR. Furthermore, long-term UCN-2 treatment in hypertensive rats diminishes the development of hypertension-induced LV hypertrophy and the deterioration of its contractile function[135]. Moreover, long-term UCN treatment not only had hypotensive effects but may also inhibited development of vascular remodeling in mesenteric arteries in spontaneously hypertensive rats[146]. These beneficial effects of UCN-2 may represent a novel approach for antihypertensive therapy.

In a recent study, patients who underwent coronary angiography with the pre-diagnosis of coronary artery disease were examined and distributed according to their ejection fraction (EF). Those patients with moderate to severe systolic dysfunction (SD) showed decreased serum UCN-2 levels, while patients with mild to moderate SD showed increased levels of the peptide when compared to patients without SD. In contrast, the presence of diastolic

dysfunction or coronary artery disease appeared to have little effect on circulating UCN-2 concentrations[147].

Urocortin-2 as a Therapy for Heart Failure in Humans

Recently, a small number of clinical studies in humans have confirmed some data obtained from animal studies. In fact, UCN-2 administration in healthy humans induces a dose-related increase in CO, HR and left ventricular ejection fraction (LVEF) in association with decreased systemic vascular resistance[92]. Moreover, UCN-2 and -3 promotes a potent prolonged arterial vasodilatation without causing tachyphylaxis, with these effects being partly dependent on endothelial NO and cytochrome P450 metabolites of arachidonic acid[148].

In humans with both mild[149] and acute decompensated HF[91], UCN-2 administration resulted in a markedly augmented CO without significant reflex tachycardia and an improved vascular function. Pronounced falls in systemic arterial pressure were also seen with higher doses of UCN-2[91]. UCN-2 also induced vasorelaxation of coronary arteries isolated from patients with HF, independently of endothelial integrity[150]. In addition to positive effects on cardiovascular parameters when used as a treatment in HF, UCNs may also serve as possible biomarkers in the identification of early HF[151].

Based on these clinical studies, detailed in Table 6, it appears that UCN-2, alone or in combined therapy, is able to regulate the cardiovascular system which points towards a therapeutic application for this peptide in HF.

TABLE 6. Clinical trials with Urocortin-2 as a therapy for Heart Failure

Refs	Model	Treatment	Outcome
92	8 Healthy humans	Subjects received placebo, 25µg and 100µg of UCN-2 intravenously over the course of 1h.	↑ Cardiac output; ↑ Heart rate; ↑Left ventricular ejection fraction; ↓ Systemic vascular resistance.
148	18 Healthy humans	Volunteers were subjected to a bilateral forearm venous occlusion plethysmography during intra-arterial UCN-2 (3.6-120pmol/min), UCN-3 (1.2-36nmol/min) and substance P (2-8pmol/min).	Potent and prolonged arterial vasodilatation without tachyphylaxis.
149	8 Male patients with HF	Received placebo and 25µg and 100µg of UCN-2 intravenously over 1h.	↑ Cardiac output; ↑ Left ventricular ejection fraction; ↓ Mean arterial pressure; ↓ Systemic vascular resistance; ↓ Cardiac work.

Other Biological Effects of Urocortin-2

UCN-2 is also expressed in the central nervous system and it seems to be involved in the regulation of the stress response, anxiety and depression[152], as well as in the control of appetite[98]. Male, but not female, UCN-2-knockout animals demonstrate an altered social behavior, with more passive social interactions and reduced aggressiveness in comparison to wild-type animals. Moreover, UCN-2 appears to modulate the aggressive behavior in male mice[153] further evidence that this peptide is involved in the regulation of stress-related behaviors.

In terms of appetite control, a recent study has reported that $CRHR_1$ agonists, UCN-1 and $stressin_1$-A, reduced feeding and induced interoceptive stress, while UCN-2 had a more potent suppressive effect on feeding, via a $CRHR_2$-dependent mechanism, without eliciting malaise[154]. UCN-2 also appears to be responsible for a decrease in gastric emptying[152] which aids in appetite inhibition. These differences between UCNs in their regulation of these various functions seem to be consistent with their pharmacological differences.

AIMS

Based on the published findings referenced in the previous chapter, we hypothesize that by activating $CRHR_2$ in animals with PAH, through UCN-2 administration, we might protect not only the pulmonary vasculature, but also the RV myocardium and thus increase animal survival, attenuate PAH severity and improve RV function.

Therefore, we purpose to investigate the role of the UCN-2/$CRHR_2$ system in the pathophysiology of PAH and progression to HF, while evaluating the efficacy of UCN-2 as a possible novel therapeutic strategy for this disease.

Our specific goals are:

1. to determine changes in the expression of UCN-2 and its receptor, and of downstream signaling pathways in the heart tissue from healthy rats and from rats with PAH induced by monocrotaline (MCT);
2. to assess changes in animal survival, RV myocardial function and the severity of PAH *in vivo* (hemodynamic and echocardiographic studies), changes in myocardial structure and histology and its patterns of gene expression, in healthy animals and in animals with PAH and HF with or without chronic UCN-2 treatment.

METHODS

All the procedures in this work followed the recommendations of the Guide for the Care and Use of Laboratory Animals, published by the US National Institutes of Health (NIH Publication No. 85-23, Revised 1996), and are accredited by the Portuguese Direção Geral de Alimentação e Veterinária (DGAV) and approved by Fundação para a Ciência e a Tecnologia (FCT PTDC/DTP-FTO/0130/2012).

Animal Model

Animals were grouped 3 per cage, in a controlled environment with a light-darkness cycle of 12:12h and an established temperature of 22ºC, with water and food *ad libitum*. Before MCT administration an echocardiographic evaluation was performed as a guarantee that the potentially ill animals (with cardiac disease) did not follow the protocol. Between 24 to 25 days after MCT administration, the animals were submitted again to an echocardiographic study and to invasive hemodynamic evaluation. After morphometric assessment, samples were collected and processed for histological and molecular biology studies.

Seven week-old male Wistar rats (Charles River Laboratories, Barcelona, Spain) weighing 180-200g, were randomly assigned to receive either a subcutaneous (s.c.) injection of MCT (60mg/kg, Sigma-Aldrich) or an equal volume of vehicle, sodium chloride (NaCl, B. Braun, 0.9%). A freshly aqueous solution of MCT was prepared, wherein 300mg was dissolved in 2.36mL of 1M HCl, diluted with distilled water to about 1.60mL and neutralized with 1.52mL of 1M NaOH. The pH was settled at 7.00.

Fourteen days after MCT/vehicle administration, animals were randomly assigned into 4 subgroups: CTRL, untreated animals; MCT, animals with induced PAH and without pharmacological treatment; CTRL + UCN-2, animals without PAH and with UCN-2 treatment; MCT + UCN-2, animals with induced PAH and with UCN-2 treatment. The pharmacological treatment consisted on a daily intraperitoneal (i.p.) injection of 2.5µg/kg twice a day of hUCN-2 (Bachem, Bubendorf, Switzerland) during 10 days, while the vehicle treatment consisted on sodium chloride.

The drug dosages, administration routes and treatment duration were selected based on previous studies from other research teams[135] and on our preliminary dose-finding studies (unpublished data). Moreover and according with Reagan-Shaw's equation[155] (depicted below in which *animal km=37* and *human km=6*) the UCN-2 dose administered in our animals is the

same that has been used in human clinical trials[92, 149]. Initially an aqueous solution of hUCN-2 was prepared by dissolving 1mg in 1mL of NaCl. Part of the stock was diluted again in NaCl until we reach a final work concentration of 0.002mg/mL.

$$Human\ equivelent\ dose\ (mg/kg) = Animal\ dose(mg/kg) \times \frac{Animal\ Km}{Human\ Km}$$

Functional Studies

Cardiac function was evaluated both in healthy and MCT-induced PAH animals, with or without pharmacological treatment, in order to clarify the involvement of UCN-2/$CRHR_2$ system not only in the pathophysiology of PAH, but also in the progression of functional RV changes that accompany PAH and lead to HF.

The echocardiographic assessment allowed for a non-invasive monitoring and characterization of PAH progression and ventricular function in the different experimental groups. Invasive hemodynamic evaluation was performed using high-fidelity pressure-volume catheters that provided us an accurate determination of systolic and diastolic function parameters.

Echocardiography Studies

For this purpose, animals from the different experimental groups were sedated with 100µg/kg fentanyl and 5mg/kg midazolam via i.p. injection and anesthetized by inhalation of 8% sevoflurane (Penlon Sigma Delta, UK) in vented containers. Endotracheal intubation was performed using a 14 gauge catheter and mechanical ventilation controlled by a rodent ventilator (MouseVent G500, Kent Scientific, Connecticut, USA) with an animal weight-defined tidal volume. Anesthesia was maintained with 2.5-3.0% vol/vol sevoflurane, titrated according to the toe pinch reflex.

Animals were placed in left lateral decubitus. After applying warm echocardiography gel, a 15MHz sensorial probe (Sequoia 15L8W) was gently placed on the thorax. Acquisitions (Siemens Acuson Sequoia C512) were averaged from three consecutive heartbeats. Bi-dimensional and M-mode images were obtained for determination of RV structure and function, respectively. End-diastolic dimension (RVEDD), RAA and TAPSE were obtained in apical projection of 4 cavities. Pulmonary artery diameter (PAD) was measured in parasternal short-axis view. Conventional Doppler was used to evaluate pulmonary blood flow, with the

determination of pulmonary artery acceleration (PAAT) and ejection (PAET) times, peak systolic velocity (PAPSV) and the velocity time integral (PAVTI). The PAAT/PAET ratio was determined, and the SV, CO and cardiac index (CI) were calculated as follows:

$$SV_{(mL)} = PAVTI \times \left[\pi \left(\frac{PAD}{2}\right)^2\right]$$

$$CO_{(mL/min)} = SV \times Heart\ Rate$$

$$CI_{(mL/min/100g)} = \frac{CO}{Body\ weight \times 100}$$

Invasive Hemodynamic Evaluation

After the echocardiographic evaluation, and as previously described[156], the animal position was adjusted to right lateral decubitus for proper orientation of the heart for instrumentation. Animal temperature was monitored and regulated with a warming pad and a rectal temperature sensor, and digitally controlled together with pulse oxymetry measured through a paw sensor (PhysioSuite, Kent Scientific, Connecticut, USA), and ECG (Animal Bio Amp, ADinstruments, Oxford, UK) (shown in Figure 5A). Anesthesia was maintained with sevoflurane (2.5-3.0% vol/vol).

The internal femoral vein was catheterized using a 24G catheter, under surgical microdissection (Wilde M651, Leica microsystems, Cambridge, UK) for infusion (Multi-Phaser, NE-100, New Era Pump Systems, NY, USA) of warm lactate Ringer's solution at a rate of 32mL/kg/h (Figure 5B and 5C). A left thoracotomy was performed, pericardium and pleura were carefully dissected and the phrenic nerve was severed (Figure 5D). A 3-0 surgical silk was passed around the inferior vena cava (IVC) for transient occlusion during the protocol. Pressure-volume catheters were inserted through the apex of the RV and positioned along the long axis (SPR-869, Millar Instruments, Texas, USA). A flow probe was implanted around the ascending aorta (MA2.5PSB, 2.5mm, Precision S-Series, Transonic Systems, NY, USA) and connected to an ultrasonic transit time volume flowmeter (TS420, transit-time perivascular flowmeter, Transonic Systems, NY, USA). The experimental preparation was allowed to stabilize for 15 minutes, and during the procedure blood loss was controlled through saline bolus.

Baseline and IVC occlusions recordings were obtained with ventilation suspended at end-expiration. Pressure and volume signals were continuously acquired (MVPS 300, Millar instruments, Texas, USA), digitally recorded at a sampling rate of 1000Hz (ML880 PowerLab

16/30, ADInstruments, Oxford, UK) and analyzed off-line (LabChart 7 Pro, ADInstruments, Oxford, UK, and PVAN 3.5, Millar Instruments, Texas, USA). Parallel conductance for the volume catheter was computed after bolus injection of 50µL hypertonic saline (10% sodium chloride) and the calibration for factor alpha (field inhomogeneity) was determined through the CO measured by the aortic flow probe and the ultrasonic transit time volume flowmeter.

Following anesthetic overdose, blood was retrieved for storage and further analysis. Animals were exsanguinated and heparinized blood was collected and used for volume calibration with standard cuvettes (P/N 910-1048, Millar Instruments, Texas, USA).

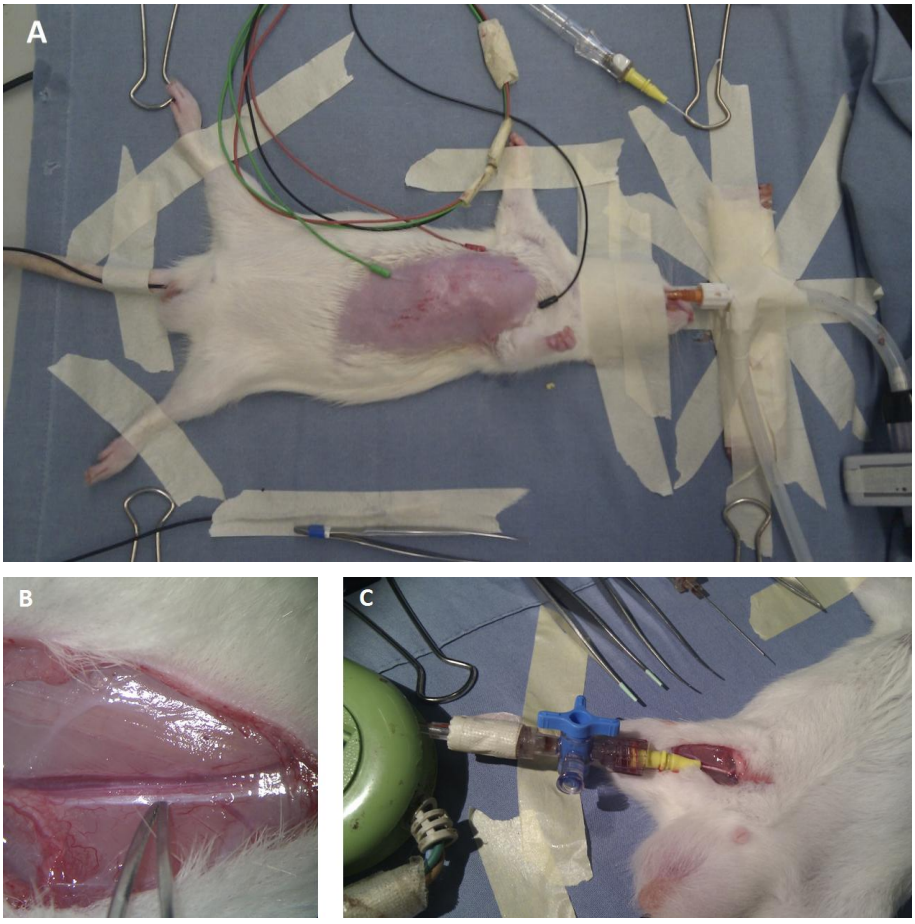

FIGURE 2. Preparation of the rat for the hemodynamic evaluation. **A)** Position of the rat for the hemodynamic instrumentation, **B)** femoral vein exposure and dissection and **C)** IV catheter placement and **D)** thorax exposure after left thoracotomy.

The baseline hemodynamic parameters analyzed were: HR, CO, RV end-systolic (ESP) and end-diastolic (EDP) pressure, end-diastolic volume (EDV), SV, EF and the isovolumic relaxation constant (τlog). IVC occlusion-derived end-systolic (ESPVR Ees) and end-diastolic (EDPVR k1) pressure volume relantionship slopes were also determined. PVR was calculated as follows:

$$PVR = ESP/CO$$

Morphometric and Histological Analysis

RV structural alterations, such as hypertrophy, are associated with PAH-progression[157], therefore morphometric and histological analysis was mandatory in this context.

Immediately after exsanguination of the anesthetized/instrumented animal, heart, lungs, liver and gastrocnemius were excised and weighted. RV and LV + Septum (LV+S) were carefully dissected and weighted separately. Although tissue weight is usually normalized to the animal body weight, HF is associated with cachexia[158] and therefore, normalizing tissue weights of MCT-injected animals might lead to an overestimate of cardiac hypertrophy. In order to eliminate bodyweight as a confounding factor in tissue weight normalization, tibia length, which remains constant throughout adulthood, was measured and served as a normalizer[159].

Samples for histology were submersed in a fixative solution of 10% formaldehyde. After the initial fixation step, samples underwent dehydration (using ethanol in decreasing

percentages), diaphanisation (using xylene) and impregnation in liquid paraffin (54ºC). Later they were placed and properly oriented in metal molds and serial sections of 4µm were obtained from RV samples, in a Minot-type microtome. Hematoxylin and eosin (HE) stained sections of the RV were used to measure cardiomyocyte cross-sectional area. Sections were digitally photographed (Olympus XC30 Digital colour Camera, Olympus, PA, USA) and measured using imaging software (cell^{B}, Olympus, PA, USA). Fifty muscle fibers per animal were analyzed and only nuclei-centered cardiomyocyte were considered for analysis of cardiomyocyte dimensions.

Molecular Studies

These studies focused on the gene expression and protein activation analysis of the main components of UCN-2/$CRHR_2$ system (peptide, receptors and downstream signaling pathways) as well as of known markers of heart failure in the different experimental groups.

mRNA Expression

In order to allow posterior molecular analysis, RV samples were collected and stored in RNAlater (Quiagen), frozen in liquid nitrogen and kept at -80ºC until manipulation. RNA was completely extracted by the silicon membrane and guanidinium-thiocyanate method (RNeasy Mini Kit, Quiagen, 74104), according to the manufacturer's instructions. Concentration and purity of RNA were measured by NanoDrop® ND-1000 spectrophotometer (Thermo Fisher Scientific), assuming as ideal ratio values of A260/A280 between 1.8 and 2.1. mRNA relative expression quantification was performed by two-step Real-Time Polymerase Chain Reaction (RT-PCR). Using animal samples from the CTRL group, standard curves were built to all the studied genes and tissues, correlating the initial total mRNA quantity and the threshold cycle. Reverse transcription was performed in a conventional thermocycler (Whatmann Biometra, 050-901) and consisted in 10 minutes at 22ºC, 50 minutes at 50ºC, and 10 minutes at 95ºC. Ten percent of the obtained cDNA was amplified and detected by RT-PCR (Step-One™ Applied biosystems) using the probe SYBR Green (PerfeCta® SYBR Green FastMix, Rox, Kit, Quanta Biosciences) according to the manufacturer's instructions.

Amplification curves were analyzed with the equipment software (v2.2.2) through absolute quantification. Melting curves of each PCR reaction were used in order to exclude the formation of primer-dimers and unspecific products, confirming the purity of the amplified

product. GAPDH was chosen as reference gene, since no significant changes were observed in the different groups. Final gene expression results were presented in Arbitrary Units (AU), being the CTRL group means values after GAPDH normalization correspondent to 1AU. All assays were performed twice, in order to ensure the security of the obtained results. The primers used in the molecular analysis (Table 7) were designed in-house with appropriate software (DNAstar™).

TABLE 7. List of used primers

Gene	Primers Sequence
GAPDH	P_1- $^{5'}$TGG CCT TCC GTG TTC CTA CCC$^{3'}$ P_2- $^{5'}$CCG CCT GCT TCA CCA CCT TCT$^{3'}$
UCN-2	P_1- $^{5'}$CGT TGG CAT AAC GCC TCA C$^{3'}$ P_2- $^{5'}$GGA CAC AGA GCT GGG AGT TG$^{3'}$
$CRHR_2$	P_1- $^{5'}$TGC AAC TCA TCG ACC ACG AA$^{3'}$ P_2- $^{5'}$CAG GTA GCA GCC TTC CAC AA$^{3'}$
ET-1	P_1- $^{5'}$CGG GGC TCT GTA GTC AAT GTG$^{3'}$ P_2- $^{5'}$CCA TGC AGA AAG GCG AAT GTG$^{3'}$
BNP	P_1- $^{5'}$CAG AGC TGG GGA AAG AAG AG$^{3'}$ P_2- $^{5'}$GGA CCA AGG CCC TAC AAA AGA$^{3'}$
HIF-1α	P_1- $^{5'}$TCA TAG GCG GTT TCT TGT AGC$^{3'}$ P_2- $^{5'}$CTA ACA AGC CGG AGG AC$^{3'}$
Caspase-3	P_1- $^{5'}$CGG GTG CGG TAG AGT AAG$^{3'}$ P_2- $^{5'}$CTG GAC TGC GGT ATT GAG ACA$^{3'}$
Caspase-8	P_1- $^{5'}$ACC AAA TGA AGA GCA AAC CTC G$^{3'}$ P_2- $^{5'}$TTT TCT GTC CCG CAT GTT GC$^{3'}$

Abbreviation: BNP, brain natriuretic peptide; $CRHR_2$, corticotrophin-releasing hormone receptor type 2; ET-1, endothelin 1; GAPDH, glyceraldehyde 3-phosphate dehydrogenase; HIF-1α, hipoxia inducible factor 1 alpha; UCN-2, urocortin-2.

Protein Expression

Samples from RV of each animal were homogenized on ice in 300µL RIPA lysis buffer (Cell Signaling Technology) containing protease inhibitors (Protease Inhibitor Cocktail, Sigma-Aldrich, St. Louis, USA), and phosphatase inhibitors (Phosphatase Inhibitor Cocktail 2 and 3, Sigma-Aldrich, St. Louis, USA). Tissue was then centrifuged at 12.000 RPMs for 20 min at 4°C. Supernatants were collected, and total protein concentration was determined using the Bradford assay (Bio-Rad Laboratories, CA, USA). Samples were treated with Laemmli loading buffer (Cell Signaling Technology) and boiled for 5 minutes at 95ºC. Samples, with 20µg of protein, were loaded onto a 10% SDS-PAGE gel (Bio-Rad Laboratories, CA, USA), run, and electroblotted onto a 0.2µm nitrocellulose membrane (Bio-Rad Laboratories, CA, USA). Pre-

stained molecular weight marker proteins (Bio-Rad Laboratories, CA, USA) were used as size standards for the SDS-PAGE. Ponceau staining was performed to verify the quality of the transfer and to ensure equal protein loading. Blots were blocked in 5% BSA (Bovine Serum Albumin, Sigma-Aldrich, St. Louis, USA) for 1 hour at room temperature. Incubated overnight at 4ºC with the antibodies listed in Table 8, in separate experiences, at a dilution of 1:1000.

TABLE 8. List of used primary antibodies

Protein	Antibody's Identification
Akt	Akt (pan) (C67E7), Rabbit mAb, Cell Signaling Technology
p-Akt	Phospho-Akt (Ser473) (587F11), Mouse mAb, Cell Signaling Technology
ERK1/2	p44/42 MAPK (Erk1/2) (3A7), Mouse mAb, Cell Signaling Technology
p-ERK1/2	Phospho-p44/42 MAPK (Erk1/2) (Thr202/Tyr204), Rabbit pAb, Cell Signaling Technology
p38	p38α MAPK (L53F8), Mouse mAb, Cell Signaling Technology
p-p38	Phospho-p38 MAPK (Thr180/Tyr182) (D3F9), Rabbit mAb, Cell Signaling Technology
$STAT_3$	Stat3 (124H6), Mouse mAb, Cell Signaling Technology
p-$STAT_3$	Phospho-Stat3 (Tyr705) (D3A7), Rabbit mAb, Cell Signaling Technology
$CRHR_2$	Anti-Corticotropin Releasing Factor Receptor 2, Rabbit pAb, Abcam, Cambridge, UK
GAPDH	GAPDH (0411), Mouse mAb, Santa Cruz Biotechnology, Inc.

Abbreviation: Akt, protein kinase B; $CRHR_2$, corticotropin-releasing hormone receptor type 2; ERK1/2, extracellular-signal regulated kinases 1 and 2; GAPDH, glyceraldehyde 3-phosphate dehydrogenase; GSK-3β, glycogen synthase kinase 3 beta; p38, p38 mitogen-activated protein kinase; $STAT_3$, signal transducer and activator of transcription 3.

After primary antibody removal, membranes were washed with Tris-Buffered Saline (Cell Signaling Technology) with 0.01% Tween-20 – TBS-T (Sigma-Aldrich, St. Louis, USA) and incubated with secondary antibodies (IRDye 680LT, Goat-anti-Mouse Ab and 800CW, Goat-anti-Rabbit Ab, LI-COR Biosciences, Lincoln, USA) in 2% skimmed nonfat milk at a 1:25000 dilution for 1 hour at room temperature. After washing the membranes with TBS-T, membranes were scanned using an Odyssey scanner (infrared imaging system, LI-COR Biosciences, Lincoln, USA) and analyzed using the Odyssey provided software (version 3.0).

Statistical Analysis

Statistical analysis was performed using *GraphPad Software* (vs.6). 2-way ANOVA was used to statistically analyze all the presented parameters. Holm-Sidak's method for post hoc comparisons between groups and Kaplan-Meier survival analysis (log-rank test) were

performed. Group data are presented as means ± SEM. Differences with $p<0.05$ were considered statistically significant.

RESULTS

Survival Analysis

Excluding animals that underwent terminal hemodynamic evaluation, Kaplan-Meier analysis demonstrated that the survival rate for MCT treated animals was significantly higher (76%) when compared with MCT untreated animals (44%) as is demonstrated in Figure 3.

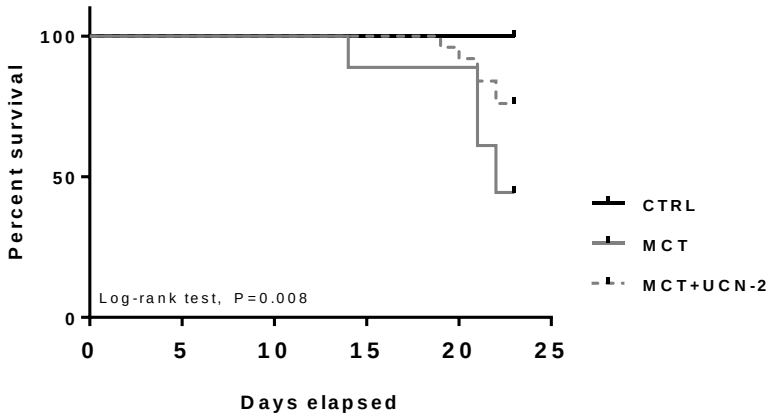

FIGURE 3. Kaplan-Meier survival curves. MCT rats treated with UCN-2 had a significantly higher survival rate than MCT rats (log-rank test, P=0.008). CTRL (n=13); CTRL+UCN-2 (n=10); MCT (n=10) and MCT+UCN-2 (n=15).

Functional Studies

Echocardiographic Evaluation

The full echocardiographic study is presented in Table 9. The bi-dimensional analysis showed that MCT-treated animals developed RH dilation, as shown by an increase in RV end-diastolic diameter (RVEDD) and right atria area (RAA), as well as a deviation of the interventricular septum (IVS) towards the left side of the heart (Figure 4B), while treatment attenuated RH structural alterations (Figure 4C). Echo-measured RV function was also improved with UCN-2 treatment, as measured by M-mode through the tricuspid annular plane systolic excursion (TAPSE), which was decreased in MCT animals.

Doppler imaging analysis revealed a deficit in the pulmonary flow in the MCT group with decreased peak systolic velocity (PAPSV), pulmonary artery acceleration time (PAAT) and ejection time (PAET), when compared with healthy animals, which affected the PAAT/PAET ratio. Treatment with UCN-2 improved blood flow in the pulmonary artery, with normalization of the PAAT/PAET ratio. Moreover, indexes of overall cardiac function, such as CO and CI, were also improved with pharmacological UCN-2 intervention.

TABLE 9. Echocardiographic evaluation

Echocardiographic Parameters	CTRL		MCT	
	Vehicle	UCN-2	Vehicle	UCN-2
PAPSV (m/s)	0.98 ± 0.06	0.96 ± 0.04	0.79 ± 0.03*	0.80 ± 0.04*
PAAT (ms)	25.7 ± 2.61	31.7 ± 1.87*	13.6 ± 0.57*	20.0 ± 1.11$^{\#}$
PAET (ms)	81.8 ± 2.46	78.3 ± 1.43	68.3 ± 1.69*	75.9 ± 1.79$^{\#}$
RAA (cm^2)	0.17 ± 0.01	0.20 ± 0.02	0.30 ± 0.03*	0.22 ± 0.01$^{\#}$
RVEDD (cm)	0.39 ± 0.01	0.37 ± 0.01	0.50 ± 0.01*	0.45 ± 0.01*$^{\#}$
TAPSE (cm)	0.23 ± 0.01	0.25 ± 0.01	0.12 ± 0.02*	0.18 ± 0.01*$^{\#}$
PAAT/PAET	0.28 ± 0.04	0.40 ± 0.02*	0.20 ± 0.01*	0.26 ± 0.01$^{\#}$
CO (mL/min)	168 ± 22.4	176 ± 14.0	86.3 ± 14.7*	137 ± 10.4*$^{\#}$
CI (mL/min/100g BW)	56.4 ± 7.1	59.6 ± 5.1	33.1 ± 4.6*	52.3 ± 3.9$^{\#}$

CTRL (n=13); CTRL+UCN-2 (n=10); MCT (n=10) and MCT+UCN-2 (n=15). **Abbreviations:** BW, body weight; CI, cardiac index; CO, cardiac output; PAAT, pulmonary artery acceleration time; PAET, pulmonary artery ejection time; PAPSV, pulmonary artery peak systolic velocity; RAA, right atria area; RVEDD, right ventricle end-diastolic diameter; TAPSE, tricuspid annular plane systolic excursion. *p<0.05 vs CTRL, $^{\#}$p<0.05 vs MCT.

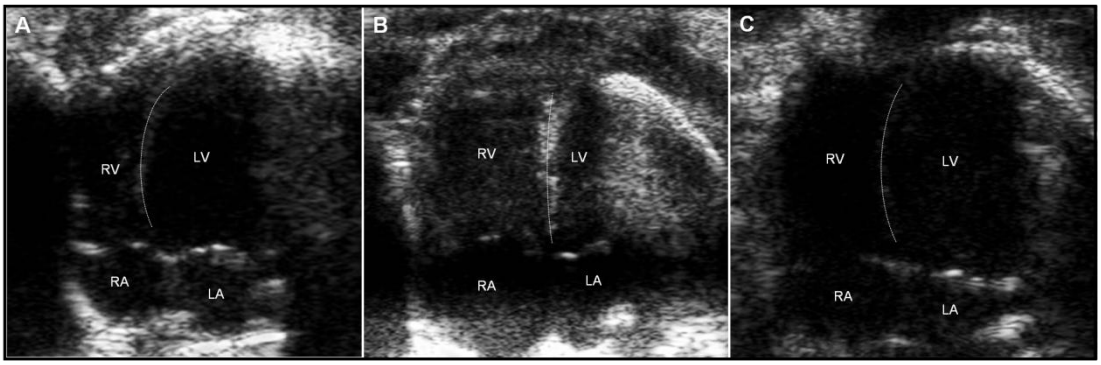

FIGURE 4. Representative echocardiographic images. Representative images from the CTRL (A), MCT (B) and MCT+UCN-2 (C) groups showing an apical 4-chamber view. MCT animals reveal RV hypertrophy and deviation of the IVS (indicated by the white line) to the left side of the heart (B). Treatment with UCN-2 restored both RV dilation and IVS structure (C). CTRL (n=13); CTRL+UCN-2 (n=10); MCT (n=10) and MCT+UCN-2 (n=15). **Abbreviations:** IVS, interventricular septum; LA, left atrium; LV, left ventricle; RA, right atrium and RV, right ventricle.

Invasive Hemodynamic Analysis

The complete hemodynamic study is detailed in Table 10 and representative pressure-volume loops are shown in Figure 5. Baseline RV hemodynamics revealed impaired RV function with both systolic and diastolic alterations in non-treated PAH animals. The MCT group presented a lower HR and decreased CO. Pulmonary resistances (PVR), representative of increased RV overload, were also increased in the MCT group. Moreover, systolic function was

deteriorated with increased end-systolic pressure (ESP) and decreased ejection fraction (EF), as well as higher IVC occlusion-derived end-systolic pressure volume relationship slope (ESPVR E_{es}). Diastolic impairment was also evident in MCT animals. End-diastolic pressure (EDP) and the isovolumic relaxation time constant (τ) were elevated in these animals. The load-independent end-diastolic pressure volume relationship slope (EDPVR k_1) was also increased in the MCT group when compared to controls. RV dilation was obvious with increased end-diastolic volumes (EDV) and a compromised SV, representative of the deteriorated ventricular function in these animals. Treatment with UCN-2 reversed RV dilation and improved both systolic and diastolic function, resulting in an overall improved right ventricular structure and function.

TABLE 10. Invasive hemodynamic evaluation

Hemodynamic Parameters	CTRL		MCT	
	Vehicle	UCN-2	Vehicle	UCN-2
HR (bmp)	387 ± 6	381 ± 3	357 ± 13*	383 ± 11$^{\#}$
CO (mL/min)	64.4 ± 2.6	64.4 ± 3.2	34.5 ± 5.6*	46.6 ± 2.2*$^{\#}$
		Baseline RV		
ESP (mmHg)	22.3 ± 0.8	22.9 ± 1.0	59.7 ± 2.5*	47.6 ± 3.6*$^{\#}$
EDP (mmHg)	3.7 ± 0.3	4.0 ± 0.3	6.0 ± 0.7*	4.3 ± 0.3$^{\#}$
EDV (μL)	222.1 ± 11.2	230.2 ± 9.4	280.0 ± 13.5*	212.9 ± 12.2$^{\#}$
SV (μL)	167.2 ± 7.4	178.2 ± 9.1	91.8 ± 12.5*	121.6 ± 4.8*$^{\#}$
EF (%)	74.6 ± 2.6	72.9 ± 3.4	32.1 ± 3.5*	59.5 ± 2.7*$^{\#}$
τ_{log} (ms)	7.18 ± 0.78	7.35 ± 0.78	9.60 ± 0.85*	7.76 ± 0.51*$^{\#}$
PVR (mmHg/mL/min)	0.35 ± 0.02	0.36 ± 0.02	2.02 ± 0.16*	1.07 ± 0.11*$^{\#}$
		Pressure-volume Relationships$^{\$}$		
ESPVR E_{es} (mmHg/μL)	0.081 ± 0.007	0.083 ± 0.008	0.288 ± 0.029*	0.213 ± 0.022*$^{\#}$
EDPVR k_1	0.0065 ± 0.0008	0.0056 ± 0.0009	0.0151 ± 0.0026*	0.0095 ± 0.0020*$^{\#}$

$^{\$}$Obtained by IVC occlusions. CTRL (n=13); CTRL+UCN-2 (n=10); MCT (n=10) and MCT+UCN-2 (n=15). **Abbreviations:** CO, cardiac output; EDP, end-diastolic pressure; EDV, end-diastolic volume; EDPVR k_1, end-diastolic pressure-volume relationship's slope; EF, ejection fraction; ESP, end-systolic pressure; ESPVR E_{es}, end-systolic pressure-volume relationship's slope; HR, heart rate; PVR, pulmonary vascular resistance; SV, stroke volume; τ_{log}, isovolumic relaxation time constant. *p<0.05 vs CTRL, $^{\#}$p<0.05 vs MCT.

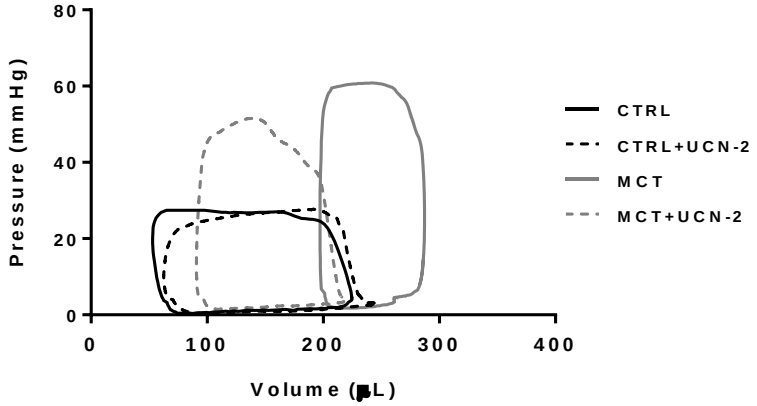

FIGURE 5. Representative pressure-volume loops. Representative pressure-volume loops of the different study groups, obtained by transient inferior vena cava (IVC) occlusions. MCT untreated animals revealed higher EDP and EDV while treatment with UCN-2 was able to attenuate both.

Morphometric and Histological Analysis

Animals from the MCT group presented RV hypertrophy as shown by the increase in RV weight (RVW)/LV + Septum weight (LV+SW) and RVW/tibia length (TL) ratios. Lung weight (LW) was also increased and gastrocnemius weight (GcW) was decreased (decreased GcW/TL ratio) in the animals from this group. Liver weight (LiW) showed no difference between groups. UCN-2 treated animals presented decreased RV hypertrophy and no changes in both lung and liver weight compared with MCT animals (Table 11). RV hypertrophy in the MCT group, was further confirmed by histological measurement of cardiomyocyte cross-sectional area (CSA) (MCT: 366 ± 25 μm^2) when compared to CTRL (255 ± 26 μm^2). UCN-2 treatment was capable to reverse MCT-induced hypertrophy (MCT+UCN-2: 287 ± 26 μm^2) (Figure 6).

TABLE 11. Morphometrical analysis

Morphometric Ratios	CTRL		MCT	
	Vehicle	UCN-2	Vehicle	UCN-2
HW/BW (g/kg)	2.48 ± 0.06	2.50 ± 0.04	3.53 ± 0.15*	3.03 ± 0.10*#
RVW//LV+SW (g/g)	0.26 ± 0.01	0.26 ± 0.01	0.48 ± 0.02*	0.41 ± 0.02*#
RVW/TL (g/cm)	0.04 ± 0.00	0.04 ± 0.00	0.08 ± 0.00*	0.06 ± 0.00*#
LW/TL (g/cm)	0.42 ± 0.02	0.41 ± 0.01	0.72 ± 0.04*	0.69 ± 0.02*
LiW/TL (g/cm)	2.97 ± 0.09	2.91 ± 0.10	2.90 ± 0.19	2.69 ± 0.07
GcW/TL (g/cm)	0.53 ± 0.02	0.52 ± 0.02	0.46 ± 0.01*	0.45 ± 0.02*

Abbreviations: BW, body weight; GcW, gastrocnemius weight; HW, heart weight; LiW, liver weight; LV+SW, left ventricle + septum weight; LW, lung weight; RVW, right ventricle weight; TL, tibia length. *p<0.05 vs CTRL, #p<0.05 vs MCT. CTRL (n=13); CTRL+UCN-2 (n=10); MCT (n=10) and MCT+UCN-2 (n=15).

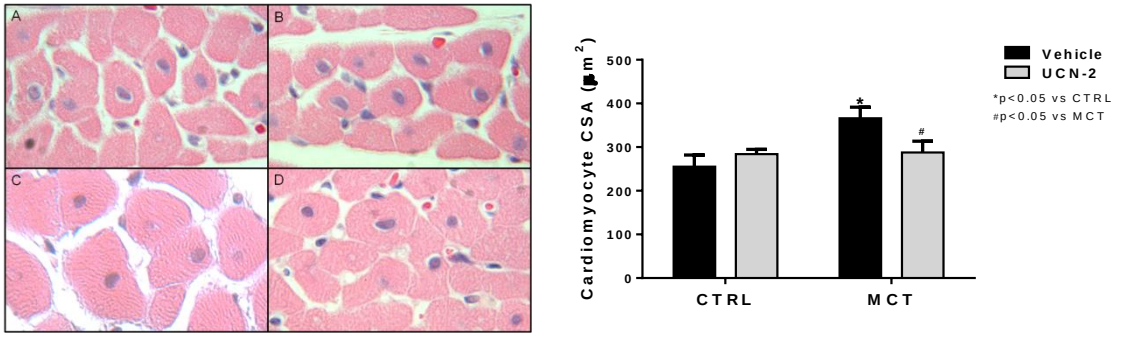

FIGURE 6. Histological analysis of cardiomyocyte structure and cross sectional area (CSA). On the left is depicted representative light microscopy images of hematoxylin-eosin (HE) stained sections of RV (400x) from CTRL (A), CTRL+UCN-2 (B), MCT (C) and MCT+UCN-2 (D), showing augmented cardiomyocyte dimensions in MCT animals. On the right is displayed a diagram with the quantification of cardiomyocyte dimensions, in which MCT animals showed an increased cardiomyocyte CSA when compared to CTRL group. Treatment was able to attenuate cardiomyocyte alterations. CTRL (n=7); CTRL+UCN-2 (n=7); MCT (n=7) and MCT+UCN-2 (n=8).

Molecular Studies

mRNA Expression

We found that in the RV of animals from the MCT group, UCN-2 mRNA levels were notably increased in relation to other study groups (MCT: 2.13 ± 0.81 AU). Moreover, it was found that chronic administration of UCN-2 in control animals did not induce significant changes in UCN-2 expression (CTRL vs CTRL+UCN-2: 1.00 ± 0.34 vs 0.51 ± 0.17 AU). In the RV of animals from the MCT+UCN-2 group, there was a normalization of the UCN-2 expression (0.23 ± 0.08 AU). $CRHR_2$ mRNA expression was decreased in the RV of MCT group animals (0.46 ± 0.08 AU) and also normalized in MCT+UCN-2 animals (0.87 ± 0.12 AU) (Figure 7).

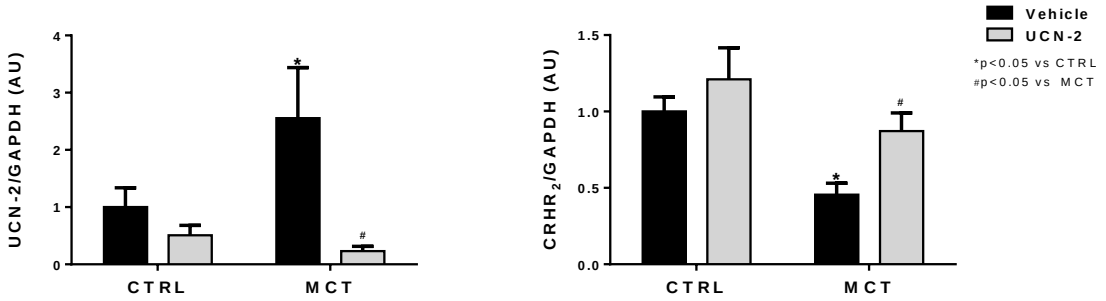

FIGURE 7. mRNA quantification of UCN-2 and $CRHR_2$ in the RV. MCT group showed increased expression of UCN-2 while MCT+UCN-2 group showed significantly lower levels of expression (left). Regarding $CRHR_2$, the MCT group showed decreased expression of the receptor that was reversed with treatment (right). The diagrams represent mean±SEM of UCN-2 and $CRHR_2$ expression. AU stands for arbitrary units. CTRL (n=5); CTRL+UCN-2 (n=6); MCT (n=5) and MCT+UCN-2 (n=8).

Additionally, we determined the gene expression levels of ET-1 and BNP, markers of ventricular hypertrophy[160] and cardiac overload[161]. In the RV of MCT animals we observed an increase in the mRNA expression of ET-1 (MCT vs CTRL: 3.39 ± 0.37 vs 1.00 ± 0.18 AU) and BNP (15.29 ± 2.50 vs 1.00 ± 0.10 AU). Hypoxia-inducible factor 1 alpha (HIF-1α) regulates the transcription of genes involved in adaptive responses to hypoxia[162] and its expression was also elevated in the MCT group (1.61 ± 0.30 vs 1.00 ± 0.16 AU). ET-1 and HIF-1α expressions were reversed with UCN-2 treatment (MCT+UCN-2: 1.84 ± 0.57 and 1.01 ± 0.15 AU, respectively) while BNP expression was attenuated by 7-fold (6.92 ± 2.14 AU) as shown in Figure 8.

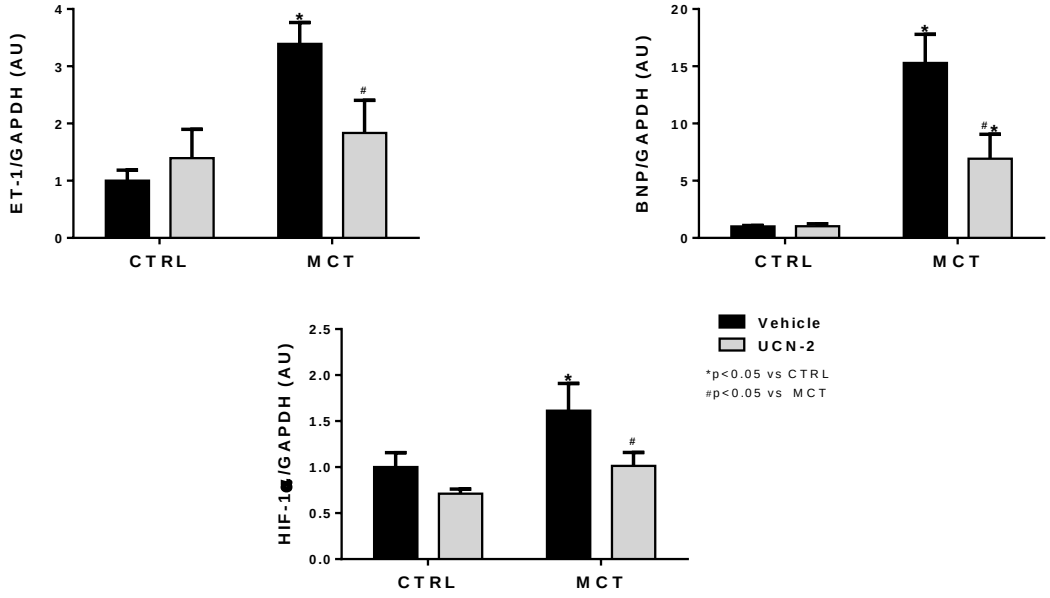

FIGURE 8. mRNA quantification of ET-1, BNP and HIF-1α in the RV. MCT group showed increased expression of ET-1, BNP and HIF-1α. UCN-2 chronic treatment attenuated BNP and reversed ET-1 and HIF-1α expressions. The diagrams represent mean±SEM of ET-1, BNP and HIF-1α expressions. AU stands for arbitrary units. CTRL (n=5); CTRL+UCN-2 (n=6); MCT (n=5) and MCT+UCN-2 (n=8).

UCN-2, as described above, has been associated with signaling pathways of cell survival. In this context we analyzed caspase-3 and caspase-8. In apoptosis-associated genes, both caspase-3 and -8 were altered with increased levels in MCT animals (MCT vs CTRL: caspase-3, 3.90 ± 0.59 vs 1.00 ± 0.13 AU and caspase-8, 2.81 ± 0.35 vs 1.00 ± 0.16 AU). Attenuation of caspase-3 (MCT+UCN-2: 2.02 ± 0.38 AU) and normalization of caspase-8 expression (1.34 ± 0.21 AU) was seen with UCN-2 treatment (Figure 9).

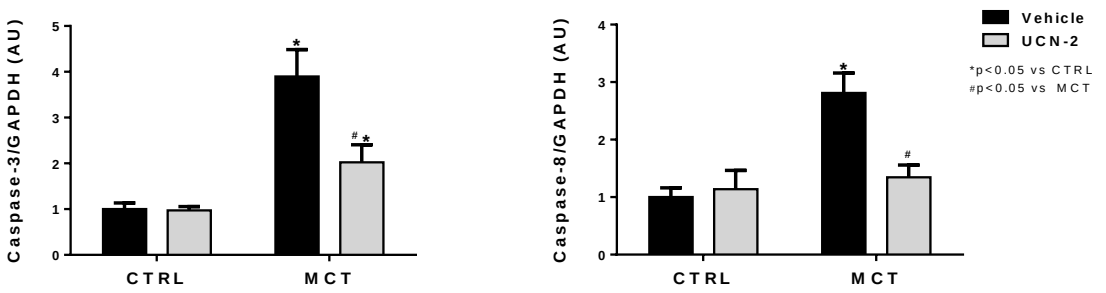

FIGURE 9. mRNA quantification of caspase-3 and caspase-8 in the RV. Both caspases were decreased in MCT group, while UCN-2 treatment was able to reverse caspase-8 and attenuate caspase-3 expression. The diagrams represent mean±SEM of caspase-3 and -8 expressions. AU stands for arbitrary units. CTRL (n=5); CTRL+UCN-2 (n=6); MCT (n=5) and MCT+UCN-2 (n=8).

Protein Expression

$CRHR_2$, a membrane-bound protein that belongs to the family of GPCRs, is the endogenous receptor with greater affinity for UCN-2 binding[107]. The expression of this receptor was particularly high in both MCT groups (MCT: 3.07 ± 0.67 and MCT+UCN-2: 3.34 ± 0.83 AU) when compared to CTRL group (1.00 ± 0.14 AU) (Figure 10).

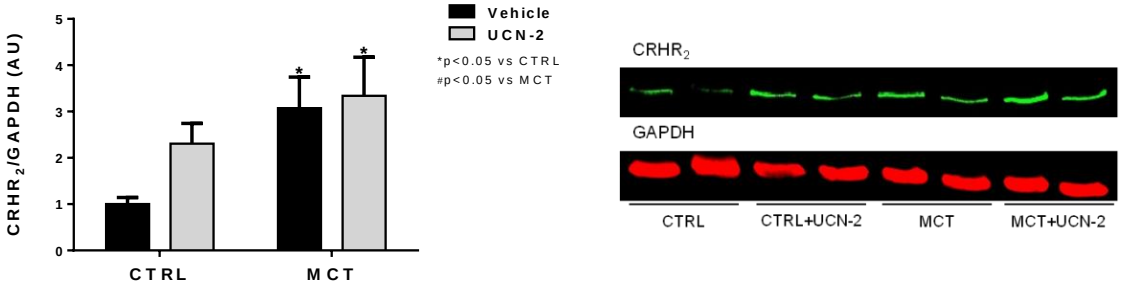

FIGURE 10. Level of $CRHR_2$ expression in the RV. $CRHR_2$ expression was higher in MCT groups. The presence of $CRHR_2$ was detected by immunoblotting utilizing total protein-specific primary antibodies. The diagrams represent mean±SEM of $CRHR_2$ bands. The $CRHR_2$ bands were normalized to GAPDH bands. Below the diagrams is depicted the representative western blot bands. AU stands for arbitrary units. CTRL (n=9); CTRL+UCN-2 (n=9); MCT (n=7) and MCT+UCN-2 (n=10).

ERK1/2 or p44/42 and p38 belong to the MAPK family and are activated in response to a wide range of extracellular stimuli including mitogens, growth factors and cytokines[163]. In MCT animals we observed a decrease in protein phosphorylation/activation of both ERKs and p38 kinases comparatively to controls (MCT vs CTRL: ERKs, 0.53 ± 0.10 vs 1.00 ± 0.11 AU and p38, 0.52 ± 0.04 vs 1.00 ± 0.14 AU). These levels were reversed with UCN-2 treatment (MCT+UCN-2: ERKs, 0.92 ± 0.11 AU and p38, 1.14 ± 0.17) (Figure 11).

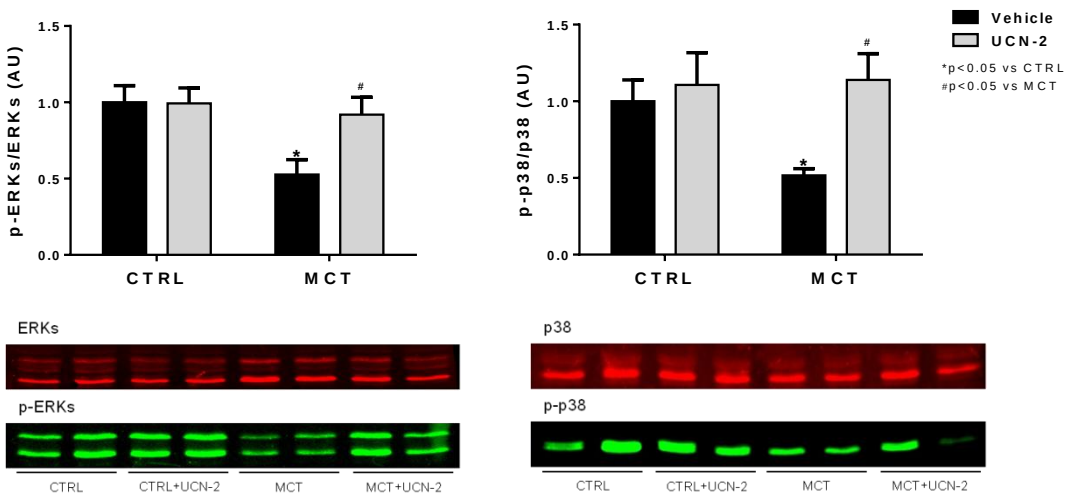

FIGURE 11. Activation level of ERKs and p38 in the RV. Both ERKs and p38 (left to right) activation was decreased in MCT animals and UCN-2 treatment was able to reverse their activation to control values. Phosphorylation was determined by immunoblotting utilizing total protein- and phosphorylation-specific primary antibodies. The diagrams represent mean±SEM of ERKs and p38 bands. Below is depicted the respective representative western blot bands. Phospho-ERKs and –p38 are denoted as p-ERKs and p-p38. AU stands for arbitrary units. CTRL (n=9); CTRL+UCN-2 (n=9); MCT (n=7) and MCT+UCN-2 (n=10).

Akt is a kinase known by its central regulatory role in several cellular processes such as cell survival and proliferation, glucose metabolism and cardiovascular homeostasis[164]. Akt activation did not show any significant differences between groups. UCN-2 treatment did not induce any difference in the phosphorylation level of Akt (Figure 12).

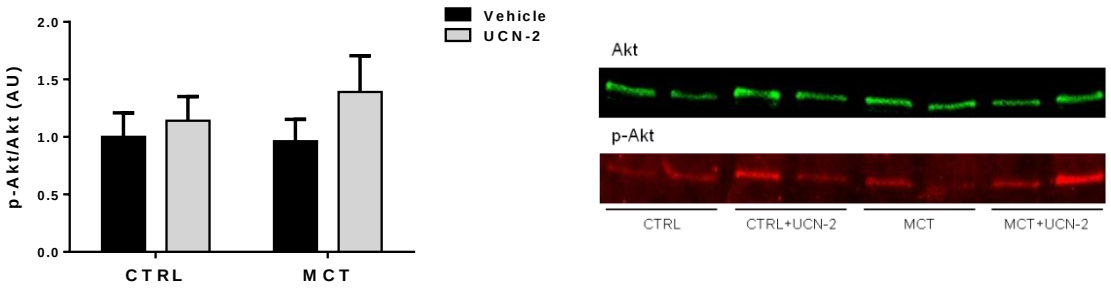

FIGURE 12. Activation level of Akt in the RV. Akt activation (on the left) did not show any difference between groups. Phosphorylation was determined by immunoblotting utilizing total protein- and phosphorylation-specific primary antibodies. The diagrams represent mean±SEM of Akt bands. Below is depicted the respective representative western blot bands. Phospho-Akt is denoted as p-Akt. AU stands for arbitrary units. CTRL (n=9); CTRL+UCN-2 (n=9); MCT (n=7) and MCT+UCN-2 (n=10).

Signal transducer and activator of transcription 3 ($STAT_3$) is a transcription factor and an important signaling molecule for several cytokines and growth factor receptors, known for possessing an oncogenic potential and anti-apoptotic activities[165]. The MCT group showed a decreased $STAT_3$ phosphorylation when compared with the CTRL group (MCT vs CTRL: 0.61 ±

0.12 vs 1.00 ± 0.10 AU). Treatment with UCN-2 resulted in restored $STAT_3$ activation (MCT+UCN-2: 1.01 ± 0.09 AU) as we can see in Figure 13.

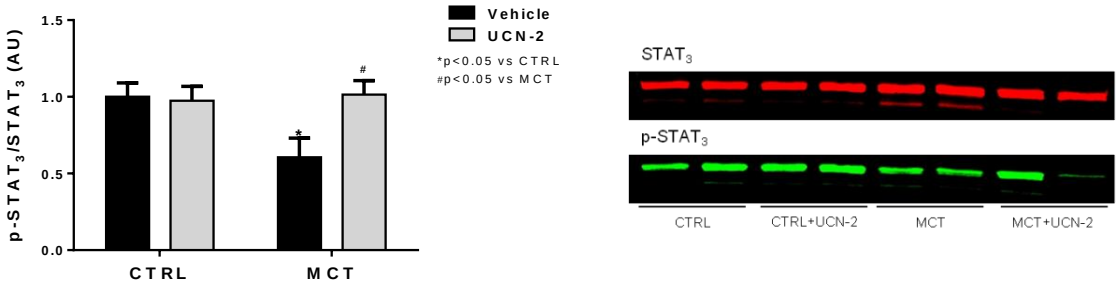

FIGURE 13. Activation level of $STAT_3$ in the RV. $STAT_3$ activation was decreased in MCT animals and UCN-2 treatment was able to reverse its reduction. Phosphorylation was determined by immunoblotting utilizing total protein- and phosphorylation-specific primary antibodies. The diagrams represent mean±SEM of $STAT_3$ bands. Below the diagrams is depicted the representative western blot bands. Phospho-$STAT_3$ is denoted as p-$STAT_3$ and AU stands for arbitrary units. CTRL (n=9); CTRL+UCN-2 (n=9); MCT (n=7) and MCT+UCN-2 (n=10).

DISCUSSION

UCN-2 treatment improves survival and RV function in MCT-induced PAH

This study demonstrated that the chronic treatment with UCN-2 in an experimental model of PAH and secondary RV failure, attenuates structural remodeling and enhances RV systolic and diastolic function.

Several studies[166-168] have demonstrated the progression of MCT-induced PAH using echo-measured indexes of RV function and structure, proving the importance of non-invasive methods in the evaluation of PAH severity and RV function, since it allows a comparable approach to that routinely used in patients[62].

In MCT-induced PAH we observed a decrease in PAAT and PAET, which significantly altered the PAAT/PAET ratio, and in systolic flow which is compromised in PAH, is associated with pulmonary systolic pressures[169] and correlates with decreased survival in PAH patients[62]. Pulmonary flow velocity, acceleration and ejection time were also restored with UCN-2 pharmacological intervention, revealing an improved pulmonary arterial function and decreased RV afterload.

Accordingly to previous studies[167, 168] we observed a significant RV and right atria chamber dilation, shown by the echo-measured RV and RAA. At this time point (4th week after MCT injection) and with a progressive increase in PVR, the RV cannot sustain the adaptive hypertrophy and eventually dilates[51]. This was shown by Hardziyenka *et al*. that measured RVEDD echocardiographycally and showed that it seems to start to increase between 20-25 days post MCT administration. Furthermore, in response to progressive pressure overload there is a shift of the IVS to the left side chamber[170], which is in agreement with our observations (Figure 4B). Moreover, echo-measured TAPSE, an indicator of RV contractile function[170], was also decreased in MCT animals. UCN-2 therapeutic intervention attenuated the adaptive hypertrophy and improved RV function and structure, as well as correcting IVS deviation. CO and CI, indexes of overall cardiac function, were also altered in MCT animals and were normalized with UCN-2 treatment.

Although no studies have invasively evaluated UCN-2's chronic treatment effect on RV function in PAH, enough studies have been performed on the LV that allows us to explain our results. Those studies showed improved cardiac performance in models of HF subjected to UCN-2 intervention. Bale *et al.* studied the acute effects of UCN-2 in a murine model of HF and although LVEDP was not different between wild-type and $CRHR_2$-deficient mice, they noticed an increase in HR, EF and CO, as well as a decrease in LVEDV and ESV[129]. In anaesthetized pigs,

intracoronary infusion of UCN-2 caused an increase in coronary blood flow and CO, accompanied by a decrease in coronary vascular resistances[89].

Recently, both humans with mild HF[149] and acute decompensated HF[91] were subjected to UCN-2 administration. In the latter, UCN-2 treatment was able to decrease systolic blood pressure and increase CO, associated with a strong reduction in total peripheral resistance. Administration of UCN-2 in humans with mild HF increased CO and LVEF and decreased mean arterial pressure, systemic vascular resistance and cardiac work, in a dose-dependent manner. In both studies UCN-2 was able to induce vasodilation and improve myocardial function.

Similarly, and despite all the structural differences between the LV and the RV, our functional RV study match what has been previously described for the LV. MCT-injected animals revealed a severe cardiac dysfunction secondary to PAH and presented RV hypercontractility, as shown by highly increased systolic pressures, as well by changes in other parameters of contractile function, namely IVC occlusion-derived ESPV relationship's slope. Diastolic dysfunction was also present in the RV of MCT animals, shown by increased stiffness (rise in RVEDP) and RV dilation (increased RVEDD). These hemodynamic alterations correspond to decompensated myocardial hypertrophy of the RV in response to pressure overload resulting from increased pulmonary vascular resistance, as previously described [171].

Treating MCT animals with UCN-2 resulted in the improvement of RV function, given that both systolic and diastolic dysfunction was enhanced and the ventricle showed improved contractile and relaxation functions. Cardiac catheterization allowed a more detailed analysis of ventricular function and corroborated echocardiographic data, nevertheless some caution is needed when interpreting the results and extrapolating previous knowledge from the LV to explain RV pathophysiology[172].

MCT-induced RV morphohistological changes are attenuated with UCN-2 treatment

UCN-2 treatment after PAH-induction resulted in accentuated decrease of cardiac hypertrophy, especially RV hypertrophy (Table 11). HW was increased in PAH animals, as previously mentioned, and this was analyzed using the HW/BW ratio. Nevertheless, in PAH, the RV is the primary affected ventricle and therefore should be the focus of the analysis, since due to the augmented PVR is under pressure overload. And in fact, the RVW/BW ratio was also increased in PAH animals, which revealed the presence of RV hypertrophy.

Despite being in agreement with all of our data regarding hypertrophy and hypertrophy-associated parameters measured, the model we're using is associated with cachexia[158] and because of that, we alternatively measured the RVW/TL ratio which is accepted as a reliable parameter for hypertrophy measurement[159]. The RVW/LV+SW ratio was consistent with the previously mentioned measurements. Lung edema and congestion is a consequence of PAH[173] and using the LW/TL ratio we observed an increase ratio in the MCT group, suggestive of PAH-associated lung fluid retention.

At the cellular level, our model of PAH developed cardiomyocyte hypertrophy, as measured by cardiomyocyte CSA. These effects were however reverted by UCN-2 administration. The reversal of hypertrophy in response to treatment underlines the functional recovery observed with non-invasive and invasive hemodynamic measurements. The RV of treated animals is under attenuated pressure overload and therefore its adaptive hypertrophic response is decreased. Less muscle mass, less developed force and consequently, attenuated developed pressures and hypercontractile state.

Expression of the UCN-2/CRHR$_2$ in PAH and alterations with UCN-2 treatment

Given that the used animal model of PAH is characterized by several structural and functional cardiac abnormalities over time, expressed by compensated RV hypertrophy at 2-3 weeks and RH failure after 3-5 weeks[170, 174] it seems relevant to search, between experimental groups, for possible differences in the expression of UCN-2 and its receptor, as well as the expression of genes encoding regulatory proteins relevant for ventricular contractile function. Moreover, these studies allowed us a better characterization of the variations occurring in the UCN-2/CRHR$_2$ system and downstream signaling in the context of PAH and progression to HF, which can provide us an explanation for the alterations detected in the functional studies.

UCN-2 and its receptor, CRHR$_2$, have been implicated in several cardiovascular diseases[91, 141, 149, 175]. In spontaneously hypertensive rats, Nishikimi *et al.* described a higher UCN mRNA expression in hypertrophied LV than in normal LV, whereas CRHR$_2$ expression was depressed[103]. Moreover, Emeto *et al.* demonstrated augmented expression of UCN-2 in biopsies from abdominal aortic aneurysm (AAA) and despite not being cardiac tissue, the same study also showed increased levels of UCN-2 in plasma samples of AAA patients, which are associated with this cardiovascular disorder[141]. Additionally, other group analyzed and compared the prognostic efficacy of both plasma UCN and NT-proBNP levels in acute myocardial infarction and correlated the high plasmatic UCN levels with increased mortality[176].

In our study we also observed increased levels of UCN-2 mRNA expression and a sharp fall in the mRNA expression of the $CRHR_2$ which complies with the studies cited above. In addition, UCN-2 levels also seem to correlate with increased morbidity and mortality[176], despite its beneficial effects. In our study, the decreased levels of $CRHR_2$ expression may be related with the increased UCN-2 expression in the RV, wherein by a mechanism of negative feedback, UCN-2 regulates $CRHR_2$ mRNA expression. UCN-2 treatment was able to reduce UCN-2 endogenous expression and augment $CRHR_2$ expression, normalizing both expressions to control levels.

Taken together, these results suggest that increased UCN-2 in the RV from MCT animals may be associated with an adaptive process of the cardiac muscle. In consequence, one can predict that UCN-2 may play an important role in the pathophysiology of PAH and progression to HF.

Increased expression of cardiac overload, hypertrophy and hypoxia markers in PAH was attenuated with UCN-2 treatment

Neurohumoral activation is associated with RV dysfunction in PAH[177] and growing evidences show that UCN-2 modulates the gene expression and/or the activity of several neurohumoral agents, such as ET-1 and BNP, involved in PAH and progression to HF[90, 143].

ET-1 plasmatic levels are elevated in PAH and are associated with disease severity[27]. In addition, its clearance from pulmonary arteries is reduced, promoting further vasoconstriction[179]. ET-1 levels are associated with the development of RV hypertrophy in MCT-induced PAH[180] and its RV expression is increased in this experimental model[181].

Plasmatic BNP levels are associated with PH[182] and increased in MCT-injected rats[181]. The production of BNP is stimulated in response to pressure-overload[183] and is associated with the extent of RV dysfunction[184]. Moreover, NT-proBNP along with UCN-2 plasmatic levels holds an enhanced prognostic value, since their levels correlate with increased mortality, as previously cited[176].

In our study, both ET-1 and BNP mRNA expressions were augmented in PAH animals up to 3-fold and 15-fold, respectively. While UCN-2 treatment was able to attenuate ET-1 to 2-fold and BNP to 7-fold, in accordance with previous studies[143, 178].

Hypoxia-inducible factor 1 alpha (HIF-1α) is a heterodimeric subunit of the transcription factor HIF-1, which regulates the transcription of genes involved in adaptive responses to

hypoxia[162]. Chu *et al.* showed that HIF-1α overexpression promotes the development of cardiac hypertrophy via up-regulation of Ca^{+2}-calcineurin under mild hypoxia conditions[185]. However, increased $[Ca^{2+}]_i$ is not only associated with hypertrophy but also with apoptotic processes under severe hypoxia situation, given that some reports showed that HIF-1α overexpression promotes apoptosis of cardiac myocytes in the presence of severe hypoxia, especially when other cellular energy substrates are lacking[186]. In our study, RV HIF-1α expression was also increased in MCT animals and UCN-2 treatment was able to reverse HIF-1α expression to control levels. The identification of a binding region for HIF-1α in human UCN-2 gene that regulates transcription in response to hypoxia, explains why both levels of UCN-2 and HIF-1α correlate. Buhler *et al.* proposed that the induction of hUCN-2 expression by low oxygen levels may confer to cardiac myocytes an advantage in ischemic conditions[187].

UCN-2 treatment reverses changes in markers of apoptosis in PAH

Apoptosis is one of the major mechanisms causing cardiomyocyte loss in failing hearts of both human patients[188] and animal models[189]. In turn, UCN-2 appears to have cardioprotective effects by preventing cardiomyocyte death[175, 190, 191].

Upon cleavage, caspase-3 is activated in the myocardium of end-stage HF patients[192] being also involved in the development of pressure overload-induced LV dysfunction, as well as hyperglycemia-induced myocardial apoptosis[193]. Studies that used the MCT-induced PAH model showed increased caspase-3 activation in those animals[194, 195] and in myocardial infarction, the overexpression of this enzyme induced myofibrillar ultrastructural damage and when subjected to myocardial ischemia-reperfusion (I/R) injury, caspase-3 transgenic mice showed increased infarct size and a pronounced susceptibility to die[196].

Caspase-8, a cysteine protease, has the ability to activate downstream caspases, including caspase-3, and therefore it is critically involved in the regulation of cellular apoptosis, as well as necrotic cell death[197]. In human cardiomyocytes, iron-induced apoptosis was linked to increased levels of caspase-8[198]. In a mouse model of HF, the inhibition of Fas-associated death domain-containing protein (FADD) had a protective role in myocardial I/R injury and was correlated with increased caspase-8 activity and downstream caspase-3 activity[197].

In our study, the high detected mRNA levels of both caspase-3 and caspase-8 in the RV of the MCT rats were reverted by UCN-2 treatment which is consistent with other studies[134, 199] and confirms the hypothesis that UCN-2/$CRHR_2$ system has anti-apoptotic proprieties.

UCN-2 treatment normalized the alterations in some elements of the UCN-2/CRHR$_2$ signaling pathway seen in MCT animals

In rats, the administration of MCT usually leads to cardiac hypertrophy that develops due to increasing oxidants, hemodynamic load and by inducing hypoxia. The mechanisms that lead to cardiac hypertrophy and progression to HF involve the activation G-proteins, calcium signaling, PI3K, PKCs and MAPKs[200]. In this study one of our goals was to find which signaling pathways are deregulated in MCT-induced PAH animals and which are involved in UCN-2 beneficial effects.

ERK1/2 or p44/42 and p38 belong to the MAPK family and are activated in response to a wide range of extracellular stimuli including mitogens, growth factors and cytokines. When activated, they have the ability to regulate other kinases and several transcription factors[163]. Defects downstream of BMP signaling pathway, involving p38 and ERKs, have been linked to PAH[201] and increased activation of ERK1/2 and p38 was found in lung tissue of MCT-induced PH model, while a suppression of this activation was observed with treatment[202].

On the other hand and for the first time, Kehat and Molkentin proposed that eccentric hypertrophy is induced by de-activation of the ERK pathway[203] and Bartelds *et al.* confirmed it by observing a decrease in phosphorylated ERK1/2 in mice subjected to volume and pressure overload[204]. Furthermore, in a model of transverse aortic constriction (TAC) that resulted in late eccentric hypertrophy with eventual development of LV dysfunction, implicated the importance of ERK1/2 downregulation and enhanced cardiomyocyte apoptosis in the transition from compensated hypertrophy to HF[205].

In relation to p38, Pérez López *et al.* showed that the disruption of the AKAP/p38 signaling complex inhibits compensatory hypertrophy in response to aortic banding-induced pressure overload and promotes early cardiac dysfunction associated with increased myocardial apoptosis and ventricular dilation[206].

In consequence, our decreased phosphorylation of both kinases in the RV of MCT animal's is in accordance with previous studies, once at the time of sample collection, the MCT animals already showed an advanced stage of HF with evident RV dilation. In addition, the reversal of both kinases to its control levels comply with prior studies that showed a boost in the activation of both ERK 1/2[88] and p38 MAPK[125], at this stage, upon UCN-2-binding to CRHR$_2$, which accordingly to Bartelds *et al.* could be a mechanism to prevent the pressure-loaded RV from dilation[204].

Akt or PKB is a serine/threonine kinase known by its critical and central regulatory role in several cellular processes such as cell survival and proliferation, glucose metabolism and cardiovascular homeostasis[164]. Akt is also a critical downstream element of the PI3K/Akt cell survival pathway, whose activity can be inhibited by Akt-mediated phosphorylation[164]. The PI3K/Akt pathway is also known to be activated by UCN-2[116] and it's particularly important in cardiac and skeletal muscle since it helps regulate PLB phosphorylation, along with PKA, controlling the inhibition of SERCA[118].

Although Akt was not significantly affected by any of the administered drugs (MCT and UCN-2) in resemblance with other studies[202, 207].

$STAT_3$ is a transcription factor and an important signaling molecule for several cytokines and growth factor receptors, known for possessing an oncogenic potential and anti-apoptotic activities[165]. In myeloma tumor cells, the blocking of Jak-STAT pathway induces apoptosis, demonstrating that $STAT_3$ signaling is essential for the survival of this type of cells[208].

Akin to cancer, PAH is characterized by an imbalance between a proliferative and an apoptotic phenotype[16]. In PASMC proliferation is enhanced due to the activation of pro-survival transcription factors, such as $STAT_3$[209]. And in fact, Courboulin *et al.* demonstrated that $STAT_3$ phosphorylation was increased in PAH-PASMCs and that treatment with a $STAT_3$ blocker reversed this state.

However, in the cardiac tissue the opposite happens. Because the RV is not able to sustain long-term pressure overload, the cardiac contractile force decreases due to apoptosis and changes in cardiomyocytes, and eventually the RV dilates[51]. Following this notion, Chen-Scarabelli *et al*. verified that cardiac cells incubated with UCN showed increased $STAT_3$ phosphorylation at Tyr705. Moreover, overexpression of $STAT_3$ in cardiac myocytes pretreated with UCN presented a reduced magnitude of cell death, when compared with UCN treatment alone. While transfection of cells with a mutant $STAT_3$ (loss of function) enhanced the extent of cell death in a dose-dependent manner[210].

Hereupon, the increased $STAT_3$ phosphorylation in the RV of the MCT treated animal's match what has been previously described for the cardiomyocytes, demonstrating the cardioprotective effect and anti-apoptotic proprieties of UCN-2.

The increased expression of $CRHR_2$ in the RV of MCT animals, obtained by western blot analysis, contrarily to its mRNA expression, may be related with our decreased activation of ERK1/2, since according to Markovic *et al.*, the endocytosis of $CRHR_2$ appears to be regulated by ERK1/2 direct phosphorylation of β-arrestin1 in an auto-regulatory mechanism that

influences the rate and extent of β-arrestin1 recruitment to the plasma membrane and interaction with $CRHR_2$[112]. Thus, the elevated presence of $CRHR_2$ in the RV from MCT animals could be associated with the deregulation seen in the pathway that leads to receptor internalization and degradation.

CONCLUSIONS AND FUTURE PERSPECTIVES

In short, we show for the first time, in an experimental model of MCT-induced PAH, that UCN-2 treatment is able to restore PAH-induced severe abnormalities in cardiac function and structure, while attenuating or reversing the expression of markers of cardiac overload, hypertrophy, hypoxia and apoptosis. We also demonstrated that the UCN-2 beneficial effects are associated and involve the modulation of several signaling pathways downstream $CRHR_2$ activation.

PAH is a chronic syndrome that is frequently diagnosed in a later stage, where HF is already settled. Therefore our approach adds the benefit of a more practical and clinical relevant therapy, since we begin the treatment after PAH was established.

The UCN-2 and its receptor have been studied in the cardiovascular system, but research so far has failed to determine its effects on both normal and diseased RV physiology. With this study, we demonstrated the effects of an increase in UCN-2 levels through exogenous administration of the peptide, which has shown that specific activation of $CRHR_2$ mediates several compensatory mechanisms that ameliorate the dysfunction and structural abnormalities associated with PAH and RVF.

However, it is also important to take into account that the animal model used in the present study does not mimic entirety human PH or PAH, nevertheless it has several pathophysiological alterations in common that allow us to enthusiastically point UCN-2 as a possible novel therapeutic approach for this incurable and with an uncertain prognosis disease.

In fact, we hope to have opened the road for further basic and translational research that could possibly lead to the establishment of UCN-2 as a novel and safe therapeutic agent for treating patients with PAH and RVF.

In spite of these results, further research is needed in order to determine specifically where UCN-2 plays its major role. The ventricular function is altered, but since in this model RV dysfunction and HF is secondary to PAH, we cannot ascertain whether RV function and structure improvement is secondary to pulmonary vascular functional enhancement and therefore decreased vascular resistances, or if UCN-2 has a direct effect on the ventricle which by itself is capable of leading to the changes we observed. In the future, in order to differentiate indirect from direct myocardial effects of UCN-2 treatment, we predict the use of an animal model of RV overload.

Beyond RV function and structure, we intent do access pulmonary function and structure as well, by *in vitro* (vascular ring preparations) and histological studies. Moreover,

our molecular results here described will allow us to design and perform further studies in order to unravel more signaling pathways underlying the beneficial effects of UCN-2/$CRHR_2$ system activation in PAH and RV HF, in both RV and lung samples.

REFERENCES

1. McLaughlin VV, Archer SL, Badesch DB, Barst RJ, Farber HW, Lindner JR, Mathier MA, McGoon MD, Park MH, Rosenson RS, Rubin LJ, Tapson VF, Varga J. Accf/aha 2009 expert consensus document on pulmonary hypertension a report of the american college of cardiology foundation task force on expert consensus documents and the american heart association developed in collaboration with the american college of chest physicians; american thoracic society, inc.; and the pulmonary hypertension association. *J Am Coll Cardiol*. 2009;53:1573-1619
2. Hoeper MM, Bogaard HJ, Condliffe R, Frantz R, Khanna D, Kurzyna M, Langleben D, Manes A, Satoh T, Torres F, Wilkins MR, Badesch DB. Definitions and diagnosis of pulmonary hypertension. *J Am Coll Cardiol*. 2013;62:D42-50
3. Galie N, Hoeper MM, Humbert M, Torbicki A, Vachiery JL, Barbera JA, Beghetti M, Corris P, Gaine S, Gibbs JS, Gomez-Sanchez MA, Jondeau G, Klepetko W, Opitz C, Peacock A, Rubin L, Zellweger M, Simonneau G. Guidelines for the diagnosis and treatment of pulmonary hypertension: The task force for the diagnosis and treatment of pulmonary hypertension of the european society of cardiology (esc) and the european respiratory society (ers), endorsed by the international society of heart and lung transplantation (ishlt). *Eur Heart J*. 2009;30:2493-2537
4. Hatano S ST. Primary pulmonary hypertension. 1975
5. Simonneau G, Galie N, Rubin LJ, Langleben D, Seeger W, Domenighetti G, Gibbs S, Lebrec D, Speich R, Beghetti M, Rich S, Fishman A. Clinical classification of pulmonary hypertension. *J Am Coll Cardiol*. 2004;43:5S-12S
6. Simonneau G, Robbins IM, Beghetti M, Channick RN, Delcroix M, Denton CP, Elliott CG, Gaine SP, Gladwin MT, Jing ZC, Krowka MJ, Langleben D, Nakanishi N, Souza R. Updated clinical classification of pulmonary hypertension. *J Am Coll Cardiol*. 2009;54:S43-54
7. Simonneau G, Gatzoulis MA, Adatia I, Celermajer D, Denton C, Ghofrani A, Gomez Sanchez MA, Krishna Kumar R, Landzberg M, Machado RF, Olschewski H, Robbins IM, Souza R. Updated clinical classification of pulmonary hypertension. *J Am Coll Cardiol*. 2013;62:D34-41
8. Sztrymf B, Coulet F, Girerd B, Yaici A, Jais X, Sitbon O, Montani D, Souza R, Simonneau G, Soubrier F, Humbert M. Clinical outcomes of pulmonary arterial hypertension in carriers of bmpr2 mutation. *American journal of respiratory and critical care medicine*. 2008;177:1377-1383
9. Humbert M, Montani D, Evgenov OV, Simonneau G. Definition and classification of pulmonary hypertension. *Handbook of experimental pharmacology*. 2013;218:3-29
10. Pietra GG, Capron F, Stewart S, Leone O, Humbert M, Robbins IM, Reid LM, Tuder RM. Pathologic assessment of vasculopathies in pulmonary hypertension. *J Am Coll Cardiol*. 2004;43:25S-32S

11. Montani D, Gunther S, Dorfmuller P, Perros F, Girerd B, Garcia G, Jais X, Savale L, Artaud-Macari E, Price LC, Humbert M, Simonneau G, Sitbon O. Pulmonary arterial hypertension. *Orphanet journal of rare diseases*. 2013;8:97

12. Cool CD, Kennedy D, Voelkel NF, Tuder RM. Pathogenesis and evolution of plexiform lesions in pulmonary hypertension associated with scleroderma and human immunodeficiency virus infection. *Human pathology*. 1997;28:434-442

13. Bjornsson J, Edwards WD. Primary pulmonary hypertension: A histopathologic study of 80 cases. *Mayo Clinic proceedings*. 1985;60:16-25

14. Dorfmuller P. Pulmonary hypertension: Pathology. *Handbook of experimental pharmacology*. 2013;218:59-75

15. Waxman AB, Zamanian RT. Pulmonary arterial hypertension: New insights into the optimal role of current and emerging prostacyclin therapies. *The American journal of cardiology*. 2013;111:1A-16A; quiz 17A-19A

16. Humbert M, Morrell NW, Archer SL, Stenmark KR, MacLean MR, Lang IM, Christman BW, Weir EK, Eickelberg O, Voelkel NF, Rabinovitch M. Cellular and molecular pathobiology of pulmonary arterial hypertension. *J Am Coll Cardiol*. 2004;43:13S-24S

17. Jeffery TK, Morrell NW. Molecular and cellular basis of pulmonary vascular remodeling in pulmonary hypertension. *Progress in cardiovascular diseases*. 2002;45:173-202

18. Davie NJ, Crossno JT, Jr., Frid MG, Hofmeister SE, Reeves JT, Hyde DM, Carpenter TC, Brunetti JA, McNiece IK, Stenmark KR. Hypoxia-induced pulmonary artery adventitial remodeling and neovascularization: Contribution of progenitor cells. *American journal of physiology. Lung cellular and molecular physiology*. 2004;286:L668-678

19. Jonigk D, Golpon H, Bockmeyer CL, Maegel L, Hoeper MM, Gottlieb J, Nickel N, Hussein K, Maus U, Lehmann U, Janciauskiene S, Welte T, Haverich A, Rische J, Kreipe H, Laenger F. Plexiform lesions in pulmonary arterial hypertension composition, architecture, and microenvironment. *The American journal of pathology*. 2011;179:167-179

20. Kherbeck N, Tamby MC, Bussone G, Dib H, Perros F, Humbert M, Mouthon L. The role of inflammation and autoimmunity in the pathophysiology of pulmonary arterial hypertension. *Clinical reviews in allergy & immunology*. 2013;44:31-38

21. Morrell NW, Adnot S, Archer SL, Dupuis J, Jones PL, MacLean MR, McMurtry IF, Stenmark KR, Thistlethwaite PA, Weissmann N, Yuan JX, Weir EK. Cellular and molecular basis of pulmonary arterial hypertension. *J Am Coll Cardiol*. 2009;54:S20-31

22. Herve P, Humbert M, Sitbon O, Parent F, Nunes H, Legal C, Garcia G, Simonneau G. Pathobiology of pulmonary hypertension. The role of platelets and thrombosis. *Clinics in chest medicine*. 2001;22:451-458

23. Montani D, Chaumais MC, Guignabert C, Gunther S, Girerd B, Jais X, Algalarrondo V, Price LC, Savale L, Sitbon O, Simonneau G, Humbert M. Targeted therapies in pulmonary arterial hypertension. *Pharmacology & therapeutics*. 2014;141:172-191

24. Tuder RM, Cool CD, Geraci MW, Wang J, Abman SH, Wright L, Badesch D, Voelkel NF. Prostacyclin synthase expression is decreased in lungs from patients with severe pulmonary hypertension. *American journal of respiratory and critical care medicine*. 1999;159:1925-1932

25. Maron BA, Loscalzo J. Pulmonary hypertension: Pathophysiology and signaling pathways. *Handbook of experimental pharmacology*. 2013;218:31-58

26. Giaid A, Yanagisawa M, Langleben D, Michel RP, Levy R, Shennib H, Kimura S, Masaki T, Duguid WP, Stewart DJ. Expression of endothelin-1 in the lungs of patients with pulmonary hypertension. *The New England journal of medicine*. 1993;328:1732-1739

27. Rubens C, Ewert R, Halank M, Wensel R, Orzechowski HD, Schultheiss HP, Hoeffken G. Big endothelin-1 and endothelin-1 plasma levels are correlated with the severity of primary pulmonary hypertension. *Chest*. 2001;120:1562-1569

28. Gangopahyay A, Oran M, Bauer EM, Wertz JW, Comhair SA, Erzurum SC, Bauer PM. Bone morphogenetic protein receptor ii is a novel mediator of endothelial nitric-oxide synthase activation. *The Journal of biological chemistry*. 2011;286:33134-33140

29. Butcher RW, Sutherland EW. Adenosine 3',5'-phosphate in biological materials. I. Purification and properties of cyclic 3',5'-nucleotide phosphodiesterase and use of this enzyme to characterize adenosine 3',5'-phosphate in human urine. *The Journal of biological chemistry*. 1962;237:1244-1250

30. Francis SH, Busch JL, Corbin JD, Sibley D. Cgmp-dependent protein kinases and cgmp phosphodiesterases in nitric oxide and cgmp action. *Pharmacological reviews*. 2010;62:525-563

31. Nagendran J, Archer SL, Soliman D, Gurtu V, Moudgil R, Haromy A, St Aubin C, Webster L, Rebeyka IM, Ross DB, Light PE, Dyck JR, Michelakis ED. Phosphodiesterase type 5 is highly expressed in the hypertrophied human right ventricle, and acute inhibition of phosphodiesterase type 5 improves contractility. *Circulation*. 2007;116:238-248

32. Wharton J, Strange JW, Moller GM, Growcott EJ, Ren X, Franklyn AP, Phillips SC, Wilkins MR. Antiproliferative effects of phosphodiesterase type 5 inhibition in human pulmonary artery cells. *American journal of respiratory and critical care medicine*. 2005;172:105-113

33. Waxman AB. Pulmonary hypertension in heart failure with preserved ejection fraction: A target for therapy? *Circulation*. 2011;124:133-135

34. Suntharalingam J, Hughes RJ, Goldsmith K, Doughty N, George P, Toshner M, Sheares KK, Pepke-Zaba J. Acute haemodynamic responses to inhaled nitric

oxide and intravenous sildenafil in distal chronic thromboembolic pulmonary hypertension (cteph). *Vascular pharmacology*. 2007;46:449-455

35. Weir EK, Reeve HL, Huang JM, Michelakis E, Nelson DP, Hampl V, Archer SL. Anorexic agents aminorex, fenfluramine, and dexfenfluramine inhibit potassium current in rat pulmonary vascular smooth muscle and cause pulmonary vasoconstriction. *Circulation*. 1996;94:2216-2220

36. Yuan JX, Aldinger AM, Juhaszova M, Wang J, Conte JV, Jr., Gaine SP, Orens JB, Rubin LJ. Dysfunctional voltage-gated k+ channels in pulmonary artery smooth muscle cells of patients with primary pulmonary hypertension. *Circulation*. 1998;98:1400-1406

37. MacLean MR, Herve P, Eddahibi S, Adnot S. 5-hydroxytryptamine and the pulmonary circulation: Receptors, transporters and relevance to pulmonary arterial hypertension. *British journal of pharmacology*. 2000;131:161-168

38. Herve P, Launay JM, Scrobohaci ML, Brenot F, Simonneau G, Petitpretz P, Poubeau P, Cerrina J, Duroux P, Drouet L. Increased plasma serotonin in primary pulmonary hypertension. *The American journal of medicine*. 1995;99:249-254

39. Guilluy C, Sauzeau V, Rolli-Derkinderen M, Guerin P, Sagan C, Pacaud P, Loirand G. Inhibition of rhoa/rho kinase pathway is involved in the beneficial effect of sildenafil on pulmonary hypertension. *British journal of pharmacology*. 2005;146:1010-1018

40. Guilluy C, Eddahibi S, Agard C, Guignabert C, Izikki M, Tu L, Savale L, Humbert M, Fadel E, Adnot S, Loirand G, Pacaud P. Rhoa and rho kinase activation in human pulmonary hypertension: Role of 5-ht signaling. *American journal of respiratory and critical care medicine*. 2009;179:1151-1158

41. Loyd JE, Primm RK, Newman JH. Familial primary pulmonary hypertension: Clinical patterns. *The American review of respiratory disease*. 1984;129:194-197

42. Cogan JD, Pauciulo MW, Batchman AP, Prince MA, Robbins IM, Hedges LK, Stanton KC, Wheeler LA, Phillips JA, 3rd, Loyd JE, Nichols WC. High frequency of bmpr2 exonic deletions/duplications in familial pulmonary arterial hypertension. *American journal of respiratory and critical care medicine*. 2006;174:590-598

43. Humbert M, Sitbon O, Chaouat A, Bertocchi M, Habib G, Gressin V, Yaici A, Weitzenblum E, Cordier JF, Chabot F, Dromer C, Pison C, Reynaud-Gaubert M, Haloun A, Laurent M, Hachulla E, Simonneau G. Pulmonary arterial hypertension in france: Results from a national registry. *American journal of respiratory and critical care medicine*. 2006;173:1023-1030

44. Machado RD, Aldred MA, James V, Harrison RE, Patel B, Schwalbe EC, Gruenig E, Janssen B, Koehler R, Seeger W, Eickelberg O, Olschewski H, Elliott CG, Glissmeyer E, Carlquist J, Kim M, Torbicki A, Fijalkowska A, Szewczyk G, Parma J, Abramowicz MJ, Galie N, Morisaki H, Kyotani S, Nakanishi N, Morisaki T, Humbert M, Simonneau G, Sitbon O, Soubrier F, Coulet F, Morrell NW,

Trembath RC. Mutations of the tgf-beta type ii receptor bmpr2 in pulmonary arterial hypertension. *Human mutation*. 2006;27:121-132

45. Girerd B, Montani D, Coulet F, Sztrymf B, Yaici A, Jais X, Tregouet D, Reis A, Drouin-Garraud V, Fraisse A, Sitbon O, O'Callaghan DS, Simonneau G, Soubrier F, Humbert M. Clinical outcomes of pulmonary arterial hypertension in patients carrying an acvrl1 (alk1) mutation. *American journal of respiratory and critical care medicine*. 2010;181:851-861

46. Harrison RE, Flanagan JA, Sankelo M, Abdalla SA, Rowell J, Machado RD, Elliott CG, Robbins IM, Olschewski H, McLaughlin V, Gruenig E, Kermeen F, Halme M, Raisanen-Sokolowski A, Laitinen T, Morrell NW, Trembath RC. Molecular and functional analysis identifies alk-1 as the predominant cause of pulmonary hypertension related to hereditary haemorrhagic telangiectasia. *Journal of medical genetics*. 2003;40:865-871

47. Nasim MT, Ogo T, Ahmed M, Randall R, Chowdhury HM, Snape KM, Bradshaw TY, Southgate L, Lee GJ, Jackson I, Lord GM, Gibbs JS, Wilkins MR, Ohta-Ogo K, Nakamura K, Girerd B, Coulet F, Soubrier F, Humbert M, Morrell NW, Trembath RC, Machado RD. Molecular genetic characterization of smad signaling molecules in pulmonary arterial hypertension. *Human mutation*. 2011;32:1385-1389

48. Morrell NW, Yang X, Upton PD, Jourdan KB, Morgan N, Sheares KK, Trembath RC. Altered growth responses of pulmonary artery smooth muscle cells from patients with primary pulmonary hypertension to transforming growth factor-beta(1) and bone morphogenetic proteins. *Circulation*. 2001;104:790-795

49. Chin KM, Kim NH, Rubin LJ. The right ventricle in pulmonary hypertension. *Coronary artery disease*. 2005;16:13-18

50. Vonk Noordegraaf A, Galie N. The role of the right ventricle in pulmonary arterial hypertension. *European respiratory review : an official journal of the European Respiratory Society*. 2011;20:243-253

51. Bogaard HJ, Abe K, Vonk Noordegraaf A, Voelkel NF. The right ventricle under pressure: Cellular and molecular mechanisms of right-heart failure in pulmonary hypertension. *Chest*. 2009;135:794-804

52. Sano M, Minamino T, Toko H, Miyauchi H, Orimo M, Qin Y, Akazawa H, Tateno K, Kayama Y, Harada M, Shimizu I, Asahara T, Hamada H, Tomita S, Molkentin JD, Zou Y, Komuro I. P53-induced inhibition of hif-1 causes cardiac dysfunction during pressure overload. *Nature*. 2007;446:444-448

53. Velez-Roa S, Ciarka A, Najem B, Vachiery JL, Naeije R, van de Borne P. Increased sympathetic nerve activity in pulmonary artery hypertension. *Circulation*. 2004;110:1308-1312

54. Gan C, Lankhaar JW, Marcus JT, Westerhof N, Marques KM, Bronzwaer JG, Boonstra A, Postmus PE, Vonk-Noordegraaf A. Impaired left ventricular filling due to right-to-left ventricular interaction in patients with pulmonary arterial hypertension. *American journal of physiology. Heart and circulatory physiology*. 2006;290:H1528-1533

55. Peacock AJ, Murphy NF, McMurray JJ, Caballero L, Stewart S. An epidemiological study of pulmonary arterial hypertension. *The European respiratory journal*. 2007;30:104-109

56. Baptista R, Meireles J, Agapito A, Castro G, da Silva AM, Shiang T, Goncalves F, Robalo-Martins S, Nunes-Diogo A, Reis A. Pulmonary hypertension in portugal: First data from a nationwide registry. *BioMed research international*. 2013;2013:489574

57. McLaughlin VV. Survival in patients with pulmonary arterial hypertension treated with first-line bosentan. *European journal of clinical investigation*. 2006;36 Suppl 3:10-15

58. D'Alonzo GE, Barst RJ, Ayres SM, Bergofsky EH, Brundage BH, Detre KM, Fishman AP, Goldring RM, Groves BM, Kernis JT, et al. Survival in patients with primary pulmonary hypertension. Results from a national prospective registry. *Annals of internal medicine*. 1991;115:343-349

59. Fisher MR, Forfia PR, Chamera E, Housten-Harris T, Champion HC, Girgis RE, Corretti MC, Hassoun PM. Accuracy of doppler echocardiography in the hemodynamic assessment of pulmonary hypertension. *American journal of respiratory and critical care medicine*. 2009;179:615-621

60. Grignola JC. Hemodynamic assessment of pulmonary hypertension. *World journal of cardiology*. 2011;3:10-17

61. Tonelli AR, Alnuaimat H, Mubarak K. Pulmonary vasodilator testing and use of calcium channel blockers in pulmonary arterial hypertension. *Respiratory medicine*. 2010;104:481-496

62. Bossone E, D'Andrea A, D'Alto M, Citro R, Argiento P, Ferrara F, Cittadini A, Rubenfire M, Naeije R. Echocardiography in pulmonary arterial hypertension: From diagnosis to prognosis. *Journal of the American Society of Echocardiography : official publication of the American Society of Echocardiography*. 2013;26:1-14

63. Tei C, Dujardin KS, Hodge DO, Bailey KR, McGoon MD, Tajik AJ, Seward SB. Doppler echocardiographic index for assessment of global right ventricular function. *Journal of the American Society of Echocardiography : official publication of the American Society of Echocardiography*. 1996;9:838-847

64. Forfia PR, Fisher MR, Mathai SC, Housten-Harris T, Hemnes AR, Borlaug BA, Chamera E, Corretti MC, Champion HC, Abraham TP, Girgis RE, Hassoun PM. Tricuspid annular displacement predicts survival in pulmonary hypertension. *American journal of respiratory and critical care medicine*. 2006;174:1034-1041

65. Eysmann SB, Palevsky HI, Reichek N, Hackney K, Douglas PS. Two-dimensional and doppler-echocardiographic and cardiac catheterization correlates of survival in primary pulmonary hypertension. *Circulation*. 1989;80:353-360

66. Ats statement: Guidelines for the six-minute walk test. *American journal of respiratory and critical care medicine*. 2002;166:111-117

67. Oudiz RJ, Barst RJ, Hansen JE, Sun XG, Garofano R, Wu X, Wasserman K. Cardiopulmonary exercise testing and six-minute walk correlations in pulmonary arterial hypertension. *The American journal of cardiology*. 2006;97:123-126

68. Nagaya N, Nishikimi T, Uematsu M, Satoh T, Kyotani S, Sakamaki F, Kakishita M, Fukushima K, Okano Y, Nakanishi N, Miyatake K, Kangawa K. Plasma brain natriuretic peptide as a prognostic indicator in patients with primary pulmonary hypertension. *Circulation*. 2000;102:865-870

69. Torbicki A, Kurzyna M, Kuca P, Fijalkowska A, Sikora J, Florczyk M, Pruszczyk P, Burakowski J, Wawrzynska L. Detectable serum cardiac troponin t as a marker of poor prognosis among patients with chronic precapillary pulmonary hypertension. *Circulation*. 2003;108:844-848

70. Nickel N, Kempf T, Tapken H, Tongers J, Laenger F, Lehmann U, Golpon H, Olsson K, Wilkins MR, Gibbs JS, Hoeper MM, Wollert KC. Growth differentiation factor-15 in idiopathic pulmonary arterial hypertension. *American journal of respiratory and critical care medicine*. 2008;178:534-541

71. Lankeit M, Dellas C, Panzenbock A, Skoro-Sajer N, Bonderman D, Olschewski M, Schafer K, Puls M, Konstantinides S, Lang IM. Heart-type fatty acid-binding protein for risk assessment of chronic thromboembolic pulmonary hypertension. *The European respiratory journal*. 2008;31:1024-1029

72. Sitbon O, Humbert M, Jais X, Ioos V, Hamid AM, Provencher S, Garcia G, Parent F, Herve P, Simonneau G. Long-term response to calcium channel blockers in idiopathic pulmonary arterial hypertension. *Circulation*. 2005;111:3105-3111

73. Montani D, Savale L, Natali D, Jais X, Herve P, Garcia G, Humbert M, Simonneau G, Sitbon O. Long-term response to calcium-channel blockers in non-idiopathic pulmonary arterial hypertension. *Eur Heart J*. 2010;31:1898-1907

74. Liu C, Chen J, Gao Y, Deng B, Liu K. Endothelin receptor antagonists for pulmonary arterial hypertension. *The Cochrane database of systematic reviews*. 2013;2:CD004434

75. Barst RJ, Rubin LJ, Long WA, McGoon MD, Rich S, Badesch DB, Groves BM, Tapson VF, Bourge RC, Brundage BH, Koerner SK, Langleben D, Keller CA, Murali S, Uretsky BF, Clayton LM, Jobsis MM, Blackburn SD, Shortino D, Crow JW. A comparison of continuous intravenous epoprostenol (prostacyclin) with conventional therapy for primary pulmonary hypertension. *The New England journal of medicine*. 1996;334:296-301

76. Dhillon S, Keating GM. Bosentan: A review of its use in the management of mildly symptomatic pulmonary arterial hypertension. *American journal of cardiovascular drugs : drugs, devices, and other interventions*. 2009;9:331-350

77. Marsboom GRJ, S. P. Models for pulmonary hypertension. *Drug Discovery Today: Disease Models*. 2004;Vol. I, No. 3

78. Schroll S, Arzt M, Sebah D, Nuchterlein M, Blumberg F, Pfeifer M. Improvement of bleomycin-induced pulmonary hypertension and pulmonary fibrosis by the

endothelin receptor antagonist bosentan. *Respiratory physiology & neurobiology*. 2010;170:32-36

79. Campbell AI, Zhao Y, Sandhu R, Stewart DJ. Cell-based gene transfer of vascular endothelial growth factor attenuates monocrotaline-induced pulmonary hypertension. *Circulation*. 2001;104:2242-2248

80. Sato K, Webb S, Tucker A, Rabinovitch M, O'Brien RF, McMurtry IF, Stelzner TJ. Factors influencing the idiopathic development of pulmonary hypertension in the fawn hooded rat. *The American review of respiratory disease*. 1992;145:793-797

81. West J, Fagan K, Steudel W, Fouty B, Lane K, Harral J, Hoedt-Miller M, Tada Y, Ozimek J, Tuder R, Rodman DM. Pulmonary hypertension in transgenic mice expressing a dominant-negative bmprii gene in smooth muscle. *Circulation research*. 2004;94:1109-1114

82. Schnader J, Schloo BL, Anderson W, Stephenson LW, Fishman AP. Chronic pulmonary hypertension in sheep: Temporal progression of lesions. *The Journal of surgical research*. 1996;62:243-250

83. Zagorski J, Debelak J, Gellar M, Watts JA, Kline JA. Chemokines accumulate in the lungs of rats with severe pulmonary embolism induced by polystyrene microspheres. *J Immunol*. 2003;171:5529-5536

84. Pak OJ, W.; Ghofrani, H. A.; Seeger, W.;Grimminger, F.;Schermuly, R. T.; Weissmann, N. Animal models of pulmonary hypertension: Role in translational research. *Drug Discovery Today: Disease Models*. 2010;Vol. 7, No. 3-4

85. Hauger RL, Grigoriadis DE, Dallman MF, Plotsky PM, Vale WW, Dautzenberg FM. International union of pharmacology. Xxxvi. Current status of the nomenclature for receptors for corticotropin-releasing factor and their ligands. *Pharmacological reviews*. 2003;55:21-26

86. Kimura Y, Takahashi K, Totsune K, Muramatsu Y, Kaneko C, Darnel AD, Suzuki T, Ebina M, Nukiwa T, Sasano H. Expression of urocortin and corticotropin-releasing factor receptor subtypes in the human heart. *The Journal of clinical endocrinology and metabolism*. 2002;87:340-346

87. Oki Y, Sasano H. Localization and physiological roles of urocortin. *Peptides*. 2004;25:1745-1749

88. Brar BK, Chen A, Perrin MH, Vale W. Specificity and regulation of extracellularly regulated kinase1/2 phosphorylation through corticotropin-releasing factor (crf) receptors 1 and 2beta by the crf/urocortin family of peptides. *Endocrinology*. 2004;145:1718-1729

89. Grossini E, Molinari C, Mary DA, Marino P, Vacca G. The effect of urocortin ii administration on the coronary circulation and cardiac function in the anaesthetized pig is nitric-oxide-dependent. *European journal of pharmacology*. 2008;578:242-248

90. Rademaker MT, Cameron VA, Charles CJ, Richards AM. Integrated hemodynamic, hormonal, and renal actions of urocortin 2 in normal and paced sheep: Beneficial effects in heart failure. *Circulation*. 2005;112:3624-3632

91. Chan WY, Frampton CM, Crozier IG, Troughton RW, Richards AM. Urocortin-2 infusion in acute decompensated heart failure: Findings from the unicorn study (urocortin-2 in the treatment of acute heart failure as an adjunct over conventional therapy). *JACC. Heart failure*. 2013;1:433-441

92. Davis ME, Pemberton CJ, Yandle TG, Fisher SF, Lainchbury JG, Frampton CM, Rademaker MT, Richards AM. Urocortin 2 infusion in healthy humans: Hemodynamic, neurohormonal, and renal responses. *J Am Coll Cardiol*. 2007;49:461-471

93. Vaughan J, Donaldson C, Bittencourt J, Perrin MH, Lewis K, Sutton S, Chan R, Turnbull AV, Lovejoy D, Rivier C, et al. Urocortin, a mammalian neuropeptide related to fish urotensin i and to corticotropin-releasing factor. *Nature*. 1995;378:287-292

94. Grace CR, Perrin MH, Cantle JP, Vale WW, Rivier JE, Riek R. Common and divergent structural features of a series of corticotropin releasing factor-related peptides. *J Am Chem Soc*. 2007;129:16102-16114

95. Karteris E, Hillhouse EW, Grammatopoulos D. Urocortin ii is expressed in human pregnant myometrial cells and regulates myosin light chain phosphorylation: Potential role of the type-2 corticotropin-releasing hormone receptor in the control of myometrial contractility. *Endocrinology*. 2004;145:890-900

96. Vaughan JM, Donaldson CJ, Fischer WH, Perrin MH, Rivier JE, Sawchenko PE, Vale WW. Posttranslational processing of human and mouse urocortin 2: Characterization and bioactivity of gene products. *Endocrinology*. 2013;154:1553-1564

97. Liaw CW, Grigoriadis DE, Lorang MT, De Souza EB, Maki RA. Localization of agonist- and antagonist-binding domains of human corticotropin-releasing factor receptors. *Mol Endocrinol*. 1997;11:2048-2053

98. Lovenberg TW, Liaw CW, Grigoriadis DE, Clevenger W, Chalmers DT, De Souza EB, Oltersdorf T. Cloning and characterization of a functionally distinct corticotropin-releasing factor receptor subtype from rat brain. *Proceedings of the National Academy of Sciences of the United States of America*. 1995;92:836-840

99. Pal K, Swaminathan K, Xu HE, Pioszak AA. Structural basis for hormone recognition by the human crfr2{alpha} g protein-coupled receptor. *The Journal of biological chemistry*. 2010;285:40351-40361

100. Wille S, Sydow S, Palchaudhuri MR, Spiess J, Dautzenberg FM. Identification of amino acids in the n-terminal domain of corticotropin-releasing factor receptor 1 that are important determinants of high-affinity ligand binding. *Journal of neurochemistry*. 1999;72:388-395

101. Hillhouse EW, Grammatopoulos DK. The molecular mechanisms underlying the regulation of the biological activity of corticotropin-releasing hormone receptors: Implications for physiology and pathophysiology. *Endocrine reviews*. 2006;27:260-286

102. Takahashi K, Totsune K, Murakami O, Saruta M, Nakabayashi M, Suzuki T, Sasano H, Shibahara S. Expression of urocortin iii/stresscopin in human heart and kidney. *J Clin Endocrinol Metab*. 2004;89:1897-1903

103. Nishikimi T, Miyata A, Horio T, Yoshihara F, Nagaya N, Takishita S, Yutani C, Matsuo H, Matsuoka H, Kangawa K. Urocortin, a member of the corticotropin-releasing factor family, in normal and diseased heart. *American journal of physiology. Heart and circulatory physiology*. 2000;279:H3031-3039

104. Davis ME, Pemberton CJ, Yandle TG, Lainchbury JG, Rademaker MT, Nicholls MG, Frampton CM, Richards AM. Urocortin-1 infusion in normal humans. *The Journal of clinical endocrinology and metabolism*. 2004;89:1402-1409

105. Davis ME, Pemberton CJ, Yandle TG, Lainchbury JG, Rademaker MT, Nicholls MG, Frampton CM, Richards AM. Effect of urocortin 1 infusion in humans with stable congestive cardiac failure. *Clin Sci (Lond)*. 2005;109:381-388

106. Patel K, Rademaker MT, Kirkpatrick CM, Charles CJ, Fisher S, Yandle TG, Richards AM. Comparative pharmacokinetics and pharmacodynamics of urocortins 1, 2 and 3 in healthy sheep. *British journal of pharmacology*. 2012;166:1916-1925

107. Hsu SY, Hsueh AJ. Human stresscopin and stresscopin-related peptide are selective ligands for the type 2 corticotropin-releasing hormone receptor. *Nature medicine*. 2001;7:605-611

108. Rossant CJ, Pinnock RD, Hughes J, Hall MD, McNulty S. Corticotropin-releasing factor type 1 and type 2alpha receptors regulate phosphorylation of calcium/cyclic adenosine 3',5'-monophosphate response element-binding protein and activation of p42/p44 mitogen-activated protein kinase. *Endocrinology*. 1999;140:1525-1536

109. Shaywitz AJ, Greenberg ME. Creb: A stimulus-induced transcription factor activated by a diverse array of extracellular signals. *Annual review of biochemistry*. 1999;68:821-861

110. Karalis KP, Venihaki M, Zhao J, van Vlerken LE, Chandras C. Nf-kappab participates in the corticotropin-releasing, hormone-induced regulation of the pituitary proopiomelanocortin gene. *The Journal of biological chemistry*. 2004;279:10837-10840

111. Brar BK, Jonassen AK, Stephanou A, Santilli G, Railson J, Knight RA, Yellon DM, Latchman DS. Urocortin protects against ischemic and reperfusion injury via a mapk-dependent pathway. *The Journal of biological chemistry*. 2000;275:8508-8514

112. Markovic D, Punn A, Lehnert H, Grammatopoulos DK. Molecular determinants and feedback circuits regulating type 2 crh receptor signal integration. *Biochimica et biophysica acta*. 2011;1813:896-907

113. Nemoto T, Mano-Otagiri A, Shibasaki T. Urocortin 2 induces tyrosine hydroxylase phosphorylation in pc12 cells. *Biochemical and biophysical research communications*. 2005;330:821-831

114. Calderon-Sanchez E, Delgado C, Ruiz-Hurtado G, Dominguez-Rodriguez A, Cachofeiro V, Rodriguez-Moyano M, Gomez AM, Ordonez A, Smani T. Urocortin induces positive inotropic effect in rat heart. *Cardiovascular research*. 2009;83:717-725

115. Van Kolen K, Dautzenberg FM, Verstraeten K, Royaux I, De Hoogt R, Gutknecht E, Peeters PJ. Corticotropin releasing factor-induced erk phosphorylation in att20 cells occurs via a camp-dependent mechanism requiring epac2. *Neuropharmacology*. 2010;58:135-144

116. Brar BK, Stephanou A, Knight R, Latchman DS. Activation of protein kinase b/akt by urocortin is essential for its ability to protect cardiac cells against hypoxia/reoxygenation-induced cell death. *Journal of molecular and cellular cardiology*. 2002;34:483-492

117. Walther S, Pluteanu F, Renz S, Nikonova Y, Maxwell JT, Yang LZ, Schmidt K, Edwards JN, Wakula P, Groschner K, Maier LS, Spiess J, Blatter LA, Pieske B, Kockskamper J. Urocortin 2 stimulates nitric oxide production in ventricular myoctytes via akt- and pka-mediated phosphorylation of enos at serine 1177. *American journal of physiology. Heart and circulatory physiology*. 2014

118. Chen Y, Zhao J, Du J, Xu G, Tang C, Geng B. Hydrogen sulfide regulates cardiac sarcoplasmic reticulum ca(2+) uptake via k(atp) channel and pi3k/akt pathway. *Life sciences*. 2012;91:271-278

119. Yang LZ, Kockskamper J, Khan S, Suarez J, Walther S, Doleschal B, Unterer G, Khafaga M, Machler H, Heinzel FR, Dillmann WH, Pieske B, Spiess J. Camp- and ca(2)(+) /calmodulin-dependent protein kinases mediate inotropic, lusitropic and arrhythmogenic effects of urocortin 2 in mouse ventricular myocytes. *British journal of pharmacology*. 2011;162:544-556

120. Grossini E, Molinari C, Mary DA, Uberti F, Ribichini F, Caimmi PP, Vacca G. Urocortin ii induces nitric oxide production through camp and ca2+ related pathways in endothelial cells. *Cellular physiology and biochemistry : international journal of experimental cellular physiology, biochemistry, and pharmacology*. 2009;23:87-96

121. Grossini E, Caimmi PP, Molinari C, Mary DA, Uberti F, Vacca G. Modulation of calcium movements by urocortin ii in endothelial cells. *Cellular physiology and biochemistry : international journal of experimental cellular physiology, biochemistry, and pharmacology*. 2010;25:221-232

122. Cantarella G, Lempereur L, Lombardo G, Chiarenza A, Pafumi C, Zappala G, Bernardini R. Divergent effects of corticotropin releasing hormone on endothelial cell nitric oxide synthase are associated with different expression of crh type 1 and 2 receptors. *British journal of pharmacology*. 2001;134:837-844

123. Ikeda K, Tojo K, Otsubo C, Udagawa T, Hosoya T, Tajima N, Nakao K, Kawamura M. Effects of urocortin ii on neonatal rat cardiac myocytes and non-myocytes. *Peptides*. 2005;26:2473-2481

124. Kageyama K, Suda T. Urocortin-related peptides increase interleukin-6 output via cyclic adenosine 5'-monophosphate-dependent pathways in a7r5 aortic smooth muscle cells. *Endocrinology*. 2003;144:2234-2241

125. Huang M, Kempuraj D, Papadopoulou N, Kourelis T, Donelan J, Manola A, Theoharides TC. Urocortin induces interleukin-6 release from rat cardiomyocytes through p38 map kinase, erk and nf-kappab activation. *Journal of molecular endocrinology*. 2009;42:397-405

126. Walther S, Awad S, Lonchyna VA, Blatter LA. Nfat transcription factor regulation by urocortin ii in cardiac myocytes and heart failure. *American journal of physiology. Heart and circulatory physiology*. 2014;306:H856-866

127. Venkatasubramanian S, Newby DE, Lang NN. Urocortins in heart failure. *Biochem Pharmacol*. 2010;80:289-296

128. Yang LZ, Kockskamper J, Heinzel FR, Hauber M, Walther S, Spiess J, Pieske B. Urocortin ii enhances contractility in rabbit ventricular myocytes via crf(2) receptor-mediated stimulation of protein kinase a. *Cardiovascular research*. 2006;69:402-411

129. Bale TL, Hoshijima M, Gu Y, Dalton N, Anderson KR, Lee KF, Rivier J, Chien KR, Vale WW, Peterson KL. The cardiovascular physiologic actions of urocortin ii: Acute effects in murine heart failure. *Proceedings of the National Academy of Sciences of the United States of America*. 2004;101:3697-3702

130. Meili-Butz S, Buhler K, John D, Buser P, Vale WW, Peterson KL, Brink M, Dieterle T. Acute effects of urocortin 2 on cardiac function and propensity for arrhythmias in an animal model of hypertension-induced left ventricular hypertrophy and heart failure. *European journal of heart failure*. 2010;12:797-804

131. Liu CN, Yang C, Liu XY, Li S. In vivo protective effects of urocortin on ischemia-reperfusion injury in rat heart via free radical mechanisms. *Canadian journal of physiology and pharmacology*. 2005;83:459-465

132. Tao J, Xu H, Yang C, Liu CN, Li S. Effect of urocortin on l-type calcium currents in adult rat ventricular myocytes. *Pharmacological research : the official journal of the Italian Pharmacological Society*. 2004;50:471-476

133. Charles CJ, Jardine DL, Rademaker MT, Richards AM. Urocortin 2 induces potent long-lasting inhibition of cardiac sympathetic drive despite baroreflex activation in conscious sheep. *The Journal of endocrinology*. 2010;204:181-189

134. Scarabelli TM, Pasini E, Stephanou A, Comini L, Curello S, Raddino R, Ferrari R, Knight R, Latchman DS. Urocortin promotes hemodynamic and bioenergetic recovery and improves cell survival in the isolated rat heart exposed to ischemia/reperfusion. *J Am Coll Cardiol*. 2002;40:155-161

135. Dieterle T, Meili-Butz S, Buhler K, Morandi C, John D, Buser PT, Rivier J, Vale WW, Peterson KL, Brink M. Immediate and sustained blood pressure lowering by urocortin 2: A novel approach to antihypertensive therapy? *Hypertension*. 2009;53:739-744

136. Kageyama K, Furukawa K, Miki I, Terui K, Motomura S, Suda T. Vasodilative effects of urocortin ii via protein kinase a and a mitogen-activated protein kinase in rat thoracic aorta. *Journal of cardiovascular pharmacology*. 2003;42:561-565

137. Chen CY, Doong ML, Rivier JE, Tache Y. Intravenous urocortin ii decreases blood pressure through crf(2) receptor in rats. *Regul Pept*. 2003;113:125-130

138. Chen ZW, Huang Y, Yang Q, Li X, Wei W, He GW. Urocortin-induced relaxation in the human internal mammary artery. *Cardiovascular research*. 2005;65:913-920

139. Huang Y, Chan FL, Lau CW, Tsang SY, He GW, Chen ZY, Yao X. Urocortin-induced endothelium-dependent relaxation of rat coronary artery: Role of nitric oxide and k+ channels. *British journal of pharmacology*. 2002;135:1467-1476

140. Bale TL, Giordano FJ, Hickey RP, Huang Y, Nath AK, Peterson KL, Vale WW, Lee KF. Corticotropin-releasing factor receptor 2 is a tonic suppressor of vascularization. *Proceedings of the National Academy of Sciences of the United States of America*. 2002;99:7734-7739

141. Emeto TI, Moxon JV, Biros E, Rush CM, Clancy P, Woodward L, Moran CS, Jose RJ, Nguyen T, Walker PJ, Golledge J. Urocortin 2 is associated with abdominal aortic aneurysm and mediates anti-proliferative effects on vascular smooth muscle cells via corticotrophin releasing factor receptor 2. *Clin Sci (Lond)*. 2014;126:517-527

142. Honjo T, Inoue N, Shiraki R, Kobayashi S, Otsui K, Takahashi M, Hirata K, Kawashima S, Yokozaki H, Yokoyama M. Endothelial urocortin has potent antioxidative properties and is upregulated by inflammatory cytokines and pitavastatin. *Journal of vascular research*. 2006;43:131-138

143. Rademaker MT, Charles CJ, Ellmers LJ, Lewis LK, Nicholls MG, Richards AM. Prolonged urocortin 2 administration in experimental heart failure: Sustained hemodynamic, endocrine, and renal effects. *Hypertension*. 2011;57:1136-1144

144. Rademaker MT, Charles CJ, Nicholls MG, Richards AM. Urocortin 2 inhibits furosemide-induced activation of renin and enhances renal function and diuretic responsiveness in experimental heart failure. *Circulation. Heart failure*. 2009;2:532-540

145. Brar BK, Stephanou A, Okosi A, Lawrence KM, Knight RA, Marber MS, Latchman DS. Crh-like peptides protect cardiac myocytes from lethal ischaemic injury. *Molecular and cellular endocrinology*. 1999;158:55-63

146. Chen J, Tao J, Zhang R, Xu Y, Soong T, Li S. Urocortin inhibits mesenteric arterial remodeling in spontaneously hypertensive rats. *Peptides*. 2009;30:1117-1123

147. Topal E, Yagmur J, Otlu B, Atas H, Cansel M, Acikgoz N, Ermis N. Relationship of urocortin-2 with systolic and diastolic functions and coronary artery disease: An observational study. *Anadolu kardiyoloji dergisi : AKD = the Anatolian journal of cardiology*. 2012;12:115-120

148. Venkatasubramanian S, Griffiths ME, McLean SG, Miller MR, Luo R, Lang NN, Newby DE. Vascular effects of urocortins 2 and 3 in healthy volunteers. *Journal of the American Heart Association*. 2013;2:e004267

149. Davis ME, Pemberton CJ, Yandle TG, Fisher SF, Lainchbury JG, Frampton CM, Rademaker MT, Richards M. Urocortin 2 infusion in human heart failure. *Eur Heart J*. 2007;28:2589-2597

150. Smani T, Calderon E, Rodriguez-Moyano M, Dominguez-Rodriguez A, Diaz I, Ordonez A. Urocortin-2 induces vasorelaxation of coronary arteries isolated from patients with heart failure. *Clinical and experimental pharmacology & physiology*. 2011;38:71-76

151. Wright SP, Doughty RN, Frampton CM, Gamble GD, Yandle TG, Richards AM. Plasma urocortin 1 in human heart failure. *Circulation. Heart failure*. 2009;2:465-471

152. Dautzenberg FM, Hauger RL. The crf peptide family and their receptors: Yet more partners discovered. *Trends in pharmacological sciences*. 2002;23:71-77

153. Breu J, Touma C, Holter SM, Knapman A, Wurst W, Deussing JM. Urocortin 2 modulates aspects of social behaviour in mice. *Behav Brain Res*. 2012;233:331-336

154. Fekete EM, Zhao Y, Szucs A, Sabino V, Cottone P, Rivier J, Vale WW, Koob GF, Zorrilla EP. Systemic urocortin 2, but not urocortin 1 or stressin 1-a, suppresses feeding via crf2 receptors without malaise and stress. *British journal of pharmacology*. 2011;164:1959-1975

155. Reagan-Shaw S, Nihal M, Ahmad N. Dose translation from animal to human studies revisited. *FASEB journal : official publication of the Federation of American Societies for Experimental Biology*. 2008;22:659-661

156. Lourenco AP, Vasques-Novoa F, Oliveira-Pinto J, Fontoura D, Roncon-Albuquerque R, Jr., Leite-Moreira AF. Haemodynamic and neuroendocrine effects of tezosentan in chronic experimental pulmonary hypertension. *Intensive care medicine*. 2012;38:1050-1060

157. Archer SL, Weir EK, Wilkins MR. Basic science of pulmonary arterial hypertension for clinicians: New concepts and experimental therapies. *Circulation*. 2010;121:2045-2066

158. Lourenco AP, Vasques-Novoa F, Fontoura D, Bras-Silva C, Roncon-Albuquerque R, Jr., Leite-Moreira AF. A western-type diet attenuates pulmonary hypertension with heart failure and cardiac cachexia in rats. *The Journal of nutrition*. 2011;141:1954-1960

159. Yin FC, Spurgeon HA, Rakusan K, Weisfeldt ML, Lakatta EG. Use of tibial length to quantify cardiac hypertrophy: Application in the aging rat. *The American journal of physiology*. 1982;243:H941-947

160. Bupha-Intr T, Haizlip KM, Janssen PM. Role of endothelin in the induction of cardiac hypertrophy in vitro. *PloS one*. 2012;7:e43179

161. Booth J, Pinney J, Davenport A. N-terminal probnp--marker of cardiac dysfunction, fluid overload, or malnutrition in hemodialysis patients? *Clinical journal of the American Society of Nephrology : CJASN*. 2010;5:1036-1040

162. Kido M, Du L, Sullivan CC, Li X, Deutsch R, Jamieson SW, Thistlethwaite PA. Hypoxia-inducible factor 1-alpha reduces infarction and attenuates progression of cardiac dysfunction after myocardial infarction in the mouse. *J Am Coll Cardiol*. 2005;46:2116-2124

163. Roux PP, Blenis J. Erk and p38 mapk-activated protein kinases: A family of protein kinases with diverse biological functions. *Microbiology and molecular biology reviews : MMBR*. 2004;68:320-344

164. Burgering BM, Coffer PJ. Protein kinase b (c-akt) in phosphatidylinositol-3-oh kinase signal transduction. *Nature*. 1995;376:599-602

165. Heim MH. The jak-stat pathway: Cytokine signalling from the receptor to the nucleus. *Journal of receptor and signal transduction research*. 1999;19:75-120

166. Jones JE, Mendes L, Rudd MA, Russo G, Loscalzo J, Zhang YY. Serial noninvasive assessment of progressive pulmonary hypertension in a rat model. *American journal of physiology. Heart and circulatory physiology*. 2002;283:H364-371

167. Urboniene D, Haber I, Fang YH, Thenappan T, Archer SL. Validation of high-resolution echocardiography and magnetic resonance imaging vs. High-fidelity catheterization in experimental pulmonary hypertension. *American journal of physiology. Lung cellular and molecular physiology*. 2010;299:L401-412

168. Koskenvuo JW, Mirsky R, Zhang Y, Angeli FS, Jahn S, Alastalo TP, Schiller NB, Boyle AJ, Chatterjee K, De Marco T, Yeghiazarians Y. A comparison of echocardiography to invasive measurement in the evaluation of pulmonary arterial hypertension in a rat model. *The international journal of cardiovascular imaging*. 2010;26:509-518

169. Naeije RaH, S. Right ventricular function in pulmonary hypertension: Physiological concepts. *European Heart Journal Supplements 9(H)*. 2007;H5-H9

170. Hardziyenka M, Campian ME, de Bruin-Bon HA, Michel MC, Tan HL. Sequence of echocardiographic changes during development of right ventricular failure in rat. *Journal of the American Society of Echocardiography : official publication of the American Society of Echocardiography*. 2006;19:1272-1279

171. Chen L, Gan XT, Haist JV, Feng Q, Lu X, Chakrabarti S, Karmazyn M. Attenuation of compensatory right ventricular hypertrophy and heart failure following monocrotaline-induced pulmonary vascular injury by the na+-h+ exchange inhibitor cariporide. *J Pharmacol Exp Ther*. 2001;298:469-476

172. Voelkel NF, Quaife RA, Leinwand LA, Barst RJ, McGoon MD, Meldrum DR, Dupuis J, Long CS, Rubin LJ, Smart FW, Suzuki YJ, Gladwin M, Denholm EM, Gail DB. Right ventricular function and failure: Report of a national heart, lung, and blood institute working group on cellular and molecular mechanisms of right heart failure. *Circulation*. 2006;114:1883-1891

173. Yamamoto S. Single lung transplantation for the treatment of monocrotaline-induced pulmonary hypertension in the rat. *Acta medica Nagasakiensia 40*. 1995;(1-4):38-43

174. Campian ME, Hardziyenka M, Michel MC, Tan HL. How valid are animal models to evaluate treatments for pulmonary hypertension? *Naunyn-Schmiedeberg's archives of pharmacology*. 2006;373:391-400

175. Brar BK, Jonassen AK, Egorina EM, Chen A, Negro A, Perrin MH, Mjos OD, Latchman DS, Lee KF, Vale W. Urocortin-ii and urocortin-iii are cardioprotective against ischemia reperfusion injury: An essential endogenous cardioprotective role for corticotropin releasing factor receptor type 2 in the murine heart. *Endocrinology*. 2004;145:24-35; discussion 21-23

176. Phrommintikul A, Sivasinprasasn S, Lailerd N, Chattipakorn S, Kuanprasert S, Chattipakorn N. Plasma urocortin in acute myocardial infarction patients. *European journal of clinical investigation*. 2010;40:874-882

177. Haworth SG. The cell and molecular biology of right ventricular dysfunction in pulmonary hypertension. *European Heart Journal Supplements 9(H)*. 2007:H10-H16

178. Charles CJ, Rademaker MT, Richards AM. Urocortin 1 modulates the neurohumoral response to acute nitroprusside-induced hypotension in sheep. *Clin Sci (Lond)*. 2007;112:485-491

179. Stewart DJ, Levy RD, Cernacek P, Langleben D. Increased plasma endothelin-1 in pulmonary hypertension: Marker or mediator of disease? *Annals of internal medicine*. 1991;114:464-469

180. Ichikawa KI, Hidai C, Okuda C, Kimata SI, Matsuoka R, Hosoda S, Quertermous T, Kawana M. Endogenous endothelin-1 mediates cardiac hypertrophy and switching of myosin heavy chain gene expression in rat ventricular myocardium. *J Am Coll Cardiol*. 1996;27:1286-1291

181. Lourenco AP, Roncon-Albuquerque R, Jr., Bras-Silva C, Faria B, Wieland J, Henriques-Coelho T, Correia-Pinto J, Leite-Moreira AF. Myocardial dysfunction and neurohumoral activation without remodeling in left ventricle of monocrotaline-induced pulmonary hypertensive rats. *American journal of physiology. Heart and circulatory physiology*. 2006;291:H1587-1594

182. Leuchte HH, Holzapfel M, Baumgartner RA, Ding I, Neurohr C, Vogeser M, Kolbe T, Schwaiblmair M, Behr J. Clinical significance of brain natriuretic peptide in primary pulmonary hypertension. *J Am Coll Cardiol*. 2004;43:764-770

183. King L, Wilkins MR. Natriuretic peptide receptors and the heart. *Heart*. 2002;87:314-315

184. Nagaya N, Nishikimi T, Okano Y, Uematsu M, Satoh T, Kyotani S, Kuribayashi S, Hamada S, Kakishita M, Nakanishi N, Takamiya M, Kunieda T, Matsuo H, Kangawa K. Plasma brain natriuretic peptide levels increase in proportion to the extent of right ventricular dysfunction in pulmonary hypertension. *J Am Coll Cardiol*. 1998;31:202-208

185. Chu W, Wan L, Zhao D, Qu X, Cai F, Huo R, Wang N, Zhu J, Zhang C, Zheng F, Cai R, Dong D, Lu Y, Yang B. Mild hypoxia-induced cardiomyocyte hypertrophy via up-regulation of hif-1alpha-mediated trpc signalling. *Journal of cellular and molecular medicine*. 2012;16:2022-2034

186. Zhou YF, Zheng XW, Zhang GH, Zong ZH, Qi GX. The effect of hypoxia-inducible factor 1-alpha on hypoxia-induced apoptosis in primary neonatal rat ventricular myocytes. *Cardiovascular journal of Africa*. 2010;21:37-41

187. Buhler K, Plaisance I, Dieterle T, Brink M. The human urocortin 2 gene is regulated by hypoxia: Identification of a hypoxia-responsive element in the 3'-flanking region. *The Biochemical journal*. 2009;424:119-127

188. Saraste A, Pulkki K, Kallajoki M, Henriksen K, Parvinen M, Voipio-Pulkki LM. Apoptosis in human acute myocardial infarction. *Circulation*. 1997;95:320-323

189. Condorelli G, Morisco C, Stassi G, Notte A, Farina F, Sgaramella G, de Rienzo A, Roncarati R, Trimarco B, Lembo G. Increased cardiomyocyte apoptosis and changes in proapoptotic and antiapoptotic genes bax and bcl-2 during left ventricular adaptations to chronic pressure overload in the rat. *Circulation*. 1999;99:3071-3078

190. Gao XF, Zhou Y, Wang DY, Lew KS, Richards AM, Wang P. Urocortin-2 suppression of p38-mapk signaling as an additional mechanism for ischemic cardioprotection. *Molecular and cellular biochemistry*. 2014

191. Tao J, Zhang Y, Soong TW, Li S. Urocortin ii inhibits the apoptosis of mesenteric arterial smooth muscle cells via l-type calcium channels in spontaneously hypertensive rats. *Cellular physiology and biochemistry : international journal of experimental cellular physiology, biochemistry, and pharmacology*. 2006;17:111-120

192. Narula J, Pandey P, Arbustini E, Haider N, Narula N, Kolodgie FD, Dal Bello B, Semigran MJ, Bielsa-Masdeu A, Dec GW, Israels S, Ballester M, Virmani R, Saxena S, Kharbanda S. Apoptosis in heart failure: Release of cytochrome c from mitochondria and activation of caspase-3 in human cardiomyopathy. *Proceedings of the National Academy of Sciences of the United States of America*. 1999;96:8144-8149

193. Cai L, Li W, Wang G, Guo L, Jiang Y, Kang YJ. Hyperglycemia-induced apoptosis in mouse myocardium: Mitochondrial cytochrome c-mediated caspase-3 activation pathway. *Diabetes*. 2002;51:1938-1948

194. Yen CH, Tsai TH, Leu S, Chen YL, Chang LT, Chai HT, Chung SY, Chua S, Tsai CY, Chang HW, Ko SF, Sun CK, Yip HK. Sildenafil improves long-term effect of endothelial progenitor cell-based treatment for monocrotaline-induced rat pulmonary arterial hypertension. *Cytotherapy*. 2013;15:209-223

195. Lee FY, Lu HI, Zhen YY, Leu S, Chen YL, Tsai TH, Chung SY, Chua S, Sheu JJ, Hsu SY, Chang HW, Sun CK, Yip HK. Benefit of combined therapy with nicorandil and colchicine in preventing monocrotaline-induced rat pulmonary arterial hypertension. *European journal of pharmaceutical sciences : official journal of the European Federation for Pharmaceutical Sciences*. 2013;50:372-384

196. Condorelli G, Roncarati R, Ross J, Jr., Pisani A, Stassi G, Todaro M, Trocha S, Drusco A, Gu Y, Russo MA, Frati G, Jones SP, Lefer DJ, Napoli C, Croce CM. Heart-targeted overexpression of caspase3 in mice increases infarct size and depresses cardiac function. *Proceedings of the National Academy of Sciences of the United States of America*. 2001;98:9977-9982

197. Fan Q, Huang ZM, Boucher M, Shang X, Zuo L, Brinks H, Lau WB, Zhang J, Chuprun JK, Gao E. Inhibition of fas-associated death domain-containing protein (fadd) protects against myocardial ischemia/reperfusion injury in a heart failure mouse model. *PloS one*. 2013;8:e73537

198. Hsieh YP, Huang CH, Lee CY, Lin CY, Chang CC. Silencing of hepcidin enforces the apoptosis in iron-induced human cardiomyocytes. *J Occup Med Toxicol*. 2014;9:11

199. Yuan Z, McCauley R, Chen-Scarabelli C, Abounit K, Stephanou A, Barry SP, Knight R, Saravolatz SF, Saravolatz LD, Ulgen BO, Scarabelli GM, Faggian G, Mazzucco A, Saravolatz L, Scarabelli TM. Activation of src protein tyrosine kinase plays an essential role in urocortin-mediated cardioprotection. *Molecular and cellular endocrinology*. 2010;325:1-7

200. Chen QM, Tu VC, Purdon S, Wood J, Dilley T. Molecular mechanisms of cardiac hypertrophy induced by toxicants. *Cardiovascular toxicology*. 2001;1:267-283

201. Nohe A, Hassel S, Ehrlich M, Neubauer F, Sebald W, Henis YI, Knaus P. The mode of bone morphogenetic protein (bmp) receptor oligomerization determines different bmp-2 signaling pathways. *The Journal of biological chemistry*. 2002;277:5330-5338

202. Kiss T, Kovacs K, Komocsi A, Tornyos A, Zalan P, Sumegi B, Gallyas F, Jr. Novel mechanisms of sildenafil in pulmonary hypertension involving cytokines/chemokines, map kinases and akt. *PloS one*. 2014;9:e104890

203. Kehat I, Molkentin JD. Extracellular signal-regulated kinase 1/2 (erk1/2) signaling in cardiac hypertrophy. *Annals of the New York Academy of Sciences*. 2010;1188:96-102

204. Bartelds B, Borgdorff MA, Smit-van Oosten A, Takens J, Boersma B, Nederhoff MG, Elzenga NJ, van Gilst WH, De Windt LJ, Berger RM. Differential responses of the right ventricle to abnormal loading conditions in mice: Pressure vs. Volume load. *European journal of heart failure*. 2011;13:1275-1282

205. Li XM, Ma YT, Yang YN, Liu F, Chen BD, Han W, Zhang JF, Gao XM. Downregulation of survival signalling pathways and increased apoptosis in the transition of pressure overload-induced cardiac hypertrophy to heart failure. *Clinical and experimental pharmacology & physiology*. 2009;36:1054-1061

206. Perez Lopez I, Cariolato L, Maric D, Gillet L, Abriel H, Diviani D. A-kinase anchoring protein lbc coordinates a p38 activating signaling complex controlling compensatory cardiac hypertrophy. *Molecular and cellular biology*. 2013;33:2903-2917

207. Mosele F, Tavares AM, Colombo R, Caron-Lienert R, Araujo AS, Ribeiro MF, Bello-Klein A. Effects of purple grape juice in the redox-sensitive modulation of right ventricular remodeling in a pulmonary arterial hypertension model. *Journal of cardiovascular pharmacology*. 2012;60:15-22

208. Catlett-Falcone R, Landowski TH, Oshiro MM, Turkson J, Levitzki A, Savino R, Ciliberto G, Moscinski L, Fernandez-Luna JL, Nunez G, Dalton WS, Jove R. Constitutive activation of stat3 signaling confers resistance to apoptosis in human u266 myeloma cells. *Immunity*. 1999;10:105-115

209. Paulin R, Courboulin A, Meloche J, Mainguy V, Dumas de la Roque E, Saksouk N, Cote J, Provencher S, Sussman MA, Bonnet S. Signal transducers and activators of transcription-3/pim1 axis plays a critical role in the pathogenesis of human pulmonary arterial hypertension. *Circulation*. 2011;123:1205-1215

210. Chen-Scarabelli C, Saravolatz Ii L, McCaukey R, Scarabelli G, Di Rezze J, Mohanty B, Barry S, Latchman D, Georgiadis V, McCormick J, Saravolatz L, Knight R, Faggian G, Narula J, Stephanou A, Scarabelli TM. The cardioprotective effects of urocortin are mediated via activation of the src tyrosine kinase-stat3 pathway. *Jak-Stat*. 2013;2:e24812

APPENDIX

Publications as Full Texts:

Santos-Ribeiro D*, Adão R*, Rademaker M, Leite-Moreira AF, Brás-Silva C. Urocortin-2 in Cardiovascular Health and Disease. Drug Discovery Today, 2014 (*in revision*).

Mendes-Ferreira P, Adão R, Maia-Rocha C, Alves BS, **Santos-Ribeiro D**, Lourenço AP, Mendes MJ, Cerqueira RJ, Castro-Chaves P, De Keulenaer GW, Leite-Moreira AF, Brás-Silva C. Neuregulin-1 improves right ventricular function and attenuates monocrotaline-induced pulmonary arterial hypertension. Cardiovascular Research, 2014 (*submitted*).

Publications as Abstracts:

Santos-Ribeiro D, Mendes-Ferreira P, Alves BS, Adão R, Maia-Rocha C, Leite-Moreira AF, Brás-Silva C. Molecular mechanisms underlying the beneficial effects of neuregulin-1 in the treatment of pulmonary arterial hypertension. 7th Meeting of Young Researchers of University of Porto 2014, Book of abstracts, page 54.

Alves BS, **Santos-Ribeiro D**, Adão R, Maia-Rocha C, Mendes-Ferreira P, Leite-Moreira AF, Brás-Silva C. Modulation of right ventricle function by neuregulin-1 – therapeutic implications in pulmonary hypertension. 7th Meeting of Young Researchers of University of Porto 2014, Book of abstracts, page 56.

Mendes-Ferreira P, **Santos-Ribeiro D**, Alves BS, Adão R, Maia-Rocha C, Leite-Moreira AF, De Keulenaer GW, Brás-Silva C. Reversão da hipertrofia ventricular direita pela neuregulina-1. Revista Portuguesa de Cardiologia 2014, vol. 33 (Especial congresso): 69-70.

Adão R, Mendes-Ferreira P, Maia-Rocha C, Alves BS, **Santos-Ribeiro D**, Falcão-Pires I, De Keulenaer GW, Leite-Moreira AF, Brás-Silva C. A neuregulina-1 modula a função dos cardiomiócitos do ventrículo direito na hipertensão arterial pulmonar. Revista Portuguesa de Cardiologia 2014, vol. 33 (Especial congresso): 164.

Maia-Rocha C, Mendes-Ferreira P, Adão R, **Santos-Ribeiro D**, Alves BS, De Keulenaer GW, Leite-Moreira AF, Brás-Silva C. Mecanismos moleculares subjacentes aos efeitos benéficos da neuregulina-1 no tratamento da hipertensão arterial pulmonar. Revista Portuguesa de Cardiologia 2014, vol. 33 (Especial congresso): 69.

Mendes-Ferreira P, **Santos-Ribeiro D**, Alves BS, Adão R, Maia-Rocha C, Leite-Moreira AF, De Keulenaer GW, Brás-Silva C. Neuregulin-1 attenuates right ventricle hypertrophy in a model of pulmonary artery banding. European Journal of Heart Failure 2014, 16 S2:112.

Maia-Rocha C, Mendes-Ferreira P, Adão R, **Santos-Ribeiro D**, Alves BS, De Keulenaer GW, Leite-Moreira AF, Brás-Silva C. Molecular mechanisms underlying the beneficial effects of neuregulin-1 in pulmonary arterial hypertension. Cardiovascular Research 2014, 103 S1:138.

Maia-Rocha C, Mendes-Ferreira P, Adão R, **Santos-Ribeiro D**, Alves BS, De Keulenaer GW, Leite-Moreira AF, Brás-Silva C. The right ventricle molecular changes associated with pulmonary arterial hypertension are attenuated by neuregulin-1 treatment. European Heart Journal 2014, 35:1046.

Santos-Ribeiro D, Adão R, Maia-Rocha C, Alves BS, Mendes-Ferreira P, Leite-Moreira AF, Brás-Silva C. Urocortin-2 improves right ventricular function in pulmonary arterial hypertension. Circulation 2014 (*in press*).

Santos-Ribeiro D, Alves BS, Adão R, Maia-Rocha C, Mendes-Ferreira P, Leite-Moreira AF, Brás-Silva C. Urocortin-2 improves right ventricular function in pulmonar arterial hypertension. Young European Scientist Meeting 2014 Abstract Book, page 61.

Alves BS, **Santos-Ribeiro D**, Adão R, Maia-Rocha C, Mendes-Ferreira P, De Keulenaer GW, Leite-Moreira AF, Brás-Silva C. Right ventricle pressure overload-induced hypertrophy is attenuated by neuregulin-1. Young European Scientist Meeting 2014 Abstract Book, page 62.

Maia-Rocha C, **Santos-Ribeiro D**, Mendes-Ferreira P, Adão R, Alves BS, De Keulenaer GW, Leite-Moreira AF, Brás-Silva C. Molecular mechanisms underlying the beneficial effects of neuregulin-1 in pulmonary arterial hypertension. Young European Scientist Meeting 2014 Abstract Book, page 63.

Adão R, Alves BS, **Santos-Ribeiro D**, Mendes-Ferreira P, Maia-Rocha C, Hamdani N, Mendes MJ, Falcão-Pires I, De Keulenaer GW, Linke W, Leite-Moreira AF, Brás-Silva C. Neuregulin-1 preserves right ventricular diastolic function in animal model of pulmonary arterial hypertension. Young European Scientist Meeting 2014 Abstract Book, page 50.

Santos-Ribeiro D, Mendes-Ferreira P, Adão R, Maia-Rocha C, Alves BS, Leite-Moreira AF, Brás-Silva C. Urocortin-2 improves right ventricular function in pulmonar arterial hypertension. Heart Without Borders – Cardiovascular Development, Disease and Repair – International Conference 2014. Abstract Book, page 91.

Mendes-Ferreira P, Adão R, Maia-Rocha C, **Santos-Ribeiro D**, Alves BS, De Keulenaer GW, Leite-Moreira AF, Brás-Silva C. Neuregulin-1 improves right ventricular function and attenuates monocrotaline-induced pulmonary arterial hypertension. Heart Without Borders –

Cardiovascular Development, Disease and Repair – International Conference 2014. Abstract Book, page 90.

Santos-Ribeiro D, Mendes-Ferreira P, Adão R, Maia-Rocha C, Alves BS, Rademaker M, Leite-Moreira AF, Brás-Silva C. Urocortin-2 improves right ventricular function in pulmonary arterial hypertension. European Journal of Heart Failure 2015 (*accepted*).

Communications at Scientific Meetings

Oral Communications

Santos-Ribeiro D, Mendes-Ferreira P, Alves BS, Adão R, Maia-Rocha C, Leite-Moreira AF, Brás-Silva C. Molecular mechanisms underlying the beneficial effects of neuregulin-1 in the treatment of pulmonary arterial hypertension. 7th Meeting of Young Researchers of University of Porto (IJUP) 2014 February. Oporto, Portugal.

Alves BS, **Santos-Ribeiro D**, Adão R, Maia-Rocha C, Mendes-Ferreira P, Leite-Moreira AF, Brás-Silva C. Modulation of right ventricle function by neuregulin-1 – therapeutic implications in pulmonary hypertension. 7th Meeting of Young Researchers of University of Porto (IJUP) 2014 February. Oporto, Portugal.

Mendes-Ferreira P, **Santos-Ribeiro D**, Alves BS, Adão R, Maia-Rocha C, Leite-Moreira AF, De Keulenaer GW, Brás-Silva C. Neuregulin-1 attenuates right ventricle hypertrophy in a model of pulmonary artery banding. Heart Failure 2014 May. Athens, Greece.

Adão R, Alves BS, **Santos-Ribeiro D**, Mendes-Ferreira P, Maia-Rocha C, Hamdani N, Mendes MJ, Falcão-Pires I, De Keulenaer GW, Linke W, Leite-Moreira AF, Brás-Silva C. Neuregulin-1 preserves right ventricular diastolic function in animal model of pulmonary arterial hypertension. 9th Young European Scientist Meeting 2014 September. Oporto, Portugal.

Poster Communications

2013

Santos-Ribeiro D, Mendes-Ferreira P, Maia-Rocha C, Adão R, Leite-Moreira AF, Brás-Silva C. The role of miRNA-146a in pulmonary arterial hypertension. Fundação Astrazeneca Innovate Competition – 5.0 iMed Conference 2013 October. Lisbon, Portugal.

Adão R, Mendes-Ferreira P, Maia-Rocha C, **Santos-Ribeiro D**, Rademaker M, Leite-Moreira AF, Brás-Silva C. UCN-2/CRHR2 system role in pulmonary hypertension – pathophysiological and therapeutic implications. Fundação Astrazeneca Innovate Competition – 5.0 iMed Conference 2013 October. Lisbon, Portugal.

2014

Mendes-Ferreira P, **Santos-Ribeiro D**, Alves BS, Adão R, Maia-Rocha C, Leite-Moreira AF, De Keulenaer GW, Brás-Silva C. Reversão da hipertrofia ventricular direita pela neuregulina-1. XXXV Congresso Português de Cardiologia 2014 Abril. Albufeira, Portugal.

Maia-Rocha C, Adão R, Mendes-Ferreira P, **Santos-Ribeiro D**, Alves BS, Leite-Moreira AF, De Keulenaer GW, Brás-Silva C. Mecanismos moleculares associados aos efeitos benéficos da neuregulina-1 no tratamento da hipertensão arterial pulmonar. XXXV Congresso Português de Cardiologia 2014 Abril. Albufeira, Portugal.

Adão R, Mendes-Ferreira P, Maia-Rocha C, Alves BS, **Santos-Ribeiro D**, Falcão-Pires I, De Keulenaer GW, Leite-Moreira AF, Brás-Silva C. a neuregulina-1 modula a função dos cardiomiócitos do ventrículo direito na hipertensão arterial pulmonar. XXXV Congresso Português de Cardiologia 2014 Abril. Albufeira, Portugal.

Maia-Rocha C, Mendes-Ferreira P, Adão R, **Santos-Ribeiro D**, Alves BS, De Keulenaer GW, Leite-Moreira AF, Brás-Silva C. Molecular mechanisms underlying the beneficial effects of neuregulin-1 in pulmonary arterial hypertension. Frontiers in Cardiovascular Biology 2014 July. Barcelona, Spain.

Maia-Rocha C, Mendes-Ferreira P, Adão R, **Santos-Ribeiro D**, Alves BS, De Keulenaer GW, Leite-Moreira AF, Brás-Silva C. the right ventricle molecular changes associated with pulmonar arterial hypertension are attenuated by neuregulin-1 treatment. European Society of Cardiology Congress 2014 August/September. Barcelona, Spain.

Santos-Ribeiro D, Alves BS, Adão R, Maia-Rocha C, Mendes-Ferreira P, Leite-Moreira AF, Brás-Silva C. Urocortin-2 improves right ventricular function in pulmonar arterial hypertension. 9th Young European Scientist Meeting 2014 September. Oporto, Portugal.

Alves BS, **Santos-Ribeiro D**, Adão R, Maia-Rocha C, Mendes-Ferreira P, De Keulenaer GW, Leite-Moreira AF, Brás-Silva C. Right ventricle pressure overload-induced hypertrophy is attenuated by neuregulin-1. 9th Young European Scientist Meeting 2014 September. Oporto, Portugal.

Maia-Rocha C, **Santos-Ribeiro D**, Mendes-Ferreira P, Adão R, Alves BS, De Keulenaer GW, Leite-Moreira AF, Brás-Silva C. Molecular mechanisms underlying the beneficial effects of neuregulin-1 in pulmonary arterial hypertension. 9th Young European Scientist Meeting 2014 September. Oporto, Portugal.

Santos-Ribeiro D, Adão R, Maia-Rocha C, Alves BS, Mendes-Ferreira P, Leite-Moreira AF, Brás-Silva C. Urocortin-2 improves right ventricular function in pulmonary arterial hypertension. American Heart Association Scientific Sessions 2014 November. Chicago, USA.

Santos-Ribeiro D, Mendes-Ferreira P, Adão R, Maia-Rocha C, Alves BS, Leite-Moreira AF, Brás-Silva C. Urocortin-2 improves right ventricular function in pulmonar arterial hypertension. Heart Without Borders – Cardiovascular Development, Disease and Repair – International Conference 2014 November. Porto, Portugal.

Mendes-Ferreira P, Adão R, Maia-Rocha C, **Santos-Ribeiro D**, Alves BS, De Keulenaer GW, Leite-Moreira AF, Brás-Silva C. Neuregulin-1 improves right ventricular function and attenuates monocrotaline-induced pulmonary arterial hypertension. Heart Without Borders – Cardiovascular Development, Disease and Repair – International Conference 2014 November. Porto, Portugal.

2015

Santos-Ribeiro D, Mendes-Ferreira P, Adão R, Maia-Rocha C, Alves BS, Rademaker M, Leite-Moreira AF, Brás-Silva C. Urocortin-2 improves right ventricular function in pulmonary arterial hypertension. Heart Failure Association Winter Research Meeting 2015 January. Les Diablerets, Switzerland (*accepted*).

Research Projects

Role of the neuregulin system in pulmonary arterial hypertension – pathophysiological and therapeutic implications. Carmen Brás Silva, Faculdade de Medicina da Universidade do Porto, PTDC/SAU-FCF/100442/2008.

Pathophysiological role and therapeutic potential of urocortin-2 in pulmonary hypertension. Carmen Brás Silva, Faculdade de Medicina da Universidade do Porto, PTDC/DTP-FTO/0130/2012.

The role of miRNA-146a in pulmonary arterial hypertension. Pedro Ferreira, **Diana Ribeiro**, Carolina Rocha, Rui Adão, Bárbara Alves, Adelino Leite Moreira, Carmen Brás Silva, Faculdade

de Medicina da Universidade do Porto, Bolsa de Estudo João Porto da Sociedade Portuguesa de Cardiologia 2013/2014.

Research Prizes

Bolsa de Estudo João Porto da Sociedade Portuguesa de Cardiologia 2013/2014 – Mendes-Ferreira P, **Santos-Ribeiro D**, Maia-Rocha C, Adão R, Alves BS, Leite-Moreira AF, Brás-Silva C. O Papel do miRNA-146a na hipertensão arterial pulmonar.

Prémio Servier de Investigação Básica da Sociedade Portuguesa de Cardiologia 2014 – Mendes-Ferreira P, Maia-Rocha C, Adão R, **Santos-Ribeiro D**, Alves BS, Cerqueira RJ, Mendes MJ, Leite-Moreira AF, Brás-Silva C. A neuregulina-1 reduz a hipertensão arterial pulmonar e a disfunção ventricular direita num modelo experimental de hipertensão pulmonar.

Physiology & Immunology Poster Presentation First Prize, 9th Young European Scientist Meeting 2014 – Maia-Rocha C, **Santos-Ribeiro D**, Mendes-Ferreira P, Adão R, Alves BS, De Keulenaer GW, Leite-Moreira AF, Brás-Silva C. Molecular mechanisms underlying the beneficial effects of neuregulin-1 in pulmonary arterial hypertension.

Physiology & Immunology Parallel Oral Session First Prize, 9th Young European Scientist Meeting 2014 – Adão R, Alves BS, **Santos-Ribeiro D**, Mendes-Ferreira P, Maia-Rocha C, Hamdani N, Mendes MJ, Falcão-Pires I, De Keulenaer GW, Linke W, Leite-Moreira AF, Brás-Silva C. Neuregulin-1 preserves right ventricular diastolic function in animal model of pulmonary arterial hypertension.